Dissertation

Neural circuits underlying colour vision and visual memory in *Drosophila melanogaster*

Dissertation der Fakultät für Biologie der Ludwig-Maximilians-Universität München
Zur Erlangung des akademischen Grades Doktor der Naturwissenschaften (Dr. rer. nat.)
München, 2014 / Christopher Dominik Schnaitmann

Erstgutachter: Prof. Dr. Alexander Borst
Zweitgutachter: Prof. Dr. Andreas Herz

Datum der Einreichung: 06. Mai 2014
Datum der Promotion: 15. Oktober 2014

Meiner geliebten Frau und
meinen Eltern gewidmet.

Contents

Table of Figures

List of Tables

List of Abbrevations

amc	amacrine cell
CS	conditioned stimulus
DA	dopamine
DRA	dorsal rim area
ERG	electroretinogram
GAL4	yeast transcription factor
GFP	green fluorescent protein
KC	Kenyon cell
L1–5	lamina monopolar cells 1-5
LED	light-emitting diode
LMC	lamina monopolar cell
MB	mushroom body
n	number of experiments
n.s.	not significant
R1-R8	photoreceptors 1-8
Rh	Rhodopsin
UAS	upstream activating sequence
US	unconditioned stimulus
UV	ultraviolet

Zusammenfassung

Mit Fokus auf das visuelle System von Fliegen behandle ich in meiner Dissertation die Identität und Funktion von Neuronen, welche zwei fundamentale Verarbeitungsschritte ausführen, die für das Überleben der meisten Tiere notwendig sind. Zum einen sind dies dem Farbensehen zugrunde liegende Neuronen und zum anderen solche, die essentiel für visuelles Gedächtnis sind.

Allgemein wird angenommen, dass Farbensehen auf Photorezeptoren mit Sensitivitäten für schmale Spektralbereiche aufbaut. Im Ommatidium von *Drosophila* exprimieren die sogenannten inneren Photorezeptoren verschiedene spektral schmalbandige Opsine. Im Gegensatz dazu haben die äußeren Photorezeptoren eine breitbandige spektrale Sensitivität und man nimmt an, dass diese ausschließlich achromatisches Sehen ermöglichen. Mit Hilfe von computergestützten Modellen und Verhaltensexperimenten zeige ich hier, dass die breitbandigen äußeren Photorezeptoren zum Farbensehen in *Drosophila* beitragen. Ein Modell mit opponenter Verarbeitung von Photorezeptorsignalen, welches das Opsin der äußeren Photorezeptoren beinhaltet, passt am besten zum spektralen Unterscheidungsverhalten von Fliegen. Um experimentell den Beitrag der einzelnen Photorezeptortypen zu ermitteln verwendete ich blinde Fliegen mit einem Defekt in der Phototransduktion (*norpA*$^{-}$) und rettete die *norpA* Funktion gezielt in einzelnen oder verschiedenen Kombinationen von Photorezeptortypen mit Hilfe des GAL4/UAS Genexpressionssystems. Erstaunlicherweise können dichromatische Fliegen mit nur äußeren Photorezeptoren und einem weiteren Rezeptortyp Farben unterscheiden, was auf die Existenz eines spezifischen Vergleichs der Signale von äußeren und inneren Photorezeptoren hindeutet. Außerdem beeinträchtigt der Block von Interneuronen, welche postsynaptisch von den äußeren Photorezeptoren sind, spezifisch das Farbensehen aber nicht die Intensitätsunterscheidung. Diese Ergebnisse zeigen zum einen, dass die äußeren Photorezeptoren mit einer komplexen und breitbandigen spektralen Sensitivität zum Farbensehen beitragen und zum anderen, dass chromatische und achromatische neuronale Netzwerke in der Fliege gemeinsame Photorezeptoren teilen.

Höher geordnete Gehirnbereiche integrieren sensorische Information verschiedener Modalitäten insbesondere visueller Natur und assoziieren deren neuronale Representation mit guten und schlechten Erfahrungen. Es ist jedoch unklar, wie unterschiedliche sensorische Gedächtnisse im Gehirn von *Drosophila* verarbeitet werden. Außerdem ist das neuronale Netzwerk, welches Farb- und Intensitätsgedächtnis zugrunde liegt völlig unbekannt. Um diese

Fragen zu beantworten etablierte ich appetitive und aversive Verhaltensassays für *Drosophila*. Diese erlauben die Gegenüberstellung von appetitivem und aversivem visuellen Gedächtnis unter Verwendung von neurogenetischen Methoden zur Netzwerkanalyse. Desweiteren sind die visuellen Verhaltensassays sehr ähnlich zu den verbreiteten olfaktorischen Lernsassays, da diese verstärkende Stimuli (Zuckerbelohnung und Elektroschockbestrafung), Konditionierungsablauf und Methoden zur Gedächtnismessung gemein haben. Dadurch wird ein direkter Vergleich der zellulären Grundlagen von visuellem und olfaktorischem Gedächtnis möglich. Ich fand, dass die gleichen Gruppen von Dopaminneuronen, welche den Pilzkörper innervieren, sowohl notwendig als auch ausreichend für die Bildung beider sensorischer Gedächtnisse sind. Außerdem ist die Expression des D1-ähnlichen Dopaminrezeptors (DopR) im Pilzkörper ausreichend um den Gedächtnisdefekt einer DopR Nullmutante (*dumb*$^{-}$) zu retten. Diese Ergebnisse sowie die Notwendigkeit des Pilzkörpers für visuelles Gedächtnis in dem benutzen Assay deuten darauf hin, dass der Pilzkörper ein Konvergenzareal ist, in welchem Repräsentationen von verschiedenen sensorischen Modalitäten assoziativer Modulation unterliegen.

Schlagwörter:

Klassische Konditionierung, Lernen, Gedächtnis, Farbensehen, Retina, Photorezeptor, Lamina, Dopamin, Belohnung, Bestrafung, Pilzkörper

Summary

Focusing at the fly visual system I am addressing the identity and function of neurons accomplishing two fundamental processing steps required for survival of most animals: neurons of peripheral circuits underlying colour vision as well neurons of higher order circuits underlying visual memory.

Colour vision is commonly assumed to rely on photoreceptors tuned to narrow spectral ranges. In the ommatidium of *Drosophila*, the four types of so-called inner photoreceptors express different narrow-band opsins. In contrast, the outer photoreceptors have a broadband spectral sensitivity and are thought to exclusively mediate achromatic vision. Using computational models and behavioural experiments, I here demonstrate that the broadband outer photoreceptors contribute to colour vision in *Drosophila*. A model of opponent processing that includes the opsin of the outer photoreceptors scores the best fit to wavelength discrimination behaviour of flies. To experimentally uncover the contribution of individual photoreceptor types, I used blind flies with disrupted phototransduction (*norpA*$^{-}$) and rescued *norpA* function in genetically targeted photoreceptors and receptor combinations. Surprisingly, dichromatic flies with only broadband photoreceptors and one additional receptor type can discriminate different colours, indicating the existence of a specific output comparison of outer and inner photoreceptors. Furthermore, blocking interneurons postsynaptic to the outer photoreceptors specifically impairs colour but not intensity discrimination. These findings show that outer receptors with a complex and broad spectral sensitivity do contribute to colour vision and reveal that chromatic and achromatic circuits in the fly share common photoreceptors.

Higher brain areas integrate sensory input from different modalities including vision and associate these neural representations with good or bad experiences. It is unclear, however, how distinct sensory memories are processed in the *Drosophila* brain. Furthermore, the neural circuit underlying colour/intensity memory in *Drosophila* remained so far unknown. In order to address these questions, I established appetitive and aversive visual learning assays for *Drosophila*. These allow contrasting appetitive and aversive visual memories using neurogenetic methods for circuit analysis. Furthermore, the visual assays are similar to the widely used olfactory learning assays and share reinforcing stimuli (sugar reward and electric shock punishment), conditioning regimes and methods for memory assessment. Thus, a direct comparison of the cellular requirements for visual and olfactory memories becomes feasible. I found that the same subsets of dopamine neurons innervating

the mushroom body are necessary and sufficient for formation of both sensory memories. Furthermore, expression of D1-like Dopamine Receptor (DopR) in the mushroom body is sufficient to restore the memory defect of a DopR null mutant (*dumb*$^{-}$). These findings and the requirement of the mushroom body for visual memory in the used assay suggest that the mushroom body is a site of convergence, where representations of different sensory modalities may undergo associative modulation.

Keywords:

Classical Conditioning, Learning, Memory, Colour Vision, Retina, Photoreceptor, Lamina, Dopamine, Reinforcement, Mushroom Body

1. Introduction

Visual systems in animals have evolved to allow processing of different parameters of visual stimuli, leading to diverse visual behaviours. Intensity differences can lead for example to simple phototactic behaviour (Lubbock, 1888) or the preference of a shape or an object (Liu et al., 2006). Stimuli that move across the retina can for example allow course control (Bahl et al., 2013) or identification of moving objects (Zhang et al., 2012). The spectral composition of light can be perceived as colour, allowing to discriminate an object of interest from others (Menzel and Backhaus, 1989), or can induce spectral specific behaviour (Gao et al., 2008). Colour vision, i.e. discrimination of spectrally different stimuli irrespective of their intensity (see also 1.2.1), is widespread throughout the animal kingdom and the underlying systems are diverse. It requires the existence of at least two photoreceptor types with different spectral sensitivities, whose responses must be compared (Rushton, 1972). Most mammals use two photoreceptor types for colour vision and are therefore dichromates (Kelber et al., 2003), while e.g. humans are trichromates based on their colour vision with three cone photoreceptor types (Gegenfurtner and Kiper, 2003). Invertebrates show a high diversity with e.g. honeybee *Apis mellifera* being trichromate (Menzel and Backhaus, 1989), monarch butterfly *Papilio xuthus* being tetrachromate (Koshitaka et al., 2008), and in some cases very complex systems like being found in mantis shrimp species with 12 types of photoreceptors of different spectral sensitivity (Cronin and Marshall, 1989). Colour information allows an animal to identify food sources like a flower with nectar or a fruit that stands out from the bland background vegetation. It also can allow an animal to avoid toxic prey/food like yellow jacket wasps or fly amanita with their warning pattern which signals the existence of a poisonous defensive mechanism. Furthermore, it may be useful to discriminate conspecifics from related species or to identify whether a conspecific is ready to mate. All these examples show that organisms derive extremely useful information from being able to discriminate colours and to associate them with important events.

The first concepts in colour vision were mostly derived from human perception and psychophysics. Back in the 19th century, several models related human colour discrimination to underlying receptor responses and mechanisms (Von Helmholtz, 1866; Hering, 1878; Maxwell, 1860). Today, photoreceptor spectral sensitivities have been directly measured, retinal ganglion cells with spatial colour opponency mechanisms have been identified, and several neural mechanisms underlying colour coding from the retina to higher brain regions have been studied (Gegenfurtner and Kiper, 2003).

Many studies demonstrated the existence of colour vision in diverse animals (Kelber et al., 2003). Although, there was important work on honeybees (Daumer, 1956; Frisch, 1914; von Helversen, 1972; Menzel and Backhaus, 1989) (see also 1.2.2), most studies that went beyond this level were from mammals. In my thesis, I aimed at the questions how colours are processed and memorized in a less complex nervous system using the fruit fly *Drosophila melanogaster*. For the study of the neural mechanisms underlying the diverse processing of visual stimuli, the fruit fly *Drosophila melanogaster* with the broad spectrum of genetic techniques available, has been shown to be a powerful model organism (Borst, 2009) (see also 1.4). The genetic manipulation of neural networks in the behaving animal allows drawing causal relationships between anatomy and function. To this extend, this is (yet) only possible in the fruit fly or the nematode *Caenorhabditis elegans* (Xu and Kim, 2011). Furthermore, in the last decades, the anatomical knowledge and the genetic accessibility to the visual system of the fly, has increased significantly (Fischbach and Dittrich, 1989; Morante and Desplan, 2008; Takemura et al., 2013, 2008) (see also 1.1). That *Drosophila* can discriminate colours irrespective of their brightness has been shown in classical conditioning experiments (Menne and Spatz, 1977), though the neural mechanisms underlying this behaviour have so far been elusive (see also 1.2.3).

This thesis is concerned with dissecting (1) the peripheral neural networks underlying true colour discrimination in *Drosophila* and (2) the neural networks allowing the fly to associate colours with sugar reward or electric shock punishment by combining behavioural analysis and genetic manipulation of neurons. Although the five photoreceptor types have been identified decades ago (Hardie, 1985), which of the five photoreceptor types contribute to colour vision has not been conclusively established (Bicker and Reichert, 1978; Fukushi, 1994; Troje, 1993). To this regard, I focused on whether signals from the broadband photoreceptors and their postsynaptic neurons are used in *Drosophila* to derive information on the wavelength composition of a visual stimulus (1). Using the same behavioural assay, I also aimed at identifying neural circuits underlying colour/intensity memory formation (2). For that, I focused on the identification of reinforcement signalling neurons underlying visual memory in flies, which have so far been unknown. Due to the shared parameters of the here presented visual and previously used olfactory assays, this work furthermore allows a direct comparison of neural circuits underlying memories of both modalities.

The results presented in this thesis have recently been published or submitted to a scientific journal (Schnaitmann et al., 2013; Vogt and Schnaitmann et al., submitted).

1.1 The visual system of *Drosophila*

1.1.1 The retina

The compound eye of *Drosophila melanogaster* consists of ~750 ommatidia, each equipped with an optical apparatus, and eight photoreceptor cells named R1 to R8 which are surrounded by pigment cells (Figure 1A, B; reviewed in Hardie, 1985). R1–R6, which are positioned around R7/8 and are therefore called the 'outer photoreceptors', extend the full depth of the retina. In contrast, R7 and R8 are restricted to the upper and lower halves of each ommatidium, respectively (Figure 1B, C; reviewed in Hardie, 1985). Photons are absorbed by Rhodopsins (i.e. opsin protein + 3-hydroxy-11-*cis*-retinal as chromophore) at a specific layered structure of photoreceptor cells arranged at the central axis of an ommatidium (Vogt and Kirschfeld, 1984). In these so called rhabdomeres, a G-protein dependent signalling cascade is triggered by the absorption of light, leading to the opening of ion channels and subsequent membrane depolarization (see 1.1.2).

R1–R8 altogether cover a wide spectral sensitivity range (ca. 300 to 600 nm) with five different types of photoreceptors expressing different Rhosopsins (Figure 2). The 'outer photoreceptors' (R1–R6) express the 'cyan'-sensitive Rhodopsin 1 and contain an additional UV–sensitizing pigment which renders those cells light-sensitive over a broad spectral range (Hardie, 1985; Salcedo et al., 1999) (Figure 2). R1–R6 of one ommatidium have slightly divergent optical axes and therefore sample different points in space. The R1–R6 photoreceptors mediate motion detection as well as phototaxis (a behaviour in which the fly moves toward a light or chooses between two lights) while its role in colour discrimination is controversial (Bicker and Reichert, 1978; Fukushi, 1994; Troje, 1993) (see also 1.2.3). These cells project exclusively to the lamina, the first neuropil of the optic lobe.

The R7 and R8 ''inner photoreceptors'' contain four different types of rhodopsin (Rh3–Rh6) and terminate exclusively in the medulla, the second neuropil of the optic lobe (Figure 1C; Fischbach and Dittrich, 1989; Salcedo et al., 1999). Based on the combination of rhodopsins in R7/8, the photoreceptors can be differentiated into two main ommatidial classes (named pale (p) and yellow (y) after fluorescence characteristics) that are distributed stochastically in the main part of the retina. R7 photoreceptors express one of two UV-sensitive opsins, Rh3 (p) (shorter wavelength) or Rh4 (y) (longer wavelength), whereas R8 photoreceptors express either the 'blue'-sensitive opsin Rh5 (p) or the 'green'-sensitive opsin Rh6 (y) (Figure 1C; Rister et al., 2013). R7/8 are thought to mediate colour

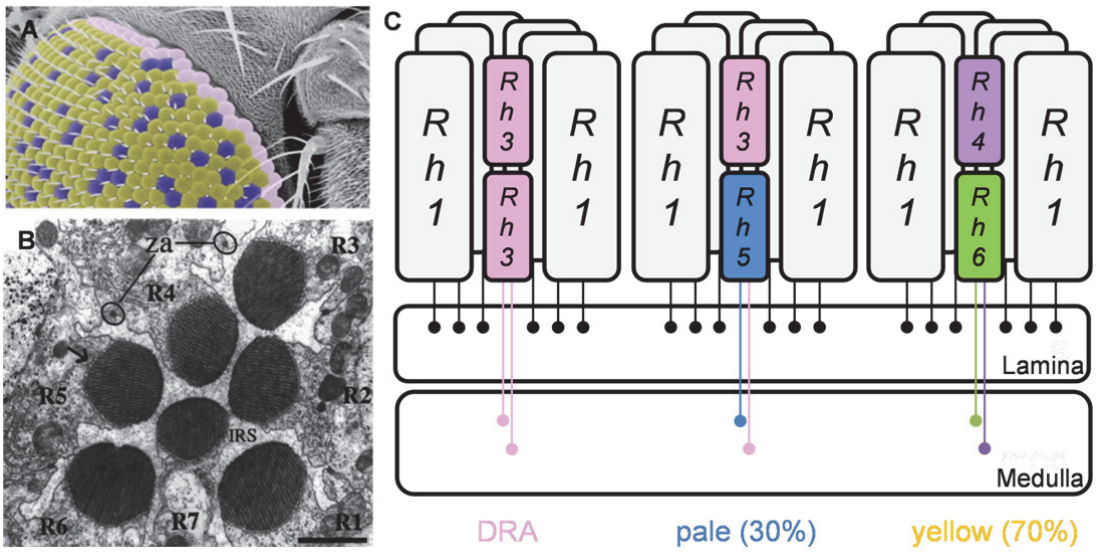

Figure 1 – The retina of *Drosophila melanogaster.* (**A**) Three types of ommatidia are to be discerned: pale (violet), yellow (yellow), and DRA (pink), the latter constituting only a single row in the dorsal part of the eye. Pale and yellow ommatidia account for 30 % and 70 % of the ommatidia, respectively, and are randomly distributed in the retina (adapted from Wernet et al., 2007). (**B**) In the horizontal section of an ommatidium, one can see that the rhabdomeres of six outer photoreceptors R1–R6 surround an inner photoreceptor rhabdomere (at this depth R7). The eighth photoreceptor R8 is found below (more proximally than) R7 (adapted from Kumar and Ready, 1995). (**C**) R1–R6 all express Rh1 rhodopsin and terminate in the lamina. The R7 and R8 inner photoreceptors typically express one out of four different types of rhodopsin (Rh3–Rh6) and terminate exclusively in the medulla. DRA ommatidia represent an exception as in both R7 and R8 the short UV-sensitive opsin Rh3 is expressed. Pale R7 and R8 photoreceptors express the short UV-sensitive opsin Rh3 and the 'blue'-sensitive opsin Rh5, respectively. Long UV-sensitive opsin Rh4 and the 'green'-sensitive opsin Rh6 are expressed in R7 and R8 of yellow type ommatidia, respectively.

vision, as they express spectrally different rhodopsins, and were shown to contribute to phototaxis (Harris et al., 1976; Yamaguchi et al., 2010). A recent study showed evidence that R7/8 in addition feed into the motion vision circuit, probably via electrical synapses between R7/8 and R1–R6, the latter being absolutely required (Wardill et al., 2012). A third type of ommatidia is found in the dorsal part of the eye. In the two most dorsal ommatidial rows, R7 and R8 both express Rh3. These ommatidia were shown to be specialized to detect the oscillation plane of polarized skylight (Labhart and Meyer, 1999).

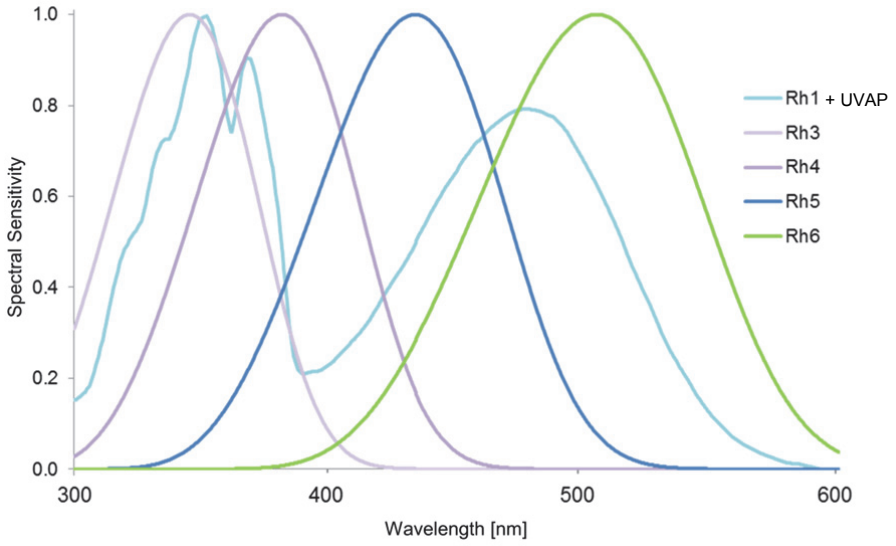

Figure 2 – Normalized spectral sensitivities of the five different Rhodopsins in the *Drosophila* eye. In R1–R6, Rh1 alone is maximally sensitive at 478 nm while an accessory pigment (UVAP) underlies their additional UV sensitivity. The maximal sensitivities of Rh3–6: 345 nm (Rh3), 375 nm (Rh4), 437 nm (Rh5), and 508 nm (Rh6) (adapted from Salcedo et al., 1999).

1.1.2 Phototransduction in *Drosophila*

Visual transduction is initiated by light-induced conversion of the 3-hydroxy-11-cis-retinal containing photopigment rhodopsin to metarhodopsin which then interacts with a heterotrimeric GTP-binding protein (G protein) (Figure 3). This heterotrimeric G protein (Gq) subsequently interacts with a phospholipase C (PLC; encoded by the gene *norpA*), which catalyses the conversion of phosphatidylinositol-4,5-bisphosphate (PIP2) to inositol-1,3,5-trisphosphate (IP3) and diacylglycerol (DAG) (Figure 3; Bloomquist et al., 1988; Devary et al., 1987; Lee et al., 1994; Scott et al., 1995). This step is critical for the phototransduction pathway, flies lacking functional *norpA* alleles being blind (Inoue et al., 1985). Activation of PLC leads to opening of cation influx channels *trp*, and *trpl* and thereby to the depolarisation of the photoreceptor cell (Figure 3; Hardie, 1991; Hardie and Minke, 1992; Ranganathan et al., 1991). A recent study suggested that excitation of *Drosophila* photoreceptors may be mediated by PLC's dual action of phosphoinositide depletion and proton release (Huang et al., 2010). The authors showed that following depletion of phosphoinositides, the light sensitive channels in *Drosophila* photoreceptors became remarkably sensitive to pH changes, that light

induces a rapid acidification in the microvilli, which is eliminated in mutants of PLC, and that TRPL channels are activated by acidification (Huang et al., 2010). Another recent study suggests that by cleaving PIP2, PLC generates rapid physical changes in the lipid bilayer that lead to contractions of the microvilli, and suggest that the resultant mechanical forces contribute to gating the light-sensitive channels (Hardie and Franze, 2012).

Following the activation of the signalling cascade, the system must be reset to be able to respond to subsequent stimulation. Deactivation of the *Drosophila* photoreceptor response is quite rapid and occurs within about 100 ms of cessation of the light stimulus (Hardie, 1991; Ranganathan et al., 1991). After exposure to light, the chromophore in *Drosophila* photoreceptor cells does not dissociate from the opsin (Hardie, 1985). For regenerating rhodopsin, the metarhodopsin requires absorption of a second photon. To inactivate metarhodopsin, however, it is bound by arrestin *arr2*, which also contributes to long-term adaptation (Arshavsky, 2003). Ca^{2+}/Calmodulin play an important role in response termination as they attenuate the activities of rhodopsin, PLC, and both groups of ion channels (Montell, 1999). Additionally, an eye specific Ca^{2+}-dependent protein kinase C ePKC (coded by *inaC*) phosphorylates TRP channels, thereby causing inactivation (Popescu et al., 2006). ePKC is also required for adaptation over a wide range of light intensities (Hardie et al., 1993).

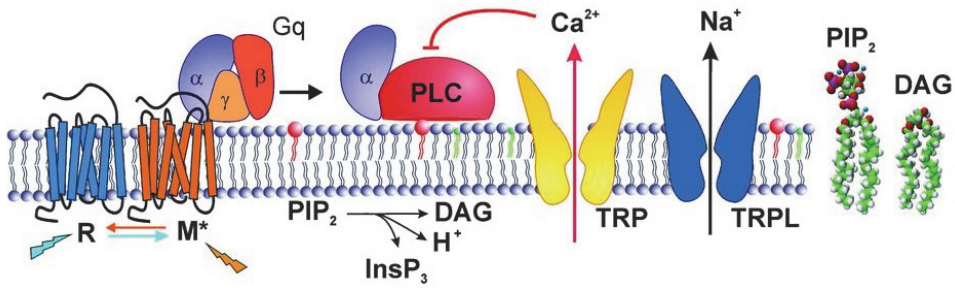

Figure 3 – Phototransduction in *Drosophila.* The light-activated metarhodopsin catalyzes release of the Gq protein α subunit to activate PLC. PLC hydrolyzes PIP_2 (red), leading to the production of IP3 and DAG. The depletion of PIP2 together with protons released by PIP2 hydrolysis were shown to potently activate the light-sensitive channels. Ca^{2+}-influx via TRP channels inhibits PLC (adapted from Hardie and Franze, 2012).

1.1.3 The optic lobe neuropil

The Lamina: The lamina neuropil has been studied extensively on the light and electron microscopic level. It contains 15 cell types, i.e. three photoreceptor types (R1–R6, R7, R8), five monopolar cell types (L1–L5), three types of medulla cells (C2, C3, T1), and the wide field tangential and amacrine cells (Figure 4A; Fischbach and Dittrich, 1989; Takemura et al., 2008). These cells are organized in so-called lamina cartridges, surrounded by glia cells (Figure 4B–C; Braitenberg, 1967). All monopolar cells and T1 project retinotopically to the medulla but arborize in different layers (Figure 4A; Fischbach and Dittrich, 1989; Takemura et al., 2008).

R1–R6 photoreceptors with parallel optical axes sampling the same point in space converge in a single lamina cartridge. This wiring principle is called neuronal superposition (Braitenberg, 1967; Kirschfeld, 1967) and causes an improvement of the signal to noise ratio by a factor of √6 (Scholes, 1969). This is due to the increased photon catch without impairment of visual acuity or resolution (Land, 1997).

The synaptic connections between the lamina cell types both at the level of the lamina and medulla are known. L1, L2, L3, and the amacrine cells (amc) receive input from R1–R6 (Hardie, 1989; Pollack and Hofbauer, 1991). L2 innervates, and reciprocally receives input from L4 cells, of its own and adjacent cartridges (Meinertzhagen and O'neil, 1991). Furthermore, L2 feeds back to R1–R6 and is electrically coupled to L1 at the medulla level (Joesch et al., 2010; Meinertzhagen and O'neil, 1991). The terminal of L5 reciprocally connects to that of L1, thus being synaptic in the medulla despite lacking synapses in the lamina (Takemura et al., 2008). The amc provides the only lamina input to the second-order interneuron T1 and probably feeds back to R1–R6 (Meinertzhagen and O'neil, 1991). The centrifugal cells C2 and C3 have connections both with L1 and L2 in the medulla (Takemura et al., 2008). R7/8 bypass the cartridge though a recent study shows evidence for functional electric connections between R7/8 and R1–R6 (Wardill et al., 2012).

Intracellular recordings from L1 and L2 revealed a strong high-pass filtering and an inversion of the signals in the lamina monopolar cells provided by R1–R6 (Järvilehto and Zettler, 1971; Straka and Ammermüller, 1991). Pharmacological studies identified histamine as the neurotransmitter of photoreceptors. Illumination of the photoreceptors causes a transient hyperpolarization of the lamina cells via the histamine receptor and chloride channel Ort (Hardie, 1989).

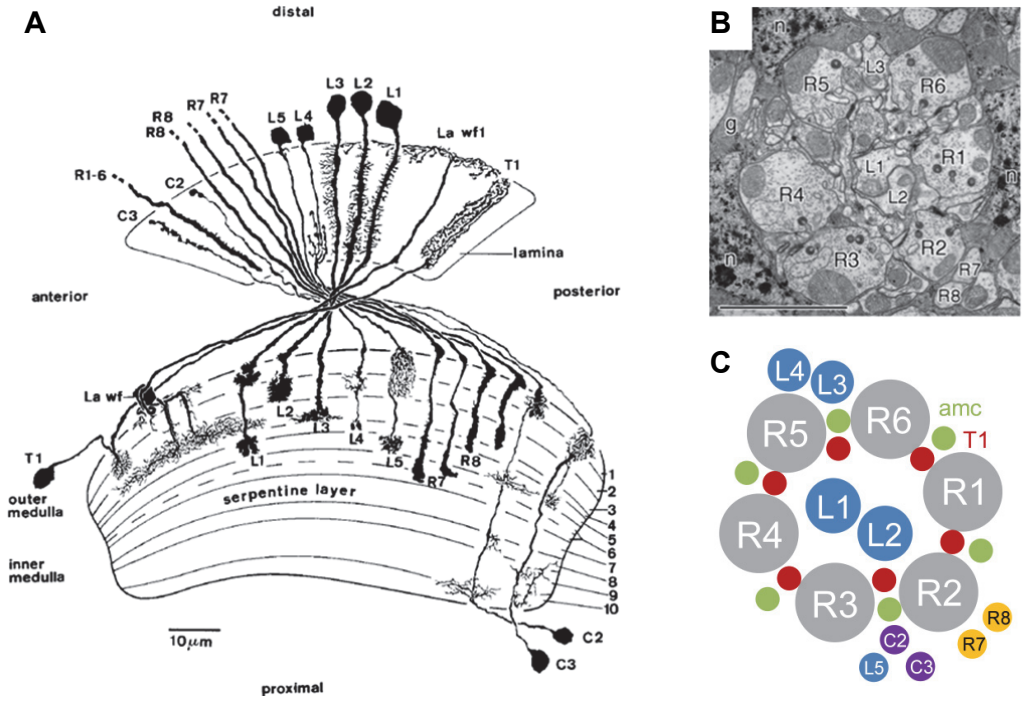

Figure 4 – Neuronal cell types of the lamina and anatomy of the lamina cartridge. (**A**) Anatomical reconstructions of retina and lamina cell types from Golgi stainings in *Drosophila*. The lamina contains five different lamina monopolar cell types (LMCs) L1–L5, which all project to the medulla. Furthermore, amacrine cells (amc), and centrifugal T1, Lamina widefield (Lawf), C2, and C3 are innervating the lamina neuropil. R1–R6 project to the lamina, while R7/8 bypass the lamina and project directly to the medulla (from Fischbach and Dittrich, 1989). (**B**) Electron microscopical (modified from Stuart et al., 2007) and (**C**) schematic cross-section through a lamina cartridge. L1 and L2 are located in the center of the cartridge, forming many synaptic connections with R1–R6. L3, and amc processes also receive direct R1–R6 input. L4, L5 and T1 are second-order interneurons.

As previously described, information from R1–R6 is projected onto four different cell types, which might result in four retinotopically organized, parallel pathways. Functionally, L1 and L2 were shown to be required and sufficient for motion vision (Katsov and Clandinin, 2008; Rister et al., 2007), L1 and L2 mediating the detection of ON-edges and OFF-edges, respectively (Joesch et al., 2010). This functional difference is reflected by their anatomical differences, L1 innervating a different layer in the medulla than L2. Also L2 but not L1 contacts L4. As L4 cells are feeding back via two backward oriented collaterals onto L2 in adjacent cartridges, one can describe the L2/L4 network as a horizontal network of lateral connections (Braitenberg, 1970; Braitenberg and Debbage, 1974; Meinertzhagen and O'neil,

1991; Strausfeld and Braitenberg, 1970). It is thought that such a network might mediate the detection of front-to-back motion (Takemura et al., 2011), though it was recently found that L4 is required for OFF motion processing in all cardinal directions (Meier et al., 2014). A function of L3 has only recently been identified. It is mediating a response to slow motion stimuli (Tuthill et al., 2013), and together with L1, it is required for dark-edge motion detection (Silies et al., 2013). Furthermore, it is speculated that L3 plays a role in colour vision, as it projects to cells in the medulla that are postsynaptic to R7/8 (Bausenwein et al., 1992; Gao et al., 2008; Strausfeld and Lee, 1991). Consistently, L3 has significantly less synaptic connections with R1–R6 than L1 and L2 (Meinertzhagen and Sorra, 2001), and it is speculated to have a higher response threshold for light intensity (Anderson and Laughlin, 2000), possibly in the range of R7/8. The function of L5 is still unknown, though its connection with L1 suggests a role in motion vision. The amc is thought to provide feedback to R1–R6 (Meinertzhagen and O'neil, 1991), suggesting that the amc/T1 pathway could be involved in lateral inhibition or adaptation (Järvilehto and Zettler, 1971).

The Medulla: Similar to the lamina, the medulla neuropil exhibits a retinotopic, columnar organization. In addition to the terminals of lamina neurons, each medulla column contains about 60 different neurons (Fischbach and Dittrich, 1989; Takemura et al., 2013). Each column can be divided into ten layers, M1–M10 (Figure 5). There are 26 types of transmedullary (Tm) cells; 12 medulla intrinsic (Mi) neurons; 13 TmY cells; and 8 distal medulla (Dm) cells (Fischbach and Dittrich, 1989). Tm cells connect the medulla and the lobula neuropils, whereas TmY bifurcate in the chiasm between the medulla and the lobula plate, and thus connect the medulla to both these neuropils (Figure 5; Fischbach and Dittrich, 1989). In addition to columnar neurons, many neurons in the medulla have been described, which extend their ramifications horizontally over different columns (Fischbach and Dittrich, 1989; Takemura et al., 2013). A detailed description of the synaptic connections between the diverse medulla neurons based on reconstructions of electron mircoscopical data has been recently published (Takemura et al., 2013).

The medulla is the first neuropil that might harbour a colour-coding neural circuit because it receives input from spectrally different channels (R7/8) and the lamina which conveys the R1–R6 signals. Many cell types have been identified in the *Drosophila* medulla that receive input from different photoreceptor types and thus are candidate colour-coding cells (Gao et al., 2008; Takemura et al., 2013). One can speculate that the Tm9 and Tm5 neurons function as colour-opponent neurons by computing the synaptic input signals that are

provided by L3 and R7/R8 (see also 1.2.1). Recently, it was shown that a multi-columnar neuron called Dm8, which collects R7- and therefore UV input, is required for phototaxis towards UV (Gao et al., 2008).

Based on anatomical studies of the medulla and lobula complex (Bausenwein et al., 1992), two parallel motion detection pathways were proposed; the L1 pathway, involving L1, Mi1, and T4 cells, and the L2 pathway, involving L2, Tm1 and T5 cells. Using 2-deoxyglucose labelling in flies perceiving motion stimuli, this model was supported (Buchner et al., 1984). Recently, two studies showed strong evidence for the existence of the proposed pathways (Maisak et al., 2013; Takemura et al., 2013). Mi1 and Tm3 were shown to be the input to four different T4 cell types with different dendritic orientations (Takemura et al., 2013). The assumed receptive fields of the Tm3 and Mi1 input to a respective T4 cell were shown to be slightly shifted (Takemura et al., 2013). Thus, these cells are strong candidates for providing the input to an elementary motion detector (Hassenstein and Reichardt, 1956). That T4 and T5 cells are indeed motion selective has been shown in functional Ca^{2+}-imaging experiments (Maisak et al., 2013). The four different types of T4 and T5 cells are

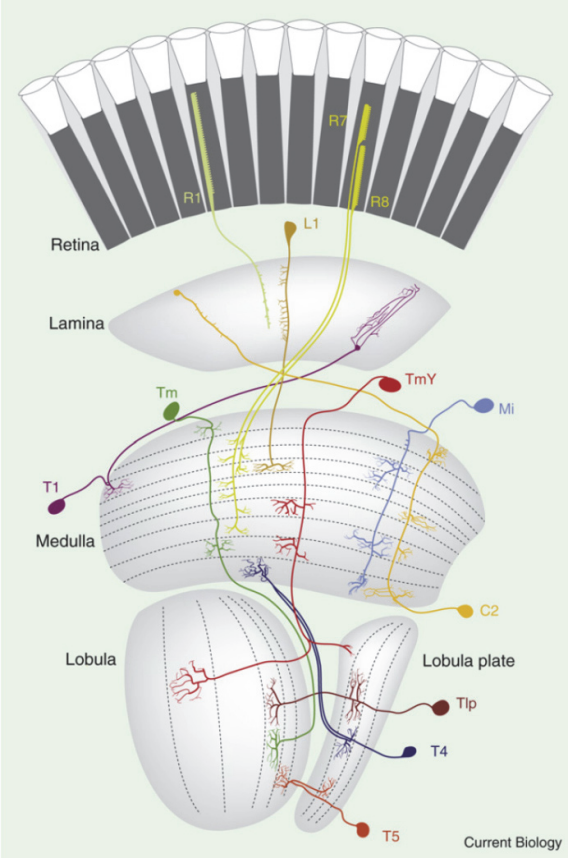

Figure 5 – Columnar cell types in the fly visual ganglia. Each column in the medulla harbours about 60 different neurons. A few columnar cell types are depicted on the left. Transmedulla neurons (Tm) connect the medulla with the lobula. Transmedulla neurons Y neurons connect medulla, lobula, and lobula plate. Mi neurons are medulla intrinsic and connect different medulla layers. Translobulaplate neurons (Tlp) connect lobula plate and lobula. T cells project from either the medulla or the lobula to the lobula plate, with their cell bodies located posterior to the lobula complex. (From Borst, 2009; modified from Fischbach and Dittrich, 1989).

directionally tuned to one of the four cardinal directions. Depending on their preferred direction, T4 and T5 cells terminate in specific sublayers of the lobula plate. Additionally, T4 and T5 functionally segregate with respect to contrast polarity: T4 cells selectively respond to moving brightness increments (ON edges), while T5 cells only respond to moving brightness decrements (OFF edges). Together, they provide a biologically plausible hardware for the sign-correct multiplication of positive and negative input signals (Egelhaaf and Borst, 1992; Eichner et al., 2011)

The Lobula complex: The third order neuropil, the lobula complex, is divided into two parts, the lobula and the lobula plate. The lobula, which consists of six layers with many columnar and non-columnar cell types being identified in Golgi stainings (Fischbach and Dittrich, 1989) or GAL4 line screen (Otsuna and Ito, 2006), has seen only little attention in functional studies so far (Mu et al., 2012; Zhang et al., 2013). It is suggested to contain both motion and colour sensitive neurons (Bausenwein et al., 1992; Buchner et al., 1984). In contrast, the lobula plate which has four layers has been extensively studied (Borst and Haag, 2002). Based on 2-deoxyglucose labelling in *Drosophila*, each layer is sensitive to a different motion direction of a moving stimulus (Bausenwein et al., 1992; Buchner et al., 1984; Maisak et al., 2013). In the lobula plate, giant neurons, called 'lobula plate tangential cells' are found, spanning a large area or even the whole neuropil (Egelhaaf et al., 1989; Single and Borst, 1998; Spalthoff et al., 2010). These cells have been identified and studied electro- and optophysiologically in many fly species including *Drosophila*, and were shown to be motion sensitive (Hausen, 1984; Joesch et al., 2010; Maisak et al., 2013). According to their sensitivity to horizontal or vertical motion stimuli, they can be grouped into various classes, such as the horizontal system (HS-cells) and the vertical system (VS-cells) (Krapp and Hengstenberg, 1996; Krapp et al., 1998; Wertz et al., 2009). The main input to these types of cells is transmitted via motion sensitive T4 and T5 cells (Maisak et al., 2013; Schnell et al., 2012).

In the lobula and lobula plate, many columnar and non-columnar cell types project to diverse central brain regions or the contralateral optic lobe (Fischbach and Dittrich, 1989; Otsuna and Ito, 2006; Strausfeld, 1976). Lobula-specific visual projection neurons are associated with only three central brain regions: posteriorlateral protocerebrum, optic tubercle, and ventrolateral protocerebrum. Most of the pathways terminate in the ventrolateral protocerebrum. The projection patterns within this neuropil are significantly different between pathways and their terminals are confined within relatively small and discrete areas of the

central brain (Otsuna and Ito, 2006). For this reason, these subregions are comparable to the glomerular structure in the antennal lobe and are often referred to as optic foci or optic glomeruli (Mu et al., 2012; Otsuna and Ito, 2006; Strausfeld, 1976).

1.2 Colour vision in insects

1.2.1 Colour and brightness

Two monochromatic visual stimuli can differ in their wavelength as well as in their intensity. If an animal has colour vision, it can tell apart such stimuli based on their spectral properties irrespective of their intensity. This intensity independence should however not be taken too literally. If for example the lights are so dim they can barely be detected or extremely bright, vision in most animals becomes achromatic (Kelber and Lind, 2010). Thus, colour vision is usually only independent over a certain range of intermediate intensities.

The term 'colour' refers to the physiological sensation and perception of spectral properties of a visual stimulus, not to its physical wavelength composition. Colour vision provides information about surface reflectance, pigmentation and other material properties (Gegenfurtner and Kiper, 2003). It is therefore likely to be important for object classification and recognition. Two spectrally different stimuli can be perceived as the same 'colour', if they cause the same kind of excitation of the photoreceptors involved in colour vision. That is because the colour perceived is based on the ratio of excitation of the photoreceptor types, and if the ratio for two stimuli is the same, the perceived colour is same as well (Rushton, 1972). As a prerequisite for colour vision, the visual system of an organism must comprise at least two photoreceptor types with different spectral sensitivities whose output is put into relation by the neural network. That a single photoreceptor type is not sufficient for colour vision is stated by the principle of univariance (Rushton, 1972). To give one example: Let's assume a monochromatic stimulus $S\lambda_1$ has a wavelength that is the same as the wavelength for which a photoreceptor has maximal sensitivity. For another stimulus $S\lambda_2$ with twice the intensity of $S\lambda_1$ and with a wavelength for which the photoreceptor has 50 % sensitivity, the photoreceptor will show the same response as to $S\lambda_1$. Thus, intensity and spectral wavelength cannot be discriminated with a single photoreceptor type. The building block of intensity invariant colour coding is the so called colour opponency, a neural mechanism in which the output of at least two photoreceptor types is compared by subtracting from each other (Figure 6; Gegenfurtner and Kiper, 2003). Colour opponent cells that receive antagonistic input from

two (or more) photoreceptor types, respectively, become excited by one photoreceptor type and inhibited by the other (Figure 6; Gegenfurtner and Kiper, 2003). This computation underlies the neural representation of spectral differences, such cell being able to code for the difference in excitation of two photoreceptor types and therefore for two wavelength ranges.

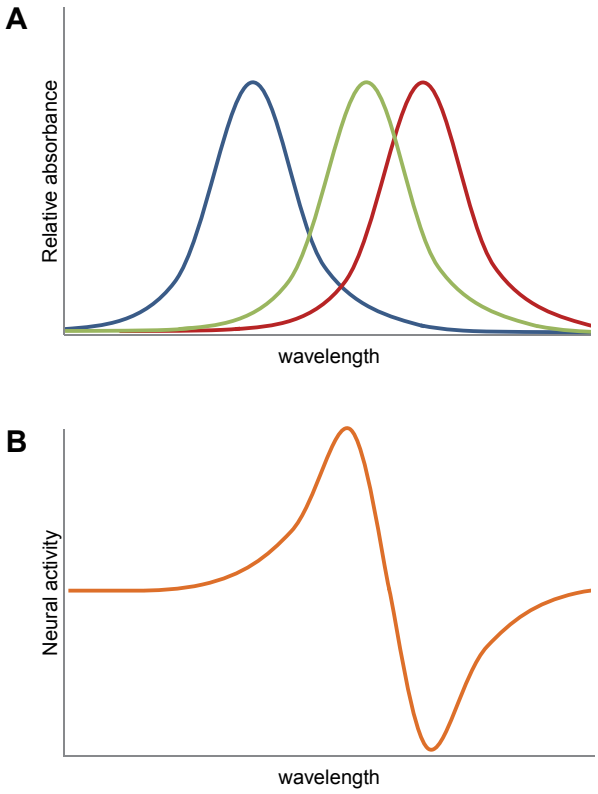

Figure 6 – Colour opponency. (**A**) Spectral sensitivities of three putative Rhodopsins which are expressed in different photoreceptor types ('blue', 'green', 'red') in an animal. All photoreceptors respond to light over a broad wavelength range and cannot code for spectral information due to the principle of univariance (Rushton, 1972). (**B**) Spectral information can only be gained by comparing the photoreceptor output of different photoreceptor types. Neural activity of a putative colour opponent cell which gets antagonistic input from the 'green' and 'red' photoreceptor types is shown. This cell shows increased neural activity for short and medium wavelength stimuli and reduced activity for long wavelength stimuli, irrespective of the stimulus intensity.

'Brightness' refers to the physiological sensation and perception of the intensity of a visual stimulus, not to its physical quantity. It is virtually the complementary information to 'colour', and is based on the weighted sum of photoreceptor excitations (Gegenfurtner and

Kiper, 2003). In addition to brightness as an object property, such achromatic summation is used by the brain to process motion, form and texture (Osorio and Vorobyev, 2005).

How to untangle colour and brightness in a behavioural experiment? Best would be to use stimuli that differ in wavelength but share the same subjective brightness for an animal. But the identification of such isoluminant stimuli in animals is difficult. Importantly, every visual subsystem underlying a specific visual behaviour may have a different sensitivity function (Harris et al., 1976; Heisenberg and Buchner, 1977). This becomes apparent if one compares the spectral sensitivity functions of the optomotor response and phototaxis of *Drosophila*, which clearly differ (Harris et al., 1976; Heisenberg and Buchner, 1977). Therefore, calibrating the intensities of visual stimuli using a specific visual behaviour and assuming these apply to another one as well may be problematic (Hernández de Salomon and Spatz, 1983). Also the method applied by von Helversen (von Helversen, 1972) in honeybees has to be critically reviewed, who determined isoluminant stimuli for each wavelength by adjusting the minimum intensity required to achieve a certain learning index. Though this approach determines isoluminance using the same task which is used for analysis of colour discrimination (associative conditioning), it has several pitfalls. First, it is only valid if the same photoreceptor types are both underlying intensity conditioning at intensity levels required to reach the learning index criterion and colour conditioning (usually higher intensities are used). Imagine for example a certain photoreceptor type is sensitive at low light intensities and sufficient for intensity conditioning, while other photoreceptor types are only sensitive at higher intensities (e.g. rods/cones in humans). The obtained isoluminance values would not reflect isoluminance under higher intensity levels. Second, if saliency does not only depend on intensity but also on the spectral properties of the stimulus, the obtained 'isoluminance' values would be false. Another approach was used by Fukushi (Fukushi, 1990), who calculated the subjective brightness of the different spectral stimuli used, based on the assumption that physiological responses from each receptor type are summed. He also weighed the outer photoreceptors R1–R6 by a factor of six because of the neural superposition (six cells feed into one lamina cartridge). Such calculations were not based on any behavioural data and a proof that subjective brightness can be calculated in such way has not been provided by the authors.

A potent approach to demonstrate intensity invariance of visual conditioning in particular, is to train animals with equal (or arbitrarily chosen) physical intensities. After training, intensities in nonreinforced tests have then to be varied over a broad range of intensities (Menne and Spatz, 1977 for *Drosophila*; Kelber and Pfaff, 1999 for the butterfly

Papilio aegeus; reviewed in Kelber et al., 2003). Such an approach, which is not based on any assumptions about the visual system, was also chosen in this study.

1.2.2 Colour vision in honey bees

In the following, I'll give a brief overview of colour vision research in the honey bee *Apis mellifera*. That is because it became one of the model organisms for colour vision from which we gained a lot insight into the underlying mechanisms in animals and particularly in insects.

Since Karl von Frisch's experiments in 1914 (Frisch, 1914) in which he demonstrated that bees are able to discriminate a blue stimulus from a series of differently intense grey stimuli, colour vision has been extensively studied in the honey bee using psychophysical, and electrophysiological experiments. For its study, the conditionable foraging behaviour has been a major advantage and allowed fast and reliable colour discrimination analyses. Daumer showed in colour mixing experiments, that the bee possesses trichromatic colour vision, similar to humans (Daumer, 1956). Daumer measured the proportions of complementary monochromatic lights that are necessary to produce metameric (physically different but indistinguishable) light mixtures. Furthermore, he found that bees ignore intensity differences over a wide range (Daumer, 1956).

In 1972, von Helversen deduced a spectral threshold function (discussed in 1.2.1) as well as a spectral discrimination function (von Helversen, 1972). Based on previous results (Daumer, 1956), intensity differences were thought to be ignored by the animals and intensities were chosen above the threshold function. He found that bees are able to discriminate wavelengths best around 490 nm (separated by 4.5 nm), and second best around 400 nm (separated by 7 nm) (Figure 7).

In animals, simultaneous colour contrast was first shown in the honey bee (Kühn, 1927). This phenomenon was quantified in a later study in which bees perceived blue on a yellow background as more blue (more saturated) than on a grey background and more yellow on a blue background than on a grey background (Neumeyer, 1980). That bees also show colour constancy was shown in colour discrimination tasks in which the background illumination was changed between training and test (Werner et al., 1988).

Intracellular recordings revealed that the honeybee eye is equipped with three classes of spectral receptors, as it has been previously suggested by behavioural results. They exhibit peak sensitivity in the ultraviolet (344 nm), blue (436 nm), and green (544 nm) wavelength range (Autrum and Zwehl, 1964; Menzel and Blakers, 1976; Menzel et al., 1986). In contrast

to *Drosophila*, each ommatidium in the honey bee contains nine photoreceptors instead of eight. The two central R7-like cells exhibit differential opsin expression ranging from UV to green sensitive opsins. As the central R8 cell homolog, the peripheral photoreceptor cell homologs R1–R6 express the green-opsin (Jackowska et al., 2007).

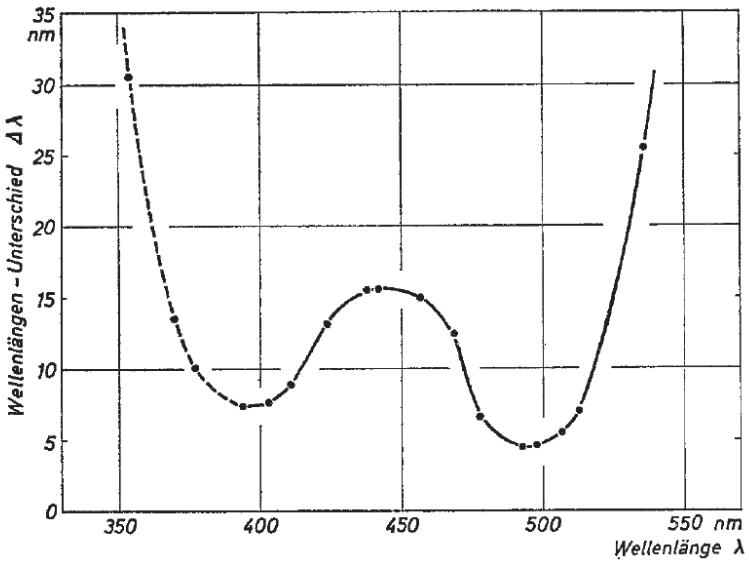

Figure 7 – Spectral discrimination function of the honey bee *Apis mellifera.* The function has two optima at about 400 nm and 490 nm, respectively (from von Helversen, 1972).

Performing intracellular recordings, Kien and Menzel (Kien and Menzel, 1977a, 1977b) found many different classes of neurons (tonic and phasic, broadband, narrow-band, different receptive fields) in the bee's visual system by measuring the cells' responses to monochromatic lights at different intensities. While some of these cells were labelled, the anatomy of most of the recorded cell types remained unknown. A few more studies described neuronal cell types and their response characteristics (broadband, narrow-band, colour opponent) in the optic lobes and the central brain of honey bee (Hertel, 1980; Yang et al., 2004) or bumblebee (Paulk et al., 2008, 2009a, 2009b). On the basis of two colour opponent types only, (type A: UV-/B+/G+ and UV+/B-/G-; type B: UV-/B+/G- and UV+/B-/G+), Backhaus (Backhaus, 1991) constructed a trichromatic colour opponent coding model that could explain the behavioural results obtained before (von Helversen, 1972).

While a considerable amount of knowledge has been accumulated about the colour vision system of the honeybee, the underlying neuronal circuitry is not well understood. This is because many cell types have been identified in physiological recordings but their anatomy and connectivity remained unknown. Therefore, the questions of neural mechanisms leading to opponent coding and the behavioural relevance of these cells remain mostly unanswered. Also the difficulty of specific interference in the nervous system of the honey bee and subsequent behavioural or physiological analysis will make it difficult to answer these questions. At this level, the potent tools for neural circuit analysis in *Drosophila* may be of advantage to address these questions (reviewed in Borst, 2009).

1.2.3 Colour vision in flies

The fly's visual system with five photoreceptor types that have different spectral sensitivities could theoretically allow fine colour discrimination over a broad range of wavelengths. Seminal behavioural studies aimed at the questions whether *Drosophila* possesses colour vision and which photoreceptor types are involved. Schuemperli found that at low light intensities, phototaxis solely depends on the photoreceptors R1–R6 while at higher light intensities, several photoreceptors contribute to phototaxis (Schümperli, 1973). By using mutants with defect photoreceptor types, Harris and colleagues showed that all photoreceptor types can contribute to phototaxis (Harris et al., 1976). A similar result was shown in a recent study that found that all photoreceptor types can contribute to spectral preference where flies choose between two spectrally different lights (Yamaguchi et al., 2010). This behaviour, which strongly depends on the intensity of the presented light stimuli, was shown to also depend on the spectral composition of light (Fischbach, 1979; Heisenberg and Buchner, 1977). The authors presented a green stimulus on one side and added in a series of experiments an increasing intensity of UV light to both sides. Interestingly, while flies in general prefer the UV stimulus with higher intensity (Jacob et al., 1977), flies chose from a certain UV intensity level on the side with pure UV and not the side with UV and green (Fischbach, 1979; Heisenberg and Buchner, 1977). It was therefore concluded that the fly possesses a 'UV-visible' spectral discrimination (visible refers to the spectrum of light that is visble to humans). Furthermore, Fischbach could demonstrate in successive colour contrast experiments that for flies the UV preference is enhanced by previous exposure of the flies to 'visible' light (Fischbach, 1979). These naïve preference behaviours which show characteristics of intensity independent spectral discrimination are termed wavelength-

specific behaviour and to be discerned from 'true' colour vision (Kelber and Osorio, 2010). The latter refers to a behaviour which is modified by experience, i.e. the association of a colour stimulus with a positive or negative reinforcing stimulus, leading for example to preference or avoidance. One rationale for this distinction is that learning requires a neural representation of colour (Kelber and Osorio, 2010). Also in flies, several studies focused on true colour vision using visual conditioning (Bicker and Reichert, 1978; Hernández de Salomon and Spatz, 1983; Menne and Spatz, 1977; Tang and Guo, 2001). In the blowfly *Lucilia cuprina*, combined behavioural experiments with a theoretical study predicted that colour discrimination in the fly is mediated exclusively through R7/R8 (Troje, 1993). However, R1–R6 as an additional input channel was excluded solely because of its complex spectral sensitivity profile and not because the model predicted R1–R6 not to be required. In contrast, another study did not exclude a contribution of R1–R6 to colour discrimination (Fukushi, 1994). In generalization experiments, *Lucilia cuprina* was shown to discriminate between blue, green and yellow stimuli (UV was not tested), though the colour choices of the flies depended on the intensities of the stimuli in the training (Fukushi, 1994). The behavioural data was later on compared with different models containing different sets of photoreceptor types contributing to colour vision. Models including R1–R6 could explain the behavioural data as good as models without these receptors, leaving open the question about the contribution of R1–R6 (Fukushi, 1994). A study by Bicker and Reichert even implicated a role of R1–R6: using mutant flies with degenerated R1–R6 photoreceptors in a visual conditioning assay, the authors found that these flies exhibit a potential colour discrimination defect (Bicker and Reichert, 1978). Therefore, evidence is so far controversial, and the functional interaction between photoreceptors in colour discrimination in flies requires further analysis.

A spectral discrimination curve was calculated after a series of visual conditioning experiments in which a certain wavelength was tested against a set of different wavelengths (Hernández de Salomon and Spatz, 1983) (Figure 8). Flies showed best discriminability in the range of 430-450 nm and around 500 nm. Unfortunately, UV was not tested and no discriminability curve was shown for this region. It is important to mention that the authors tried to control brightness by selecting stimulus intensities of the diverse wavelengths that in spectral preference tests were equally preferred to a 'white reference' light. As been discussed before, this method to obtain isoluminant stimuli has to be critically viewed and the discriminability curve may partially be based on intensity differences (see 1.2.1).

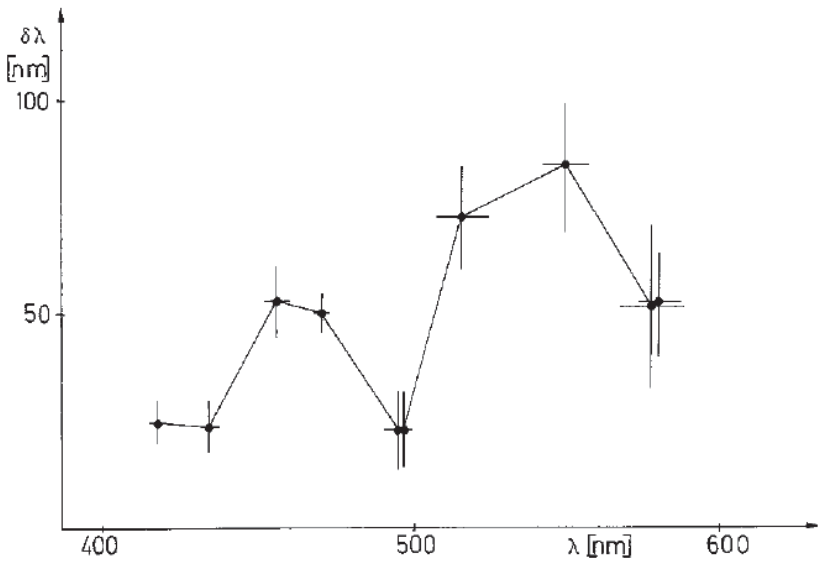

Figure 8 – Spectral discrimination function of *Drosophila melanogaster*. Δλ is defined as the wavelength difference necessary for the flies to discriminate two stimuli (a criterion of 10 % was chosen). Best discriminability was found in the violet (λ = 420 nm) and in the blue-green range (λ = 495 nm) (from Hernández de Salomon and Spatz, 1983).

Gao et al. (Gao et al., 2008) were the first to examine the role of second-order neurons in spectral preference. Using serial electron microscopy, the authors found that medulla neurons Tm5 and Tm9 receive direct synaptic input from R7 and R8, respectively, and indirect input from R1–R6 via L3. This anatomical finding qualifies them to function as colour-opponent neurons. Furthermore, the wide-field Dm8 amacrine cell was found to receive input from 13–16 UV-sensitive R7 and provides output to Tm5 (and Tm9). Using the GAL4/UAS system, cells postsynaptic to the photoreceptor cells were blocked and flies were tested in a UV/green spectral preference assay. The authors also tested the sufficiency of these neurons for this behaviour by rescuing the expression of a required histamine receptor in precisely these neurons of otherwise mutant flies. By these approaches, Dm8 was shown to be necessary and sufficient for flies to exhibit phototaxis toward ultraviolet instead of green light. In a recent study, it was found that the Tm5 subtype Tm5c receives excitatory glutamatergic input from Dm8 and that selectively inactivating Tm5c but not Tm5a or Tm5b abolishes naïve UV preference (Karuppudurai et al., 2014). Interestingly, as the Dm8 input to Tm5c is excitatory, R7 input to Dm8, and R7/R8 input to Tm5c are inhibitory via *ort*, there is so far no indication of antagonistic photoreceptor input to Tm5c. Moreover, whether Dm8 and

Tm5 neurons also contribute to intensity invariant colour discrimination requires further analysis.

Altogether, knowledge about colour vision in flies is very sparse although this organism has been proven a fruitful model organism for the study of vision (Borst, 2009).

1.3 Classical associative memory

Learning and memory is an experience dependent behaviour that allows an organism to adapt to the environment and behave more appropriately if it encounters the same situation again. Memory can be either non-associative such as habituation or sensitization to a repeatedly occurring stimulus, or associative. Two forms of associative learning, namely operant (instrumental) and classical (pavlovian) conditioning, are to be discerned. In operant conditioning, an animal learns the contingency between its own behaviour and a stimulus in the environment. After operant learning, the frequency of its own actions is increased or decreased to receive or avoid the reinforcing stimuli (Skinner, 1938). By contrast, classical conditioning allows an animal to learn the contingency between multiple sensory stimuli in the environment (Pavlov, 1927). In this case, a contingent presentation of a sensory stimulus (conditioned stimulus CS) and a reinforcing stimulus (unconditioned stimulus US) allows an animal to predict the upcoming US by perceiving the CS alone. Therefore, animals that have formed memory alter their behavioural response to the CS. This adapted behaviour is called conditioned response (CR), which ranges from a simple monosynaptic reflex to a more complex behaviour such as an animal's approach towards a stimulus source.

Since the 1970's, the fruit fly *Drosophila melanogaster* has become a suitable model organism for studying learning and memory. While many learning paradigms have been developed for a variety of sensory modalities (reviewed in Kahsai and Zars, 2011), studies about classical conditioning in the fruit fly mostly focused on olfactory memory. That is mainly because it is such a robust behaviour which only requires simple technology to be assayed (Tempel et al., 1983; Tully and Quinn, 1985). Today, the neuronal circuits and the genes underlying olfactory memory have been identified to an impressive extent, allowing to draw a detailed model of this behaviour (reviewed in Heisenberg, 2003; Keene and Waddell, 2007) (see also 1.3.1). The knowledge about the circuits, genes and cellular mechanisms underlying visual associative memory are in comparison much more limited (reviewed in Kahsai and Zars, 2011) (see also 1.3.2). Neither are the sensory visual circuits from the retina

level to the site of memory formation known, nor have the underlying reinforcement pathways been identified, as compared to olfactory memory.

What can be gained by studying visual memory (in addition to olfactory memory)? First of all, visual stimuli are of physical and not of chemical nature as odours or tastants. While odours with their single quality are perceived by many different receptors and processed in neural networks in which a specific odour is coded by a few neurons (reviewed in Heisenberg, 2003; Masse et al., 2009), visual stimuli have many qualities: spectral characteristics, motion direction, polarization, or pattern orientation, have to be extracted by neuronal circuits and often to be processed in a retinotopic manner (reviewed in Borst, 2009). The identification of the mechanisms underlying diverse visual memories and the comparison to memories of other sensory modalities, like olfactory memory, will finally allow a more comprehensive knowledge of associative memory. It will also reveal how brains deal with different sensory memories. One scenario is the processing in different dedicated circuits, which would probably require multiplying circuit motifs. A more economic scenario is the use of a shared memory circuit.

1.3.1 Olfactory memory in *Drosophila*

Soon after the discovery of mutations affecting diverse behaviours in *Drosophila* (Benzer, 1967; Konopka and Benzer, 1971), the first mutants with impaired olfactory memory were identified (Dudai et al., 1976; Quinn et al., 1979). The combination of a simple and robust memory assay and the various possibilities of genetic intervention became a new field of research. The conditioning apparatus developed by Tully and Quinn (Tully and Quinn, 1985) in which electric shock is used as reinforcing stimulus is still widely used for the study of associative learning in flies. With little modification, it also allows appetitive conditioning with sugar reward (Schwaerzel et al., 2003). In addition, many learning paradigms focusing on other sensory modalities have been developed (see also. 1.3.1 for vision; Masek and Scott, 2010 for taste; Gegear et al., 2008 for magnetic sense; Menda et al., 2011 for auditory sense), though I will focus mainly on olfactory memory at this chapter.

Depending on the training procedure, olfactory memory lasts up to several hours or even days and consists of several distinct components like short-term-, mid-term-, anaesthesia-resistant-, and long-term-memory (Margulies et al., 2005; Tully et al., 1994).

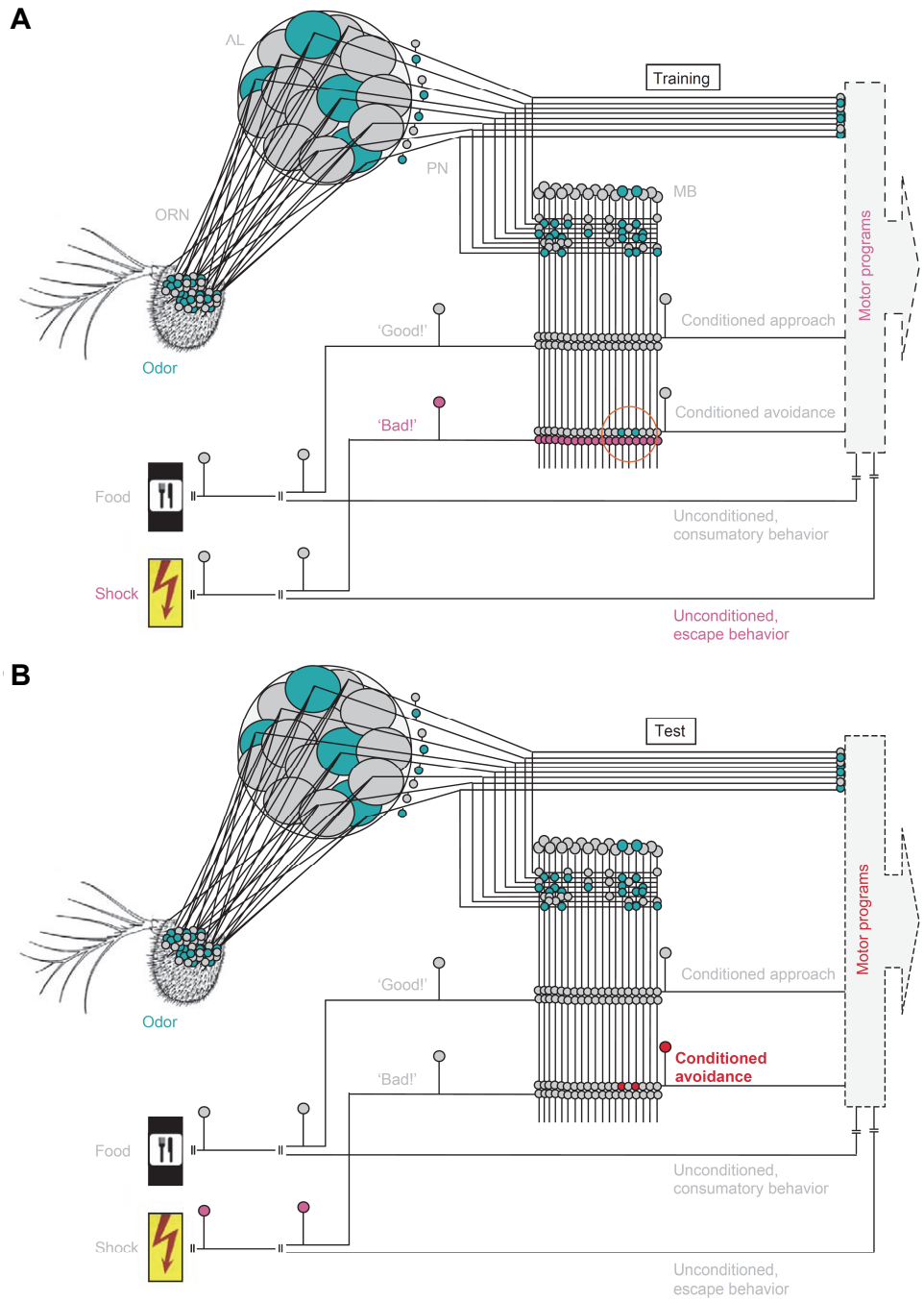

Figure 9 – Neural circuit model underlying associative olfactory memory in *Drosophila.* (**A–B**) Olfactory receptor neurons (ORNs) convey odour information from the third antennal segments and maxillary palps (not shown) to the antennal lobe. Their fibers project according to their chemospecificities to one (or few) of 40 glomeruli. The odour-induced combinatorial activation pattern is then relayed by uniglomerular projection neurons (PN) to the lateral horn and to premotor centers (box labelled 'Motor output'), as well as to the mushroom body (MB) calyx. Output from the MB is conveyed to a variety of target regions including premotor areas. Odours are represented in the mushroom bodies by sets of Kenyon cells. A memory trace for the

association between odour and reinforcement is proposed to be localized within the Kenyon cells: (**A**) during training, when the activation of a pattern of Kenyon cells representing an odour occurs simultaneously with a modulatory reinforcement signal (labelled 'Good!' and 'Bad!'; octopaminergic and dopaminergic neurons concerning reward and punishment), output from these activated Kenyon cells onto mushroom body output neurons is suggested to be strengthened. (**B**) This strengthened output is thought to mediate conditioned behaviour towards the odour when encountered during test, during which no reinforcer is present. Activated cells or synapses and motor programs are represented by filled symbols and bold lettering, respectively (adapted from Gerber et al., 2004a).

These components can be genetically dissected. Mid-term memory and anaesthesia-resistant memory specifically require the genes *amnesiac* and *radish*, respectively. Conversely, short-term memory requires the genes *rutabaga*, *dunce* and several others (Folkers et al., 1993; Isabel et al., 2004; Quinn et al., 1979; Tully and Quinn, 1985). Long-term memory differs from the other forms of memory as it is protein synthesis dependent and can be inhibited by the protein synthesis inhibitor drug cycloheximide (Tully et al., 1994).

The odour molecules are detected in the antennae, and conveyed to the primary olfactory centre, the antennal lobe. From there, the olfactory projection neurons transmit the processed olfactory information to the MB calyx and the lateral horn (Figure 9) (reviewed in Hallem et al., 2004; Masse et al., 2009). The MB is a paired structure composed of around 2000 neurons that project along a 'peduncle' before projecting more anterior into three different directions, giving rise to the αβ, α'β', and γ lobes (Aso et al., 2009). In this neuropil, the identity of odours is represented by the sparse activation pattern of its intrinsic neurons, the Kenyon cells (reviewed in Heisenberg, 2003; Masse et al., 2009). In addition to olfactory signals, aversive and appetitive reinforcement information in conveyed to the MB by dopamine and octopamine neurons (neurons with dopaminergic and octopaminergic phenotype, respectively) (Figure 9; Aso et al., 2010, 2012; Burke et al., 2012; Claridge-Chang et al., 2009; Liu et al., 2012; Schroll et al., 2006; Schwaerzel et al., 2003).

That this prominent neuropil is required for olfactory memory, was shown already several years ago by analysing MB structural mutants (Heisenberg et al., 1985) and in ablation experiments (De Belle and Heisenberg, 1994). Since then, there have been several calcium imaging studies identifying memory traces in the MB (Akalal et al., 2010; Wang et al., 2008; Yu et al., 2006). Furthermore, Kenyon cell subsets of specific mushroom body lobes were transiently silenced and found to be specifically required for memory acquisition, consolidation, or retrieval (Dubnau et al., 2001; Krashes et al., 2007; Perisse et al., 2013). Moreover, *rutabaga* dependent memory traces were restored specifically in different

mushroom body lobes (Blum et al., 2009; McGuire et al., 2003; Zars et al., 2000). Currently, it is thought that immediate odour memories require the γ lobes (Krashes et al., 2007; Qin et al., 2012), while longer-lasting memory is consolidated in the $\alpha\beta$ lobes (Krashes et al., 2007). The latter probably involves interactions among the lobes as well as between $\alpha'\beta'$ neurons and mushroom body-extrinsic neurons. Thus, all three mushroom body lobes are required for some aspect of olfactory memory.

Altogether, the MB has been considered as the site of memory formation and storage. In the current model, the aminergic neurons are hypothesized to modulate output synapses of Kenyon cells to facilitate the activation of MB-output neurons by the learned odour (Figure 9) (reviewed in Gerber et al., 2004a; Heisenberg, 2003; Keene and Waddell, 2007).

1.3.2 Visual memory in *Drosophila*

For visual associative learning in *Drosophila*, several experimental approaches have been developed, involving the visual modalities colour, intensity and form (reviewed in Heisenberg et al., 2001; Waddell and Quinn, 2001).

In pioneering studies, Menne and Spatz (Menne and Spatz, 1977), and Bicker and Reichert (Bicker and Reichert, 1978) showed that the fly can discriminate both colours and intensities of visual stimuli. Using the same assay, a spectral discrimination curve was described (Hernández de Salomon and Spatz, 1983). In another study, the genes *dunce*, *rutabaga*, *amnesiac*, and *turnip*, which are involved in olfactory memory, were also found to be required for colour/intensity memory in this assay, indicating similar processing of both memories (Folkers, 1982). For unknown reasons, colour/intensity memories have not been studied with this assay since. Even more astonishing, the neural circuit underlying colour/intensity memory is completely unknown.

Associative learning of patterns in *Drosophila* has been investigated mainly with the flight simulator setup (reviewed in Heisenberg et al., 2001). In this paradigm, tethered flies associate visual stimuli with heat punishment. By means of this setup, it was shown that different visual pattern parameters like ‘elevation’, ‘contour orientation’, ‘size’, and ‘vertical compactness’ can be learned during conditioning (Ernst and Heisenberg, 1999). Similar to colour and olfactory memory, visual memory of patterns requires *rutabaga* function and the central complex was found to be the structure, comprising *rutabaga*-dependent memory traces (Liu et al., 2006; Pan et al., 2009). The large field neurons in the first layer (F1 neurons) and

fifth layer (F5 neurons) of the fan-shaped body were found to be responsible for memory of 'contour orientation' and 'elevation', respectively (Liu et al., 2006). A memory trace was also identified in the R2/R4m neurons in the ellipsoid body which is involved in memory of all four pattern parameters (Pan et al., 2009). Similar to olfactory memory (Margulies et al., 2005), visual pattern memory was found to comprise of several components (Xia et al., 1998). Gong et al. (Gong et al., 1998) described certain common molecular mechanisms underlying learning and memory in both tasks and concluded that the previous multi-phase model of visual memory requires different genes for specific memory components.

While the mushroom bodies (MBs) are required for olfactory and gustatory memories (Heisenberg, 2003; Heisenberg et al., 1985; Masek and Scott, 2010), according to previous studies, they are not required for visual memory (Heisenberg et al., 1985; Tang and Guo, 2001; Wolf et al., 1998; Zhang et al., 2007). However, other studies suggest that visual information is indeed processed in the MB (Barth and Heisenberg, 1997; Brembs and Wiener, 2006; Liu et al., 1999; Van Swinderen, 2009). A difficulty in resolving these discrepancies results from the fact that these studies, especially when comparing stimuli with different physical nature (e.g. olfactory and visual), employed different behavioural tasks (e.g. flight orientation or binary choice by walking flies) and/or conditioning designs (Brembs and Plendl, 2008; Brembs and Wiener, 2006; Ofstad et al., 2011; Pitman et al., 2009). Thus, a more informative comparison might be obtained using comparable learning paradigms (Gerber et al., 2004b; Guo and Guo, 2005; Hori et al., 2006; Mota et al., 2011; Scherer et al., 2003).

Due to the lack of an appropriate behavioural paradigm that allows contrasting appetitive and aversive visual memory, reward and punishment processing for visual memories has not yet been addressed in *Drosophila*. Although Schwaerzel et al. (Schwaerzel et al., 2003) showed that dopamine and octopamine are necessary for aversive and appetitive olfactory conditioning, respectively, no study challenged the question whether these biogenic amines have the same function in visual associative learning. Pharmacological experiments in crickets support this analogy (Unoki et al., 2006) suggesting the same role of biogenic amines in visual memory in flies.

Several studies focused on place memory in flies (reviewed in Zars, 2009), while only a few assays involve visual cues (Foucaud et al., 2010; Neuser et al., 2008; Ofstad et al., 2011). In a spatial orientation memory task, in which flies have to remember the position of an object for several seconds after it has been removed from their environment, Neuser et al. (Neuser et al., 2008) showed that ring neurons of the ellipsoid body are necessary and their

plasticity is sufficient for a functional spatial orientation memory in flies. Furthermore, the protein kinase S6KII coded by *ignorant* is required in a distinct subset of ring neurons to display this memory. Ofstad et al. (Ofstad et al., 2011) used an assay that is similar to the Morris water-maze used for mice (Morris, 1984), in which the position of a non-heated 'safe' spot in relation to several visual cues has to be learned. Similar to the previously mentioned study, the authors identify neurons in the ellipsoid body to be required.

1.4 The model organism *Drosophila*

Drosophila melanogaster is one of the major model organisms in neuroscience. In comparison to other model organisms like mice, rat or monkey it has numerous advantages despite it's rather far phylogenetic distance to human. Fruit flies are easy and inexpensive to cultivate. They have a high fecundity and short generation time. At room-temperature, it takes only about 10 days to develop from an egg to an adult fly (Ashburner, 1989). With a presumably simple brain (3–6 orders of magnitude fewer neurons as compared to mammals), the vast amount of transgenic techniques (Elliott and Brand, 2008; see also next paragraphs), and its riche repertoire of behaviours, a comprehensive understanding of the function of a nervous system from behaviour to underlying circuits and genes (reviewed in Borst and Euler, 2011; Griffith, 2012; Sanes and Zipursky, 2010; Waddell and Quinn, 2001) can be achieved. Furthermore, despite the vast phylogenetic distance, *Drosophila melanogaster* shares many similarities in genes, neuronal circuits and behaviours with mammals (Adams et al., 2000; Hildebrand and Shepherd, 1997). Thus, the understanding of brain function in flies may reveal general mechanisms of nervous systems conserved among different species.

Traditionally, genetic studies were performed by mutagenizing a large population of flies with the subsequent identification of mutants in a screen. The mutant screen can for example be a behavioural or an anatomical analysis. Nowadays, in addition to mutant screens, a more directed approach towards circuit analysis by ectopic expression of specific genes in specific cells is used, as been described in the following paragraphs.

1.4.1 The GAL4/UAS system as a genetic tool for dissecting neuronal circuits

The GAL4/UAS system (Figure 10) is currently the most widely used technique for targeted gene expression in *Drosophila* (Brand and Perrimon, 1993; reviewed in Elliott and Brand,

2008). It allows the expression of an effector gene under the temporal and spatial control of an endogenous or cloned enhancer sequence via a transcription factor from yeast (GAL4) and an upstream activating sequence (UAS) bound by GAL4 (Figure 10).

The GAL4 element and the UAS effector element are kept in separate stocks. Many of the GAL4 driver and UAS effector stocks are available in huge public libraries (e.g. GETDB by the NP consortium or the Bloomington stock centre) or can easily be generated (Bachmann and Knust, 2008). The two components are combined in the F1 generation of a genetic cross of two selected lines. In such F1, the effector is only transcribed in those cells expressing the GAL4 protein.

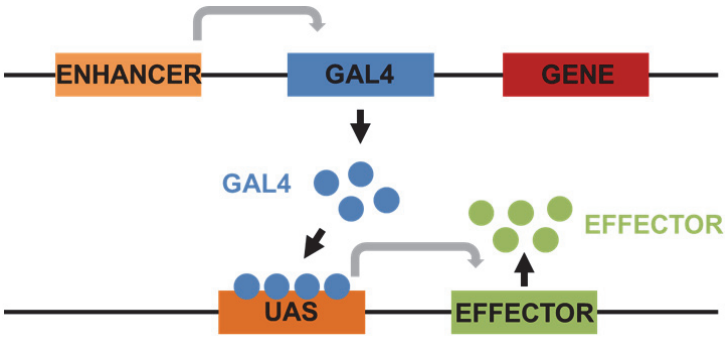

Figure 10 – The GAL4/UAS system for targeted gene expression. The transcription factor GAL4 is expressed in a spatially and temporally restricted pattern that is determined by the cloned or endogenous enhancer element. The GAL4 protein binds to its recognition site, the upstream activation sequence (UAS) and drives expression of an effector gene.

1.4.2 GAL4 driver lines

The driver line is a transgenic stock carrying the gene of the yeast transcriptional activator GAL4 in a P-element cassette in its genome (Brand and Perrimon, 1993). It is generated by germ-line transformation, with a preferential insertion of the construct in the 5' upstream, non-protein coding region of a gene (Spradling et al., 1995). The GAL4 gene requires an enhancer element to be expressed and the P-element then functions as an 'enhancer trap', as it

reflects the activity of an endogenous enhancer. Alternatively, GAL4 can also be cloned downstream of the promoter/enhancer of a desired gene, yielding a similar expression. The transcription factor GAL4 has no known targets in *Drosophila* and can drive expression of any desired gene, if the latter is cloned downstream of a GAL4 binding site, the Upstream Activation Sequence (UAS).

1.4.3 UAS effector lines

In the following, I want to briefly describe a selection of effectors that are highly useful for neural circuit analysis, most of which were also used in this study. Of particular importance is the correlation of structure (anatomy) and function. By expressing a green fluorescent protein (GFP) as an effector, the expression pattern of a GAL4 driver line can be identified under the fluorescence or confocal microscope (Yeh et al., 1995). For functional analysis, several effectors have been reported which allow the inhibition or activation of neural activity. A potent inhibitor that blocks the synaptic transmission is the temperature sensitive, dominant-negative allele of the *shibire* gene shi^{ts1} (Kitamoto, 2001). *shibire* is the coding gene of a Dynamin that is required for the endocytosis of synaptic vesicles (Koenig and Ikeda, 1983; Kosaka and Ikeda, 1983). At restrictive temperature, the synaptic vesicle pool of neurons expressing shi^{ts1} is depleted, causing the synaptic block (Delgado et al., 2000). At permissive temperature, neuronal activity is unaffected. Being reversible, this effector allows temporal control of neuronal activity i.e. to block the cells for a particular period (e.g. after development or only during a specific phase during the experiment). This effector has successfully been used to dissect the neuronal networks of diverse behaviours like olfactory memory (e.g. Krashes et al., 2007) and courtship (Kitamoto, 2002; Stockinger et al., 2005). Another neuronal inhibitor is the inward-rectified potassium channel Kir2.1 (Baines et al., 2001). If overexpressed, it causes a hyperpolarisation and shunting inhibition of cells and thereby inhibits the generation of action potentials (Johns et al., 2001). A potent neuronal activator is the temperature sensitive TRPA1 channel (Hamada et al., 2008; Pulver et al., 2009). Above 27 °C it opens and causes the influx of cations leading to a depolarisation of the cell. This effector therefore allows temporally controlled activation of neurons. Furthermore, in a mutant background of a particular gene, one can use the GAL4/UAS system to express the functional gene in specific sets of cells. This allows identifying those cells that are sufficient to rescue a particular mutant phenotype (e.g. *rutabaga* rescue: Blum et al., 2009; Liu et al., 2006).

1.4.4 Temporal control of GAL4 activity, expression pattern refinement and split-GAL4

An elegant way to add temporal control to the GAL4/UAS system is the TARGET system (temporal and regional gene expression targeting). It employs a temperature sensitive variant of GAL80 ($GAL80^{ts}$), an inhibitor of GAL4, being fused downstream of the *tubulin* promoter, driving ubiquitous expression of $GAL80^{ts}$ (McGuire et al., 2003). At 18 °C, the latter is active in all cells and prevents GAL4 from binding to the UAS. Above 30 °C, $GAL80^{ts}$ is inactive and transgene expression by GAL4 is not inhibited. By this means, developmental defects or lethality caused by the effectors can be circumvented.

To refine the expression pattern of a particular GAL4 line, a widely used approach is the use of GAL80 under the control of a genomic enhancer (enhancer trap) or a cloned promoter (Suster et al., 2004). Additional expression of GAL80 in a subset of GAL4 expressing cells allows assessing whether a phenotype is caused by the manipulation of these.

Compared to the two-component GAL4/UAS system which usually drives expression in at least a few dozen neurons (Jenett et al., 2012), intersectional strategies allow manipulation of very small sets of neurons. For example, the split-GAL4 approach restricts the expression of transgenes to the cells that express both DNA binding domain and transcription activating domain of GAL4 (Luan et al., 2006). Each domain, being under the control of a specific promoter, is fused to a heterodimerizing leucine zipper fragment so that the two domains bind tightly when expressed together in the same cell to become transcriptionally active.

1.4.5 Limitations of the GAL4/UAS system

Despite the numerous advantages of the GAL4/UAS system, it also has some limitations. First, a GAL4 line that labels the cells of interest is often not very specific and additional cells are labelled. To overcome this problem, different GAL4 lines with overlapping expression patterns can be tested, the pattern can be refined with a particular GAL80 line, or an intersectional strategy can be used. Second, transcription of the UAS effector gene is not always absent without a driver and appears to be insertion-dependent (Ito et al., 2003; Pfeiffer et al., 2010). This can be controlled by testing flies that only contain the UAS construct but not the GAL4 driver. Third, effector activity depends on the expression level of GAL4. Thus, different phenotypes may be observed when using several GAL4 lines that label cells of interest.

1.4.6 Other targeted gene expression systems

In addition to the Gal4/UAS system, several other binary systems have been developed for use in *Drosophila*. These include the LexA system, which is based on the bacterial DNA-binding protein LexA (Lai and Lee, 2006; Pfeiffer et al., 2010; Yagi et al., 2010) and the Q-system based on the fungal transcription factor Q (Potter et al., 2010). They can be used in combination, allowing independent expression of several transgenes in a fly. Furthermore, a split-LexA system similar to the split-GAL4 system has been developed for refined transgene expression (Ting et al., 2011). This split-LexA system can be concatenated with the Gal4/UAS system to refine the expression patterns of existing GAL4 lines by expressing the DNA binding domain of LexA under control of UAS and a transcription activating domain under a selected promoter (Ting et al., 2011).

2. Materials and Methods

2.1 Fly strains

Peripheral neural circuits underlying colour discrimination: All flies were raised in standard cornmeal medium at 25 °C and 60 % relative humidity under a 12/12-hour light/dark cycle. The X chromosomes of all transgenic strains were replaced with that of wild-type Canton-S (w^+). Flies were tested 2–6 days after eclosion. For *norpA* rescue experiments, correct genotypes (Table 1) of given crosses were selected before experiments. All rhodopsin GAL4 drivers were kindly provided by Claude Desplan (Mollereau et al., 2000). For *norpA* restoration, *UAS-norpA.K(1)* was used (derived from Bloomington stock number 26267). To test requirement of Rh1, the null mutant $ninaE^8$ with little photoreceptor degeneration was used (Kumar and Ready, 1995). To block the function of neuronal subsets in the lamina neuropil, the *UAS-*shi^{ts1} (Kitamoto, 2001) line was crossed to different driver lines: *+; +;* ort^{C2}*-GAL4* (Gao et al., 2008) (L1, L2, L3, Dm8), *+;vGlut-dVP16AD/CyO;* ort^{C2}*-GAL4DBD/TM6B* (Gao et al., 2008) (few L1, most Dm8), and *R48A08-GAL4* (Tuthill et al., 2013) (L1, L2, unknown medulla tangential cell type, unknown proximal medulla cell type; see http://flweb.janelia.org/ for expression pattern; Jenett et al., 2012). For anatomical analysis, the above driver lines were crossed to *y w; UAS-mCD8::GFP/CyO.*

Neural circuits underlying reinforcement signalling for visual memories: Flies were reared at 25 °C and 60 % relative humidity under a 12-12-hour light-dark cycle on a standard cornmeal-based food. As all transgenes were inserted into the w^- mutant genome, the X chromosomes of strains were replaced with that of wild-type Canton-S (w^+). I used F_1 progenies of crosses between females of genotypes *UAS-dTrpA1* (Hamada et al., 2008), *UAS-*shi^{ts} (Kitamoto, 2001), *UAS-mCD8::GFP* (Lee and Luo, 2001), or WT-females and males of genotypes *TH-GAL4* (Friggi-Grelin et al., 2003), *DDC-GAL4* (Li et al., 2000), *R58E02-GAL4* (Liu et al., 2012), *TDC2-GAL4* (Cole et al., 2005), *MB247-GAL4* (Zars et al., 2000), or Canton-S males. The $dumb^2$ null mutant was used to localize the cells that receive dopamine signals (Kim et al., 2007).

To identify a role for specific dopamine neuron subsets (neuron subsets with dopaminergic phenotype), I utilized specific split-GAL4 lines. Split-GAL4 lines have high specificity in expression pattern, since here the DNA-binding domain (dbd) and the activation domain (AD) of the GAL4-protein are independently targeted by different promoters. In this way, the UAS transgene is only expressed where the expression patterns of the two enhancers

Table 1 – Genotypes used in the *norpA* rescue experiments.

Description	Genotype	Figure
negative control	*norpA^{7}/Y; UAS-norpA/+*	16, 17A, 17B, 18A, 18C, 20B, 21A, 21C
***rh1-GAL4* rescue**	*norpA^{7}, rh1-GAL4/Y; UAS-norpA/+*	16, 19, 21A, 21C
***rh3-GAL4* rescue**	*norpA^{7}/Y; UAS-norpA/+; rh3-GAL4/+*	16
***rh4-GAL4* rescue**	*norpA^{7}/Y; UAS-norpA/rh4-GAL4*	16, 19, 20B
***rh5-GAL4* rescue**	*norpA^{7}/Y; UAS-norpA/rh5-GAL4*	16
***rh6-GAL4* rescue**	*norpA^{7}/Y; UAS-norpA/rh6-GAL4*	16, 19
***rh1-, rh4-GAL4* rescue**	*norpA^{7}, rh1-GAL4/Y; UAS-norpA/rh4-GAL4*	18B, 18C, 20A
***rh1-, rh6-GAL4* rescue**	*norpA^{7}, rh1-GAL4/Y; UAS-norpA/rh6-GAL4*	18B, 18C
***rh4-, rh6-GAL4* rescue**	*norpA^{7}/Y; UAS-norpA/rh4-GAL4, rh6-GAL4*	18B, 18C
***rh1-, rh4-, rh6-GAL4* rescue**	*norpA^{7}, rh1-GAL4/Y; UAS-norpA/rh4-GAL4, rh6-GAL4*	18A, 18C
***rh1-, rh3-, rh5-GAL4* rescue**	*rh1-GAL4, norpA^{7}/Y; UAS-norpA/rh5-GAL4; rh3-GAL4/+*	18A
***rh3-, rh4-, rh5-, rh6-GAL4* rescue**	*norpA^{7}/Y; UAS-norpA/rh5-GAL4, rh6-GAL4; panR7-GAL4/+*	21A, 21C
***rh1-, rh3-, rh4-, rh5-, rh6-GAL4* rescue**	*rh1-GAL4,norpA^{7}/Y; UAS-norpA/rh5-GAL4, rh6-GAL4; panR7-GAL4/+*	17A, 17B, 21A, 21C

intersect and therefore the functional GAL4-protein can be reconstituted (Luan et al., 2006; Pfeiffer et al., 2010). I used F_1 progenies of crosses between females of genotypes *UAS-shi^{ts}* (Kitamoto, 2001), *UAS-mCD8::GFP* (Lee and Luo, 1999), *UAS-dTrpA1* (Hamada et al., 2008) or WT-females and males of genotype *MB504B*, or Canton-S males. *MB504B* was generated using the vectors described in Pfeiffer et al., 2010 by inserting *R52H03-p65ADZp* into attp40 and *TH-ZpGdbd* into attP2.

As I was unable to distinguish genotype or sex in the behavioural videos, I sorted flies by genotype under CO_2 anaesthesia at least two days prior to experiments. Hence, 2–4 day old flies were starved in moistened empty vials to approximately 20 % mortality (Schnaitmann et al., 2010). Behavioural experiments each used 30–40 mixed males and females under dim red light in a custom-made plastic box, containing a heating element on the bottom and a fan for air circulation.

In temperature shift experiments flies were transferred into moistened empty vials while the temperature was adjusted from permissive (25 °C) to restrictive (33 °C) or vice versa. The test was performed 40–45 min after training.

2.2 Behavioural assays

Visual appetitive memory: Flies were trained and tested using a visual appetitive differential conditioning assay (Schnaitmann et al., 2010) with modifications (Figure 11A). For narrow-spectral illumination, I constructed a stimulation module using computer-controlled high-power LEDs with peak wavelengths 452 nm and 520 nm (Seoul Z-Power RGB LED) or 456 nm and 520 nm (H-HP803NB, and H-HP803PG, 3W Hexagon Power LEDs, Roithner Lasertechnik) for blue and green stimulation, respectively. LEDs were housed in a base 144 mm below the arena, which allowed homogeneous illumination of a filter paper as a screen. For separate illumination of each quadrant, the light paths of LEDs were separated by light-tight walls in a cylinder with air ducts. 'Bright' and 'dark' blue and green stimuli were used as explained throughout the manuscript. The intensities were controlled by current and calibrated using a luminance meter BM-9 (Topcon Technohouse Corporation) or a PR-655 SpectraScan® Spectroradiometer: Peripheral neural circuits underlying colour discrimination: 0.483 W sr^{-1} m^{-2} (bright-blue), 0.048 W sr^{-1} m^{-2} (dark-blue), 0.216 W sr^{-1} m^{-2} (bright-green), and 0.022 W sr^{-1} m^{-2} (dark-green), 0.437 W sr^{-1} m^{-2} (Rh4-adapted bright-blue), 0.044 W sr^{-1} m^{-2} (Rh4-adapted dark-blue), 0.874 W sr^{-1} m^{-2} (Rh4-adapted bright-green), 0.087 W sr^{-1} m^{-2} (Rh4-adapted dark-green). Neural circuits underlying reinforcement signalling for visual memories: 0.34 W sr^{-1} m^{-2} (blue) and 0.15 W sr^{-1} m^{-2} (green).

Before experiments, flies were starved at 25 °C to a mortality rate of 20–30 % (Schnaitmann et al., 2010). Flies received 4-cycle differential conditioning. Stimulation of the whole arena with one colour/intensity was paired with a sucrose reward (2 M) for 1 min, and after a 12-sec break in the dark the other colour/intensity was presented without reward. The cylindrical arena consisted of a Petri dish (Ø 92 mm, Sarstedt, Germany) on which flies could

freely move, a pipe wall, and a second Petri dish used for a lid (Figure 11A). The pipe's smooth inner surface and the lid were coated with Fluon (Fluon® GP1, Whitford Plastics Ltd., UK) to ensure that flies stayed on the filter paper at the bottom of the arena. Reward presentation was switched by inverting the whole arena, tapping the flies gently to detach them from the Petri dish, and exchanging the dishes with sugar or water. In half of the experiments, the reward/no reward sequence was reversed to cancel any effect of order. In the test period, flies were given the choice between two stimuli, presented in two quadrants each.

Conditioned response of the trained flies was recorded with CMOS cameras (FireflyMV, Point Grey Research Inc, CA) for 90 s. The learning index was based on two groups (50–100 flies each), which had been trained reciprocally in terms of the two visual stimuli used. Stimulus preference was determined by the distribution of flies in the arena. A pre-set macro for ImageJ (Rasband, W.S., U. S. National Institutes of Health, USA) was used to count the number of flies in each quadrant in every frame of the video recordings (90 frames recorded at 1 Hz) (Schnaitmann et al., 2010). Flies touching a border between two quadrants were excluded. I calculated a preference index for green (PI_G) for each time point by the difference between the number of flies on the green quadrants and the number on the blue quadrants, divided by the total number of flies counted. PI_G was calculated in both reciprocal experiments [i.e., Green rewarded (G+ B−) and Blue rewarded (G− B+)]:

$$PI_G = \frac{\#Green - \#Blue}{\#Total}$$

A Learning Index (LI) was calculated by subtracting PI_G values of the two reciprocally trained groups and by dividing the resulting value by 2:

$$LI = \frac{PI_G(G + B -) - PI_G(G - B+)}{2}$$

The LI was calculated for each frame of a recorded video and averaged over the entire test phase (1–90 s), yielding an LI that represented the average performance of the flies. For experiments with *UAS-shi*^{ts1}, flies were trained and tested at 33 °C after preincubation at the restrictive temperature for 30 min.

Visual aversive memory: For aversive electric shock conditioning, I developed a new apparatus module containing an arena with a transparent shock grid (Figure 22E). The arena itself consisted of the transparent shock grid on the bottom, a plastic ring as a wall and a glass lid. The shock grid was a custom-made ITO-coated glass plate (9 x 9 cm; Diamond Coatings Ltd., UK). ITO is a conductive transparent substance. A grid was laser-etched onto the ITO glass in order to insulate the positive and negative electrodes (lanes in the grid were 1.6 mm spaced 0.1 mm apart, Lasermicronics GmbH, Germany). I applied alternating current. The two halves of the grid can be independently controlled. The plastic ring (wall) and the glass lid were coated with diluted Fluon (10 %; Fluon GP1, Whitford Plastics Ltd., UK) to prevent flies from walking on the lid and wall. Consequently flies were forced to stay on the shock grid on the bottom of the arena. A filter paper was clamped underneath the shock grid and served as a screen.

For aversive conditioning, one second of electric shock (AC 60 V) was applied 12 times in 60 s during CS+ (CS paired with reinforcement) presentation. The consecutive CS+ and CS– presentations were interspersed with 12 s intervals without illumination (Schnaitmann et al., 2010). Training trials were repeated four times per experiment as for appetitive conditioning.

The visual stimulation was the same as being used for appetitive conditioning. Hardware for delivering the electric shock was controlled by the same custom-made software used to control the LEDs. Conditioned response was analysed the same way as for appetitive conditioning. Four setups were run in parallel.

Paired activation assay: I established a new behavioural protocol for reinforcement substitution for visual memories using *dTrpA1* expression as in olfactory conditioning (Aso et al., 2010). Flies were 'trained' as for conditioning, but the conditioned visual stimulus was paired not with sugar or shock but with high temperature that leads to thermo-activation of dTRPA1-expressing neurons (Figure 24E). Precisely, flies were transferred from an apparatus at 24 °C to a corresponding setup at 31 °C five seconds before the onset of the CS.

The two CS presentations in each training trial were intermitted by a 60 s interval at 24 °C. After four training trials, flies were kept at 24 °C for 120 s before testing at 24 °C. Control flies not expressing *dTrpA1* and wild-type flies did not show conditioned visual preference (Figure 24E–F). Significant memory in this assay is thus driven by appetitive or aversive reinforcement signals from thermo-activation.

Sugar preference and electric shock avoidance assays: Control responses to sugar and shock were measured as described previously (Schnaitmann et al., 2010). The arenas used for appetitive and aversive conditioning were backlit with IR-LEDs, and flies were given a choice between two halves of the arena, one with the US presented as in the training and one without US. Their behaviour was recorded for 60 s using the same video setup. A preference index was calculated by subtracting the numbers of flies on the US half from the numbers on the control half, divided by the total number of flies.

2.3 Electrophysiology

ERGs were measured as previously described (Garbers et al., 2012). Briefly, cold-anesthetized flies were attached to a holder with nail polish, which was also used to prevent movement of head and legs. A recording and an indifferent (reference) glass microelectrode filled with 0.1 M KCl were placed just beneath the cornea of the stimulated eye and in the thorax, respectively. The signal recorded at room temperature was amplified using an Intronix 2015f amplifier and digitally acquired using a NI PCI-6025E data acquisition board. Visual stimulation from the behavioural experiments (dark-blue or bright-green) was reproduced by using the same LEDs, intensities, and filter paper screen. Data Acquisition and stimulation were controlled with the Relacs toolbox (Benda et al., 2007). Using a modified closed-loop light clamp technique (Franceschini, 1979), WT and *norpA*-rescue flies were analysed for their spectral sensitivity ratio for blue and green LEDs. As an internal reference of the interleaved ERG (INTER ERG) (Garbers et al., 2012), I used the response to the blue LEDs set to the 'dark' intensity as in the behavioural experiments. Using an iteratively updated linear regression model, the intensity of the green LEDs were adjusted to the level that evoked the same ERG response as the blue reference LED. The ERG response was defined as the difference in the average signals 10 ms before stimulation onset and 10 ms before offset. The stimulation protocol consisted of a 100-ms green light followed by 500 ms of no stimulation before 100 ms of the blue reference light followed by 500 ms of no stimulation. An average response difference to the blue reference was calculated based on 5 cycles of the stimulation protocol and the measurement was repeated until the difference reached less than 4 % of the reference amplitude. At least eight measurements in two flies were done per genotype. Blue/green intensity ratios were calculated by normalizing the dark-green stimulus with the green LED intensity producing the same signal amplitude as the reference (dark-blue).

2.4 Immunohistochemistry

Peripheral neural circuits underlying colour discrimination: The retina of flies was prepared in agarose sections. Heads were fixed in 4 % formaldehyde in PBT (PBS, 0.3 % Triton X-100), embedded in 7 % agarose (Biomol) and sectioned horizontally at 80 µm with a vibrating microtome (Leica VT 1000S). Agarose sections were bleached in 0.1 % $NaBH_4$ for 30 minutes to reduce auto-fluorescence of the red eye pigment, and subsequently, blocked with 3 % normal goat serum for 30 min at room temperature. Preparations were incubated overnight at 4 °C with the antibodies against GFP (1:1000) and Rh6 (a gift from Claude Desplan; 1:5000) in the blocking solution. After washing with PBT, slices were incubated overnight at 4 °C with AlexaFluor-568 and 633-conjugated secondary antibodies in the blocking solution. Preparations were rinsed and mounted in Vectashield (Vector Laboratories).

Neural circuits underlying reinforcement signalling for visual memories: Adult fly brains were dissected, fixed and stained using standard protocols (Aso et al., 2009). Synapsin antibody (Klagges et al., 1996) combined with Cy3-conjugated goat anti-mouse antibody were used to visualize the neuropil. Anti-GFP antibody was used to increase the intensity of the GFP signal (rabbit polyclonal to GFP (Invitrogen) with Alexa Fluor488-conjugated goat anti-rabbit as the secondary antibody).

Confocal stacks were collected with Olympus FV-1000 microscope (Olympus). Image processing was performed with ImageJ (NIH).

2.5 Modeling Wavelength Discrimination

To compare spectral discrimination abilities, I calculated the contrast that two stimuli evoke at a hypothetical postreceptor neuronal stage (Vorobyev and Osorio, 1998). For two stimuli, let $\Delta q_i(\lambda)$ be the difference in excitation for receptor i at wavelength λ . Then for two receptor types 1 and 2 the signal contrast in a neuronal channel k that combines these two receptor signals opponently can be written as:

$$\Delta S_k^2(\lambda) = \left(\Delta q_1(\lambda) - \Delta q_2(\lambda)\right)^2 \qquad (1)$$

To predict discrimination for a visual system combining information from more than one opponent channel, I sum over the k respective mechanisms:

$$\Delta S^2(\lambda) = \sum_{k=0}^{n} w_k S_k^2(\lambda) \qquad (2)$$

where w_k is a vector of weights that scale the channels relative to each other. For the special case of wavelength discrimination, $\Delta q_i(\lambda)$ corresponds to the slope of the receptor spectral sensitivity of receptor i at wavelength λ. Calculating this relative discrimination at each wavelength λ yields an estimate of the spectral sensitivity function. I fitted this function to the data (Hernández de Salomon and Spatz, 1983) by adjusting w such that the resulting squared differences between the estimates and the data were minimized. Goodness of fit was calculated via the chi-squared statistic, treating the data as normally distributed.

2.6 Statistics

Statistical analyses were performed with the use of Prism (GraphPad Software). If groups did not violate the assumption of normal distribution one sample t-test were used to test difference from zero. Otherwise, non-parametric Wilcoxon Signed Rank Test was employed. P-values of both tests were Bonferroni corrected. For comparison of groups, which did not violate the assumption of normal distribution (Shapiro-Wilk test) and homogeneity of variance (Bartlett's test), mean performance indices were compared with a one-way ANOVA followed by planned multiple pairwise comparisons (Bonferroni correction). Experiments with data that were significantly different from the assumptions above were analysed with non-parametric Kruskal–Wallis test followed by Dunn's multiple pair-wise comparison. Where comparisons with multiple control groups gave distinct significance levels, only the most conservative result is shown.

3. Results

3.1 Peripheral neural circuits underlying colour discrimination

3.1.1 Behavioural assay for colour discrimination in *Drosophila*

I previously developed a conditioning assay where flies associate one of two spectrally different visual stimuli with sugar reward, which allows to analyse visual stimulus discrimination in *Drosophila* (Schnaitmann et al., 2010). I set out to induce modifications that allow the use of various spectral stimuli that have a smaller wavelength range and a higher intensity than the ones produced by the RGB monitor being used before (Schnaitmann et al., 2010). I here used conditioned stimuli generated by high-power light-emitting diodes (LEDs)

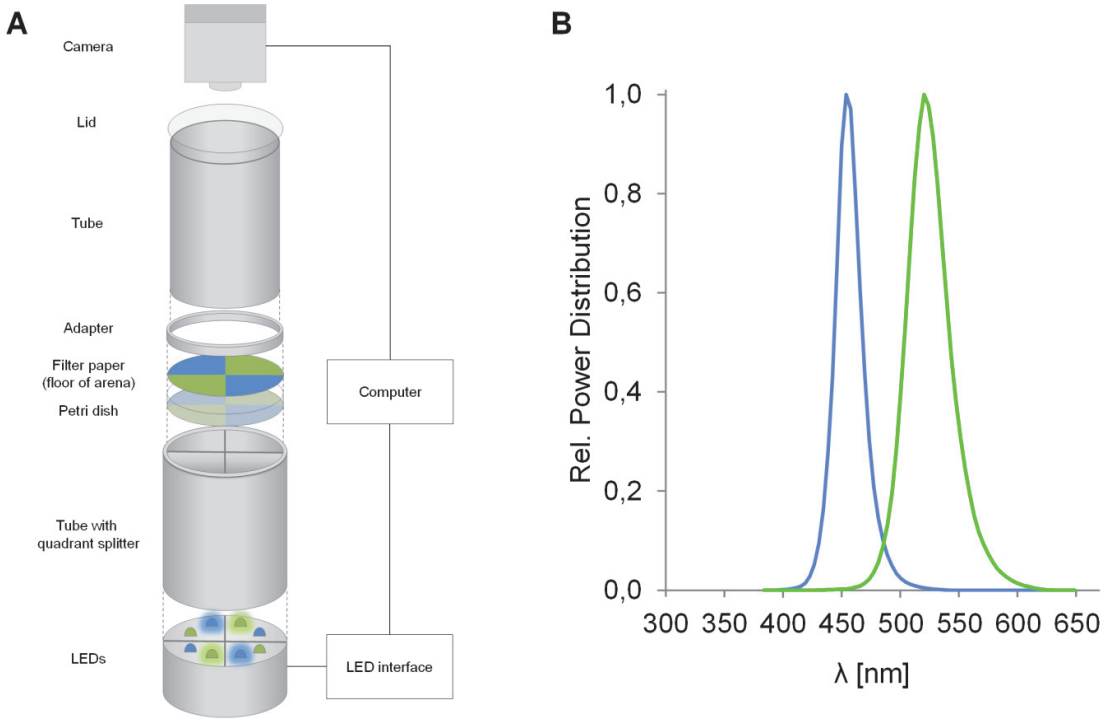

Figure 11 – An improved setup for visual appetitive memory. (**A**) Visual stimulation of the behavioural setup in (Schnaitmann et al., 2010) was modified to use LEDs instead of LCD screen. A petri dish arena containing filter paper can be illuminated from below with blue and green LEDs. The arena is partitioned into four quadrants, each of which can be illuminated independently using a custom-engineered LED interface and software. (**B**) Emission spectra of blue and green LEDs used. (Modified from Schnaitmann et al., 2013).

with peak intensities at 452 nm (blue) and 520 nm (green), respectively (Figure 11A–B). Other colour stimuli can now easily be incorporated by simply exchanging the LEDs in the apparatus with LEDs of the many spectral variants available. While flies can discriminate high-intensity blue (bright-blue) and green (bright-green) in this assay, it is not clear whether discrimination is based on colour or intensity (Figure 12A). Conditioning with differential intensities of either blue or green (1:10 ratio) resulted in significant intensity discrimination (Figure 12A), raising the possibility that blue/green discrimination might be achromatic.

To ensure that discrimination was based on colour, I introduced an intensity mismatch between training and test (Menne and Spatz, 1977): Flies were trained with low-intensity blue (dark-blue; 10 % of bright-blue) and bright-green, but were tested with bright-blue and bright-green. Flies consistently exhibited conditioned approach towards the trained colour, despite the 10-fold intensity mismatch (Figure 12B). Similarly, discrimination was not impaired when flies were trained with bright-blue/dark-green and tested with bright-blue/bright-green (Figure 12B). Finally, to assess response priority on colour and intensity cues (Bicker and Reichert, 1978; Tang and Guo, 2001), flies were trained with dark-blue/bright-green and tested

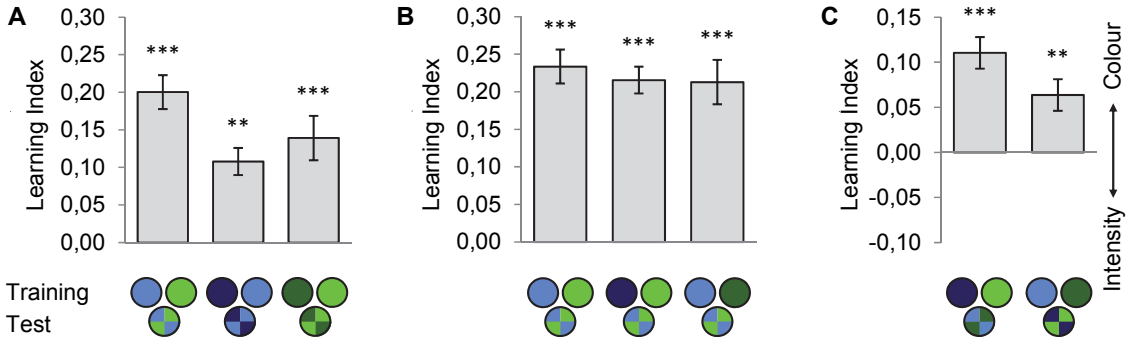

Figure 12 – Colour discrimination learning in *Drosophila*. (**A**–**C**) Conditioned stimuli, one of which is paired with a sugar reward, and test stimuli are depicted with three circles. (**A**) Wild-type flies show significant memory in the bright-blue/bright-green as well as in the intensity discrimination tasks (n = 9–18). (B) Flies choose the colour cues despite 10-fold intensity mismatch between training and test (n = 16–20). (**C**) Flies show significant colour learning despite the conflicting 10-fold intensity inversion between training and test (n = 15–16). Note that intensity learning would result in a negative learning index. Bars and error bars represent means and SEM, respectively (**p < 0.01; ***p < 0.001; ns: no significance). (Modified from Schnaitmann et al., 2013).

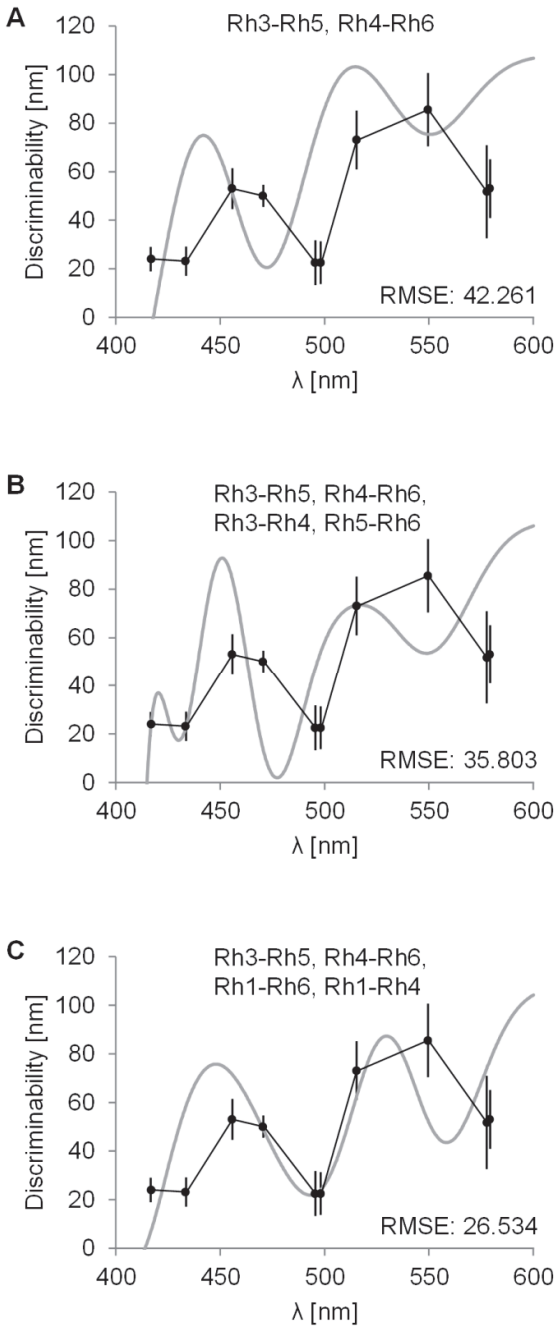

Figure 13 – Fits of models employing different combinations of colour opponent signals (gray curves) to wavelength discrimination in *Drosophila* (Hernández de Salomon and Spatz, 1983; Vorobyev and Osorio, 1998). Goodness of fit is measured by root-mean-square error corrected for the number of degrees of freedom (RMSE). (**A**) Standard model with opponent combinations of inner photoreceptor signals. (**B**) The model with the inner photoreceptors including ‘‘interommatidial’’ opponency (i.e., Rh3-Rh4 and Rh5-Rh6) fits slightly better than the standard model. (**C**) A model including outer receptor signals achieves a substantially better fit. Note that this model has the same number of parameters as the model in (B). Data points and error bars represent means and SEM, respectively. See also Figure 14. (From Schnaitmann et al., 2013).

with bright-blue/dark-green, and vice versa (intensity inversion). This experimental design allows to assess whether flies use a conflicting colour or intensity cue (Bicker and Reichert, 1978; Tang and Guo, 2001), as conditioned approach to the colour or intensity cue will result in a positive or negative learning index, respectively. Both combinations of the intensity inversion revealed choice priority on the colour cue, demonstrating that discrimination was based on spectral composition, not intensity (Figure 12C).

3.1.2 Modelling suggests that R1–R6 contribute to colour discrimination

To determine which photoreceptors feed into colour vision, I fitted a model of colour opponent processing to experimental results of wavelength discriminability in *Drosophila* (Hernández de Salomon and Spatz, 1983; Vorobyev and Osorio, 1998). The model predicts discrimination thresholds based on signals in colour opponent channels (Vorobyev and Osorio, 1998). Variants of the model that included signals from inner receptors gave poor fits to the behavioural data (Figure 13A–B), whereas goodness-of-fit was improved when including the outer photoreceptors (Figure 13C). The superior performance of models including the outer photoreceptors was mainly due to the increasing sensitivity slope of Rh1 in the region around 500 nm, where wavelength discrimination is best (Figure 14). Thus, a contribution of the outer photoreceptors to colour vision is necessary to explain the published data on wavelength discrimination in *Drosophila*.

3.1.3 Colour discrimination with restricted photoreceptor sets

To experimentally identify the receptor types responsible for colour discrimination, I generated flies with restricted sets of functional photoreceptors. I used blind mutant flies ($norpA^{7}$) that lack Phospholipase C and restored proper phototransduction by expressing $norpA^{+}$ under UAS-control and by using different combinations of *rhodopsin-GAL4* drivers (Inoue et al., 1985; Wernet et al., 2012). Specificity of GAL4 expression was verified using confocal microscopy (Figure 15). To determine functional rescue of photoreceptors, I recorded the electroretinogram (ERG) of mutant flies with single *rh-GAL4* dependent $norpA^{+}$ expression and control flies. I used the same LED stimulation as in the conditioning experiments (or UV LED for *rh3-GAL4*) and found that targeted $norpA^{+}$ expression with all *rh-GAL4* drivers restored light sensitivity (Figure 16).

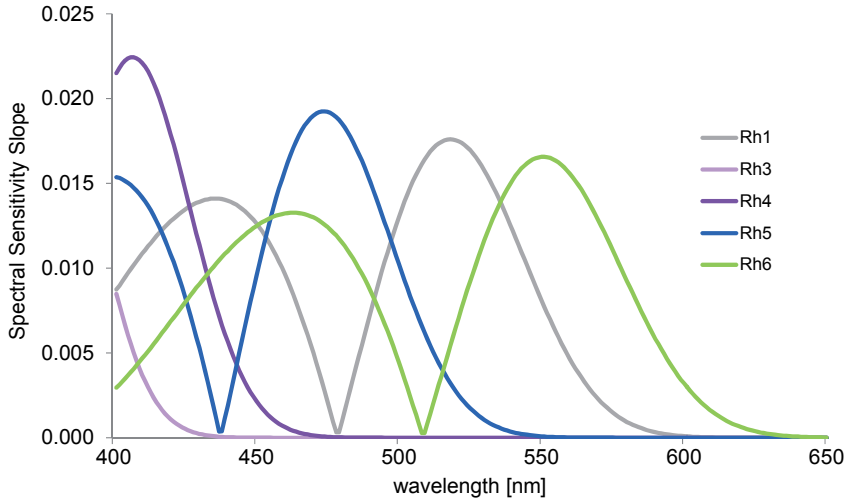

Figure 14 – Slopes of spectral sensitivity curves of the five different Rhodopsins in the *Drosophila* eye (After Salcedo et al., 1999; modified from Schnaitmann et al., 2013) .

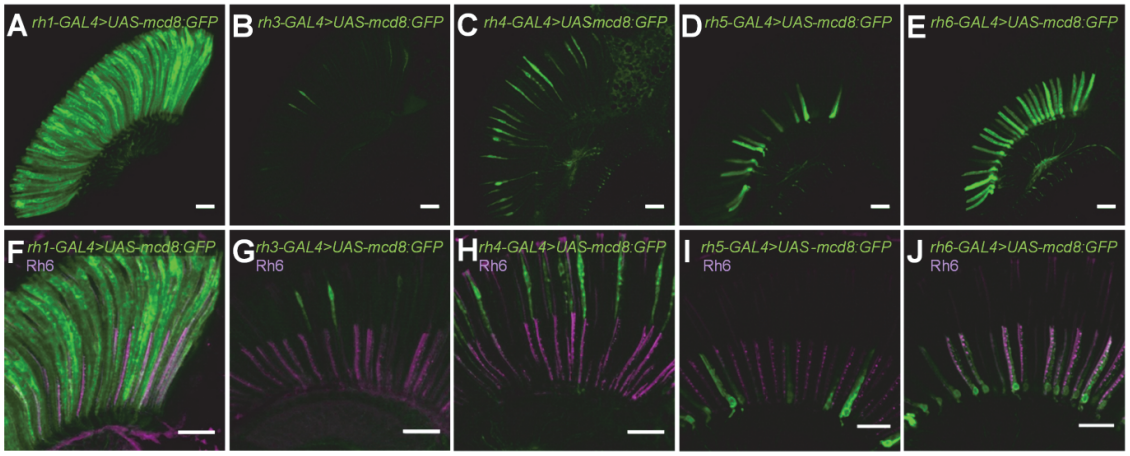

Figure 15 – Expression patterns of the different *rh-GAL4* drivers in the visual system. (**A–J**) Confocal microscopy of the optic lobe (A–E), and the retina (F–J). GAL4 expression patterns (mCD8::GFP, green) are validated using Rh6 immunostaining (magenta) as a reference. All drivers are verified to be specific for the target cells. Scale bars, 20 µm. (Modified from Schnaitmann et al., 2013).

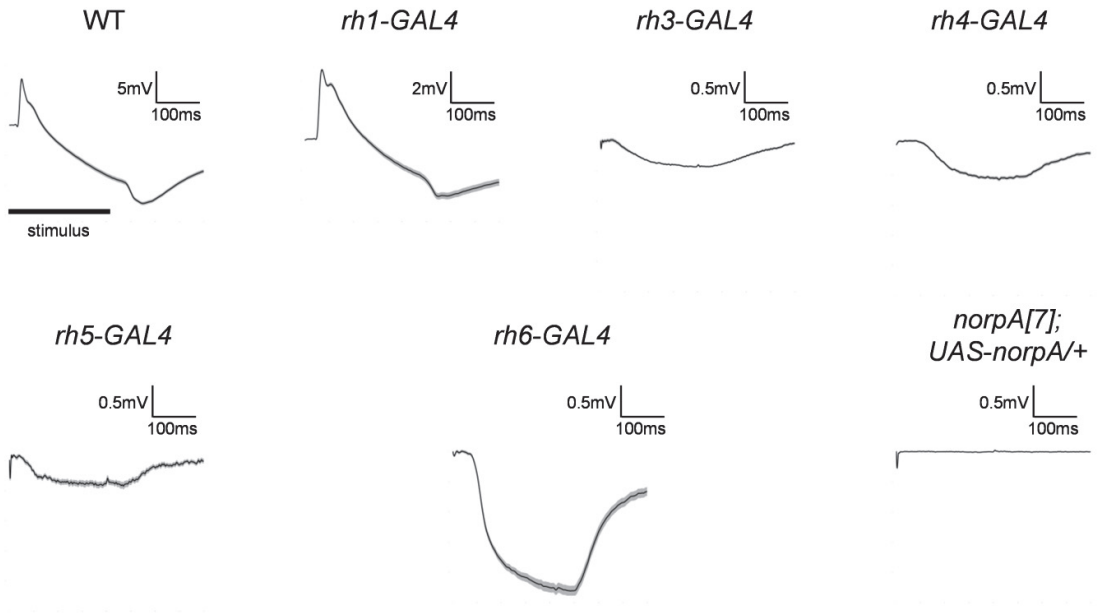

Figure 16 – Targeted *norpA*$^{+}$ expression restores photoreceptor light sensitivity in *norpA*^{7} mutant flies. ERG traces to dark-blue stimulation of *norpA*^{7} mutant flies with targeted expression of *norpA*$^{+}$ using different *rh-GAL4* drivers (n = 4–8 per genotype). For the mutant flies with *rh3-GAL4* dependent *norpA*$^{+}$ expression or without a driver, ERG traces in response to a UV LED (410 nm) or bright-blue are plotted, respectively. (Modified from Schnaitmann et al., 2013).

I targeted *norpA*$^{+}$ expression to all types of photoreceptors combining four *rh-GAL4* drivers in the same *norpA* mutant animal (i.e. *norpA*^{7}*, rh1-GAL4/Y; rh5-GAL4, rh6-GAL4/UAS-norpA; rh3+rh4-GAL4/+*) and examined colour discrimination behaviour of these flies. They fully discriminated bright-blue/bright-green at the wild-type level (Figure 17A) and exhibited a positive learning index under intensity inversion, thus demonstrating true colour discrimination (Figure 17B). I next generated *norpA* mutant flies in which either all photoreceptors in pale (*rh1-*, *rh3-* and *rh5-GAL4*) or yellow (*rh1-*, *rh4-* and *rh6-GAL4*) ommatidia were functional, using targeted *norpA*$^{+}$ expression. Interestingly, targeted *norpA* rescue in all photoreceptors of yellow, but not of pale ommatidia was fully sufficient for bright-blue/bright-green discrimination (Figure 18A). As the sugar preference of the flies with functional pale ommatidia was not impaired (data not shown), I conclude that pale ommatidia alone are not sufficient for the blue/green discrimination task (Figure 18A). They might, however, play a role for discrimination of other spectral stimulus pairs.

To determine the minimal set of photoreceptors for blue/green discrimination, I

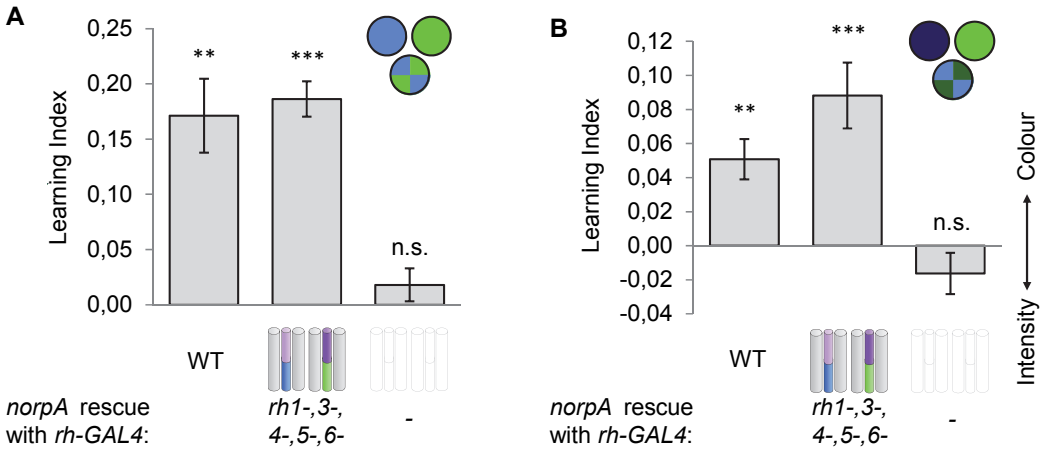

Figure 17 – Targeted *norpA*$^{+}$ expression in all photoreceptors restores colour discrimination in *norpA*^{7} mutant flies. (**A**) The targeted *norpA*$^{+}$ expression in all photoreceptor types fully restores bright-blue/bright-green discrimination learning of *norpA*^{7} mutant flies to the WT level, while *norpA*^{7} mutant flies containing the rescue construct without driver exhibit no significant discrimination (n = 9–17). (**B**) The choice of *norpA*^{7} mutant flies with targeted *norpA*$^{+}$ expression in all photoreceptors is based on colour rather than intensity in the intensity inversion experiment (n = 12–20). Bars and error bars represent means and SEM, respectively (**p < 0.01; ***p < 0.001; ns: no significance). (Modified from Schnaitmann et al., 2013).

generated *norpA* mutant flies with targeted *norpA*$^{+}$ expression in the three pairwise photoreceptor combinations in yellow ommatidia (using *rh1-/rh4-GAL4*, *rh4-/rh6-GAL4*, or *rh1-/rh6-GAL4*). The *norpA* rescue with combinations of *rh1-/rh4-GAL4* or *rh4-/rh6-GAL4* was sufficient to allow discrimination of bright-blue/bright-green (Figure 18B), whereas the *norpA* rescue with *rh1-/rh6-GAL4* was not able to rescue the mutant phenotype (Figure 18B). The mutant flies with functional Rh4-/Rh6-expressing photoreceptor types did not show colour but intensity discrimination in the intensity inversion experiment (Figure 18C). Strikingly, the intensity inversion experiment revealed that both dichromatic flies with either functional Rh1-/Rh4-expressing or Rh4-/Rh6-expressing photoreceptor types allowed spectral discrimination of blue and green stimuli (Figure 18C). Importantly, the ERG experiments showed that the blue/green intensity ratio is within 10-fold in *norpA* rescue flies with *rh1-* or *rh6-GAL4*, assuring the successful intensity inversion with dark-blue and bright-green, and *vice versa*, at the neural level (Figure 19A). Due to the high blue/green sensitivity ratio of Rh4, the dark-blue might be brighter than the bright-green for the flies with functional Rh1-/

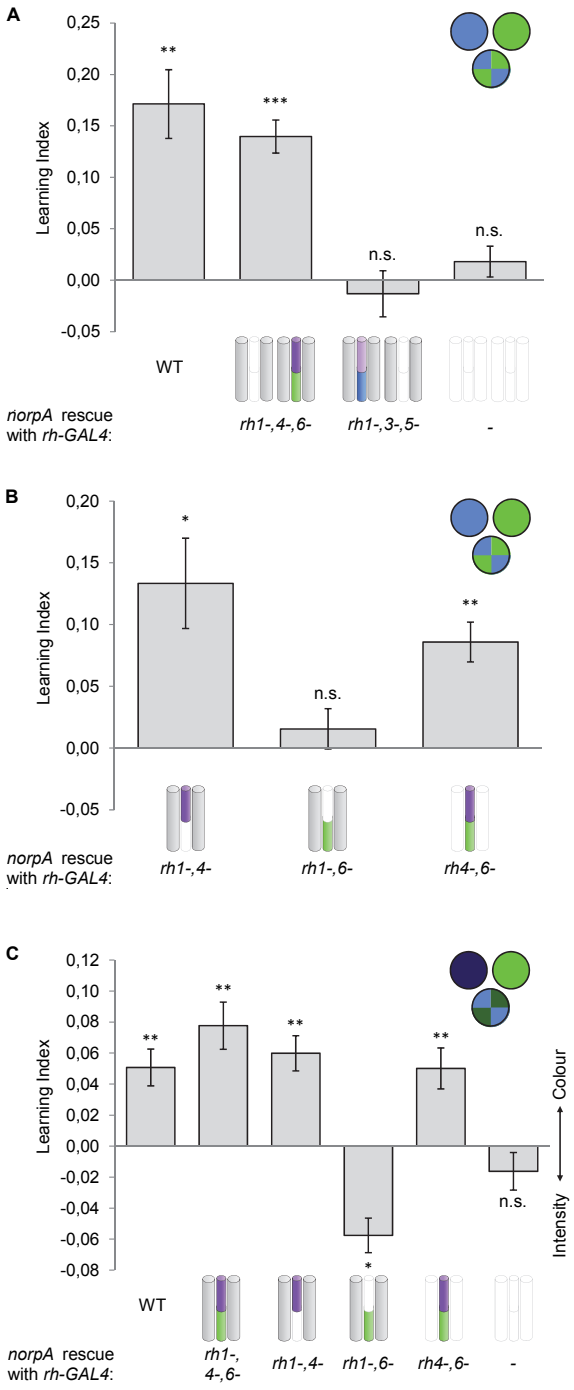

Figure 18 – Minimal sets of photoreceptors for colour discrimination. (**A**) *norpA* rescue flies with functional yellow, but not pale ommatidia, significantly discriminate bright-blue and bright-green (n = 10–17). (**B**) Bright-blue/bright-green discrimination of flies with pair-wise *norpA* rescue in yellow ommatidia. Rescue flies *with rh1-/rh4- or rh4-/rh6-GAL4s* show significant discrimination, while rescue flies with *rh1-/rh6-GAL4* cannot discriminate the stimuli (n = 8–17). (**C**) *norpA*^{7} mutants with targeted *norpA* rescues in the intensity inversion task. Pair-wise *norpA* rescues with *rh1-/rh4-* or *rh4-/rh6-GAL4* show significant colour preference rather than

intensity preference as the wild-type or 'yellow *norpA* rescue' flies. Flies with targeted *norpA* rescue with *rh1-/rh6-GAL4* significantly choose the intensity cue (n = 12–30). For WT and *norpA*^{7}*;UAS-norpA/+* in (A), and (C), the same data is plotted as in Figure 17. Bars and error bars represent means and SEM, respectively (*p < 0.05; **p < 0.01; ***p < 0.001; ns: no significance). (From Schnaitmann et al., 2013).

Rh4-expressing photoreceptor types (Figure 19A), potentially confounding the interpretation of the result (Figure 18C). I therefore performed an intensity inversion experiment where the intensities of dark-blue and bright-green during training were matched for Rh4 according to the ERG measurements (Figure 19B). Flies with functional Rh1-/Rh4-expressing photoreceptor types still used the colour cue under this condition (Figure 20A). Flies without functional photoreceptor types or with functional Rh4-expressing photoreceptor types only did not show colour discrimination (Figure 20B), confirming that a neuronal comparison of

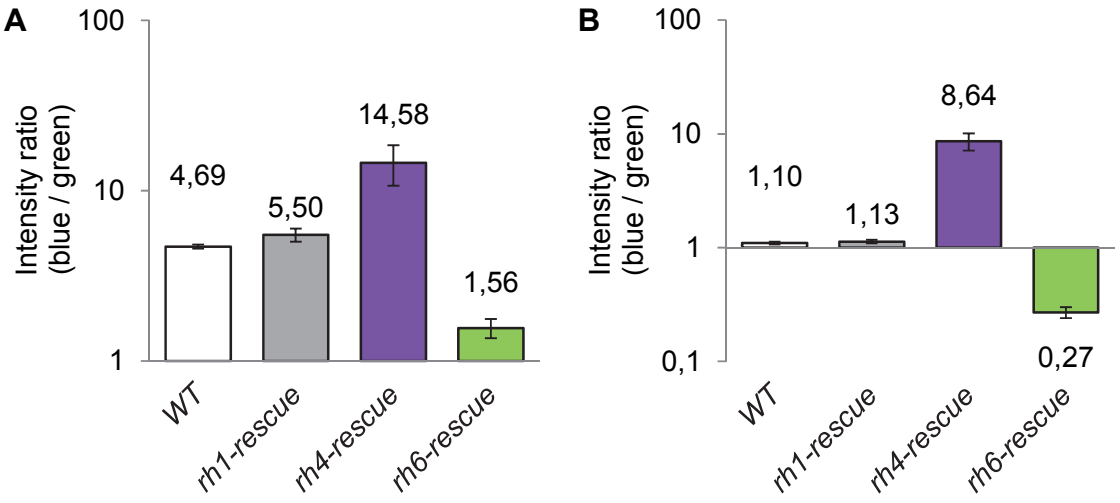

Figure 19 – Intensity ratios of blue/green stimulations in *norpA* rescue flies with single *rh-GAL4* driver. Intensities of blue and green LEDs required to elicit same-amplitude responses in the *norpA* rescue flies are measured using a modified light-clamp ERG technique (Garbers et al., 2012). Accordingly, the plotted blue/green stimulus intensity ratios are calculated for (**A**) the used RGB LEDs and (**B**) blue/green LEDs used in the experiments in Figure 20 (n = 4–8). Note that these values must be within 10-fold (between 0.1 and 10) for an intensity inversion experiment with a particular photoreceptor type. Bars and error bars represent means and standard deviation, respectively. (Modified from Schnaitmann et al., 2013).

multiple receptor outputs is required for colour vision. Altogether, these results challenge the assumption that R7/R8 provide the only input to colour vision in flies (Pichaud et al., 1999; Troje, 1993), and demonstrate that both outer and inner photoreceptors contribute to colour vision. The qualitative difference in discrimination behaviour exhibited by flies with either functional Rh1-/Rh4-expressing or Rh1-/Rh6-expressing photoreceptor types suggests differential computation underlying the signal integration of the outer photoreceptors and the different inner photoreceptor types (i.e. R7 and R8).

As *norpA* rescue in Rh4-/Rh6-expressing photoreceptor types resulted in successful colour discrimination (Figure 18C), I conclude that, R1–R6 photoreceptors are not required for blue-green discrimination under the tested conditions. To further substantiate this

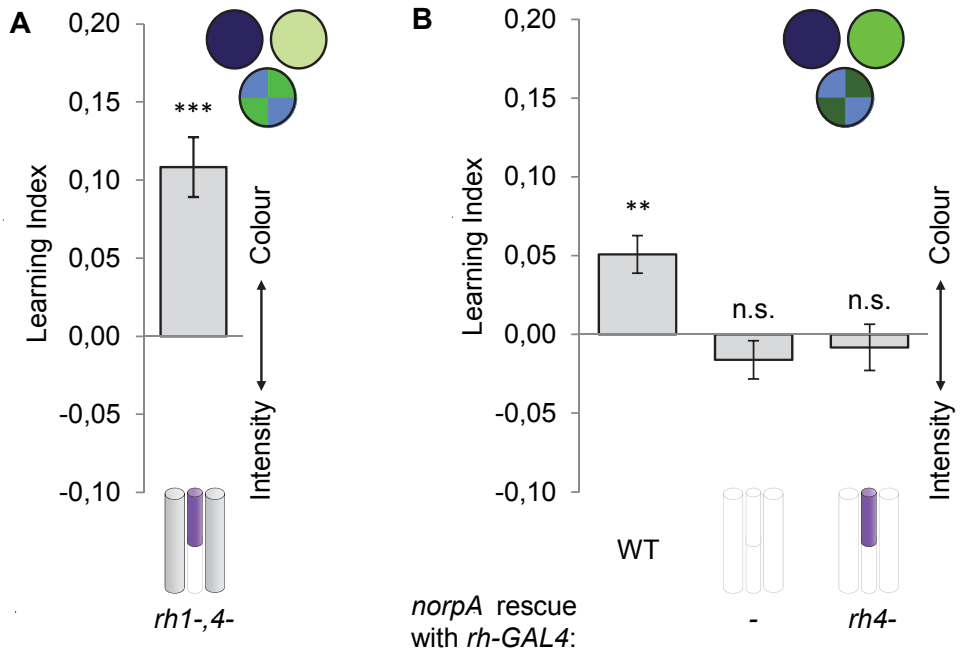

Figure 20 – Colour discrimination in flies with *norpA* rescues in Rh4- or Rh1-/Rh4-expressing photoreceptor types. (**A**) *norpA*^{7} rescue flies with *rh1-*, *rh4-GAL4* discriminate colour in the intensity inversion experiment, where the green stimulus is adjusted according to the ERG such that Rh4-expressing receptors respond equally to the dark-blue and bright-green (n = 13). (**B**) No significant colour learning is observed in the intensity inversion experiment using *norpA* rescue with only *rh4-GAL4* (n = 14–19). For WT, and *norpA*^{7}*;UAS-norpA/+* in (B), the same data is plotted as in Figure 17. Bars and error bars represent means and SEM, respectively (*p < 0.05; **p < 0.01; ***p < 0.001; ns: no significance). (From Schnaitmann et al., 2013).

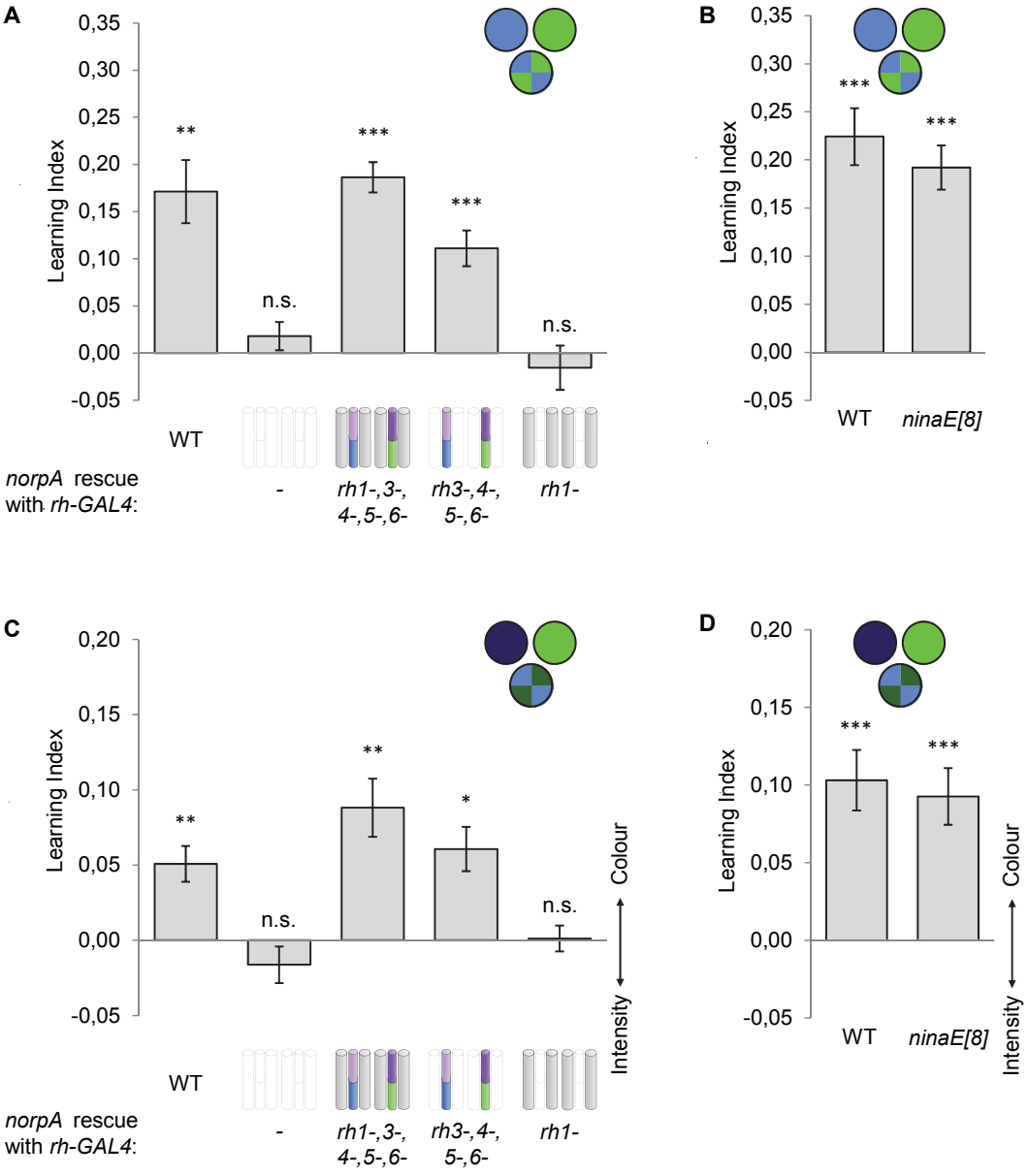

Figure 21 – Rh1 is not necessary for blue-green discrimination under the tested conditions. (**A**) Flies with *norpA* rescue in all photoreceptors or all inner photoreceptors show significant bright-blue/bright-green discrimination, while flies with rescue in the outer photoreceptors only cannot discriminate these stimuli (n = 11–20). (**B**) *ninaE*^{8} flies that lack functional outer photoreceptors show significant bright-blue/bright-green discrimination (n = 8–20). (**C**) The *norpA*-rescue in all photoreceptors or inner photoreceptors discriminate colour in the intensity inversion experiment, while the rescue in the outer photoreceptors failed (n = 11–21). (**D**) *ninaE*^{8} flies show significant discrimination in the intensity inversion experiment (n = 11–20). For WT, *rh1-,3-,4-,5-,6-GAL4-norpA*-rescue, and *norpA*^{7}*;UAS-norpA/+* in (A) and (C), the same data is plotted as in Figure 17. Bars and error bars represent means and SEM, respectively (*p < 0.05; **p < 0.01; ***p < 0.001; ns: no significance). (From Schnaitmann et al., 2013).

result, I tested flies with *norpA* rescue in all inner photoreceptors or only outer photoreceptors (Figure 21) in the blue-green and intensity inversion tasks. Targeted *norpA r*escue in the inner photoreceptors resulted in significant blue-green discrimination, whereas *norpA* rescue in the outer photoreceptors did not yield significant discrimination (Figure 21A, C). I also tested $ninaE^{8}$ mutants that lack *rh1* expression and functional outer photoreceptors with minimal degeneration of these (Kumar and Ready, 1995). In both the standard blue-green task as well as in the intensity inversion task, these flies did not show blue-green discrimination different from the wild type control (Figure 21B, D). Thus, using the described stimuli and paradigms, all my so far described experiments suggest that R1–R6 are not necessary for blue-green discrimination.

3.1.4 The blockade of lamina monopolar cells selectively impairs colour discrimination

The outer photoreceptors, unlike the inner photoreceptors, terminate in the lamina neuropil (Figure 22A). The three lamina monopolar cells (LMCs; L1, L2 and L3) convey the outputs of the outer photoreceptors directly to different layers of the medulla, where visual information of inner and outer photoreceptors converges (Fischbach and Dittrich, 1989; Meinertzhagen and O'neil, 1991) (Figure 22A). To examine the role of L1–L3 in colour discrimination, I blocked the output of these LMCs using ort^{C2}*-GAL4* (Gao et al., 2008) and *UAS-*shi^{ts1} (Kitamoto, 2001). Strikingly, this blockade caused a severe impairment in bright-blue/bright-green discrimination (Figure 22B). Intact intensity discrimination showed that appetitive visual memory and behavioural expression were not defective (Figure 22C). As ort^{C2}*-GAL4* additionally labels Dm8, amacrine cells in the medulla that receive R7 output (Gao et al., 2008) (Figure 22A), I examined a split-GAL4 driver *vglut*$\cap ort^{C2}$*-GAL4* to express shi^{ts1} specifically in Dm8 neurons as well as in a small number of L1 neurons and glia-like cells (Gao et al., 2008). These flies did not show any impairment in the bright-blue/bright-green discrimination (Figure 22D). Furthermore, I blocked LMCs with another GAL4 driver, *R48A08-GAL4*, that strongly labels L1 and L2, as well as two unknown cell types in the medulla (Tuthill et al., 2013). *R48A08-GAL4/UAS-*shi^{ts1} flies were severely impaired in discriminating bright blue and bright green, while their intensity discrimination was intact (Figures 22E–F). Thus, I conclude that the LMCs are selectively required for blue/green discrimination.

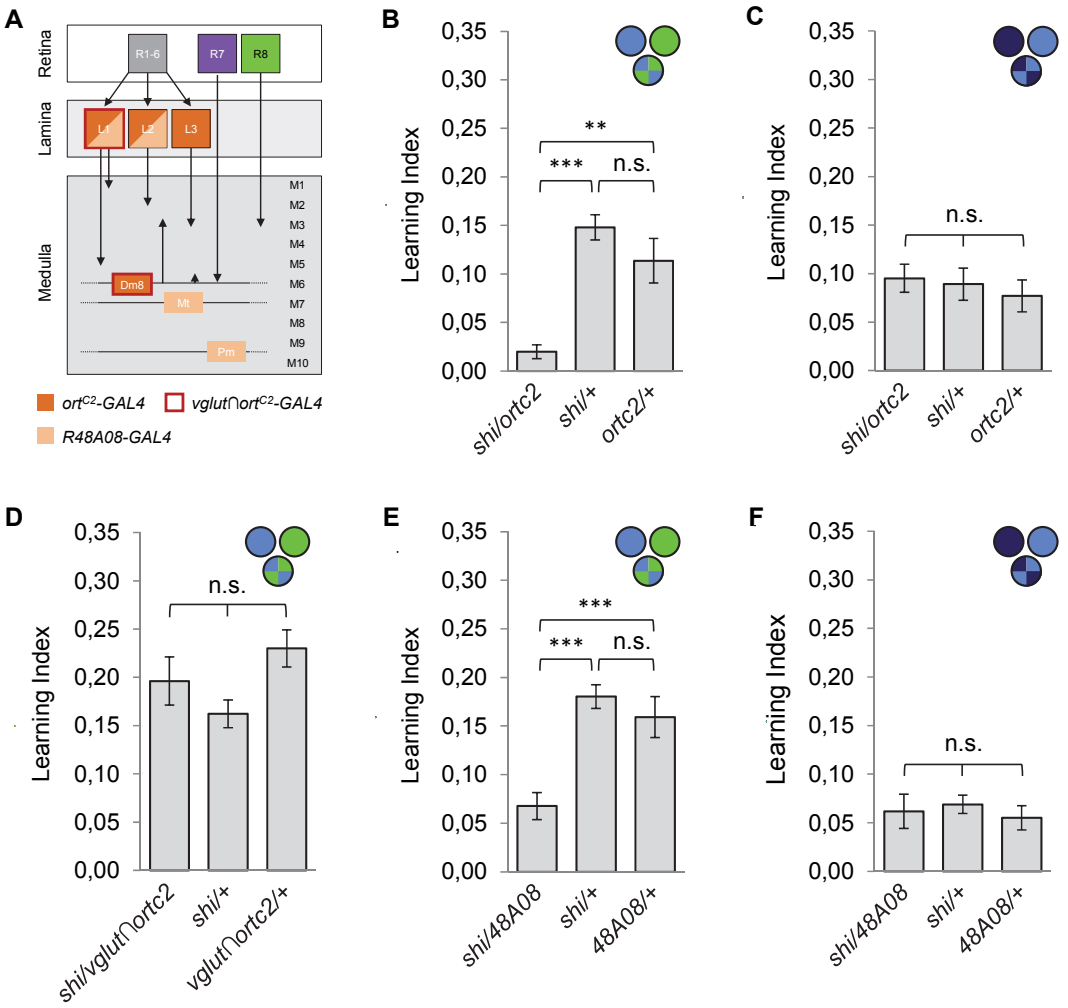

Figure 22 – Lamina monopolar cells are required for colour discrimination. (**A**) L1, L2, and L3 receive direct input from the outer photoreceptors R1–R6 and convey their signals to different layers in the medulla. Outputs of inner and outer receptors can converge in the medulla as well as in the downstream lobula complex. Cells labelled by the GAL4 drivers used in the blocking experiments are coloured with dark orange or light orange or red outline (Dm8, distal medulla cell type; Mt, medulla tangential cell type; Pm, proximal medulla cell type). (**B**) Blocking L1–L3 and Dm8 with *UAS-shi^{ts1}* and *ortC2-GAL4* specifically impaired bright-blue/bright-green discrimination (n = 13–18). (**C**) Intensity discrimination is not impaired with the same blockade (n = 15–16). (**D**) Blocking Dm8 and a few L1 cells with the split-GAL4 driver vglut∩ortC2-GAL4 does not significantly impair bright-blue/bright-green discrimination (n = 12–19). (**E**) Bright-blue/bright-green discrimination is significantly impaired by blocking L1, L2, and two other cell types with R48A08-GAL4 (n = 8–13). (**F**) Intensity discrimination is not impaired with the same blockade (n = 17–23). Bars and error bars represent means and SEM, respectively (**p < 0.01; ***p < 0.001; ns, no significance). (From Schnaitmann et al., 2013).

3.2 Neural circuits underlying reinforcement signalling of visual memories

3.2.1 A new behavioural assay for visual aversive memory

I previously developed an appetitive visual learning assay (Figure 23A–B, Schnaitmann et al., 2010). In this assay with modified visual stimulation, the visual stimuli (LEDs; Fig 23D) are projected from below through translucent sugar-soaked filter paper, the appetitive reinforcer used in olfactory conditioning. However, to contrast both appetitive and aversive visual memories a paradigm with a potent aversive reinforcer is required. While conditioning with formic acid yielded significant aversive visual memory in the assay (Schnaitmann et al., 2010), neurogenetic analyses might be difficult due to the low signal to noise ratio of the flies' performance. As electric shock is a widely used potent aversive reinforcer, also for olfactory conditioning (Quinn et al., 1974; Tully and Quinn, 1985), I aimed at integrating such stimulation into the assay. This would also allow optimal comparison of visual and olfactory memories, due to the shared reinforcement. The integration of electric shock appeared difficult, as a metal grid beneath the fly would prevent the same visual stimulation from below as in appetitive conditioning. I solved this problem by fabricating a shock grid from a transparent low-resistance material, indium tin-oxide (ITO; Figure 23B, C). An alternating electrode pattern was laser-etched into a thin layer of ITO on a glass plate (Figure 23E). Other parameters of the assay were replicated from the appetitive conditioning setup, except that the height of the arena was reduced so that flies could not escape the electric shock.

To characterize shock punishment using the transparent grid, I subjected flies to visual conditioning with four training trials as for appetitive training. During one training trial, spectrally different stimuli (green/blue colour) were presented alternately for one minute each to the flies, one of them paired with electric shock (see Materials and Methods). This punishment proved a potent aversive reinforcement. Aversive visual memory was induced at a signal to noise ratio comparable to visual appetitive memory as well as visual memory in other paradigms (Figure 23F–G). Together with the previously developed appetitive memory assay, these behavioural paradigms allow me to compare the neural requirements of appetitive and aversive visual memory. As these assays share critical features with appetitive and aversive assays for olfactory conditioning (i.e. reinforcing stimuli and behavioural tasks), visual and olfactory memories can now also be optimally compared.

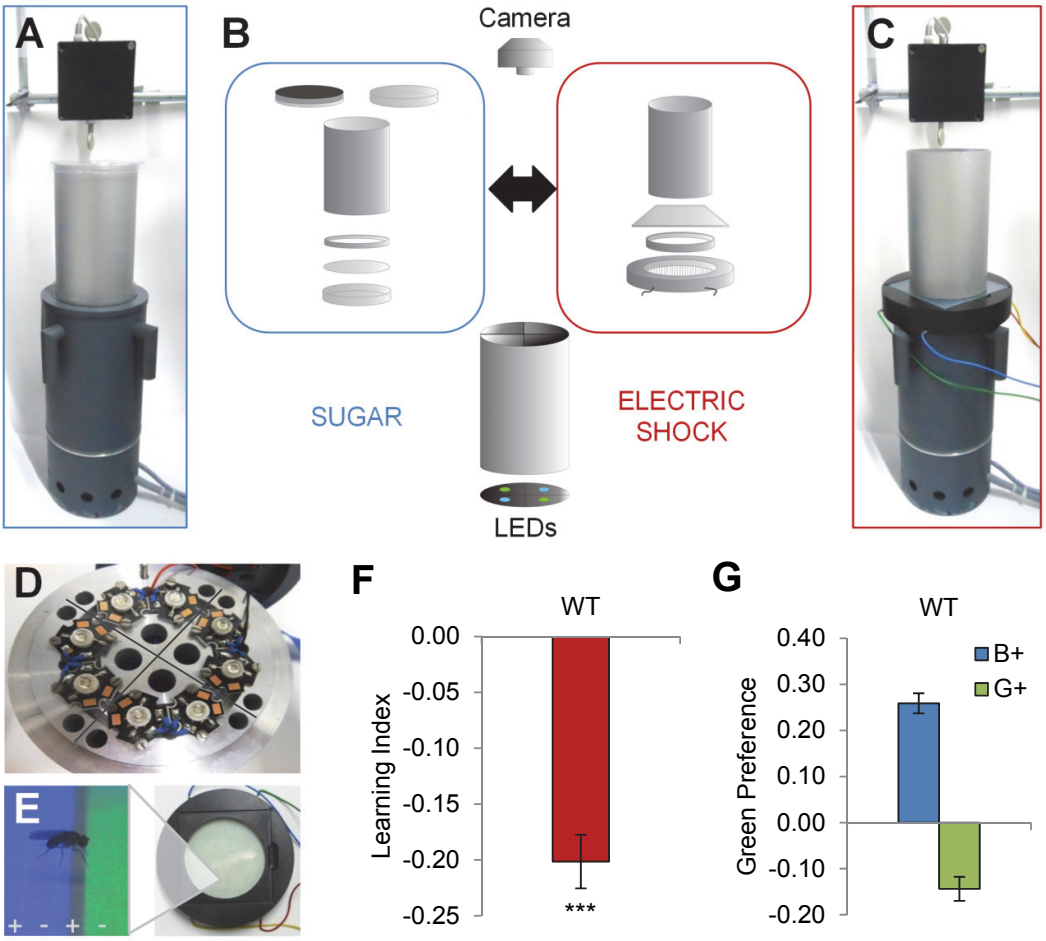

Figure 23 – A modular setup for the analysis of appetitive and aversive visual learning. (**A**–**C**) Experimental setups for appetitive and aversive visual learning. (**B**) Close up of critical components: exchangeable conditioning arenas for sugar reward (**A**) and electric shock punishment (**C**) share the same light source and video camera (**B**). (B) Appetitive conditioning setup: cylindrical Fluon-coated arena is closed at the top with opaque lid during training or transparent lid during test. An easily exchangeable Petri dish on the bottom is used to present sugar or water soaked filter paper during training and neutral filter paper during test. Filter paper is clamped in the dish by a plastic ring. Aversive conditioning setup: the circular arena consists of a transparent electric shock grid, removable Fluon-coated plastic ring and transparent lid. The cylinder on top isolates each setup from the others and creates a similar visual stimulation as in the appetitive setup. (**D**) Visual stimulus source with one blue and one green high power LED per quadrant. (**E**) The conditioning arena with the transparent electric shock grid and a magnification with visual stimulation and a fly. Electrode placement is indicated by + and – symbols. (**F**) Aversive memory comparable to appetitive memory is found when wildtype CS is trained four times with 60V electric shock (n = 18). (**G**) Green preference during test underlying data in (F). Flies prefer the green stimulus less when electric shock was paired with green (G+) in contrast to when paired with blue (G+) during training (n = 18). Bars and error bars represent mean and SEM, respectively (***p < 0.001).

3.2.2 Different sets of dopamine neurons are required for visual appetitive and aversive memory acquisition

Given the importance of monoamine neurons in memory formation (Aso et al., 2012; Burke et al., 2012; Claridge-Chang et al., 2009; Liu et al., 2012; Schwaerzel et al., 2003; Sitaraman et al., 2012), I blocked distinct sets of aminergic neurons by expressing shi^{ts1} (Kitamoto, 2001) and assessed these neurons' role in appetitive and aversive visual memories. To target these aminergic neurons, I chose *TDC2-GAL4*, *TH-GAL4* and *DDC-GAL4* driver lines that label different subsets of tyramine/octopamine and dopamine neurons (Cole et al., 2005; Friggi-Grelin et al., 2003; Li et al., 2000). I found that the requirements of these neurons for appetitive and aversive visual memories are strikingly similar to those in olfactory memories. Blocking octopamine/tyramine neurons with *TDC2-GAL4* did not cause a significant defect in sugar or shock memory (Figure 24A). In contrast, the blockade of a large fraction of dopamine neurons with *TH-GAL4* selectively reduced aversive memory (Figure 24A, see Table 2 for controls). As in olfactory learning (Liu et al., 2012), the blockade with *DDC-GAL4* that labels different sets of dopamine and serotonin neurons substantially impaired appetitive memory, but not aversive memory (Figure 24A, see Table 2 for controls).

I next analysed the temporal requirements for neurons labelled in *TH-GAL4* and *DDC-GAL4* in the learning paradigm. I measured visual memories for 30-min retention and transiently blocked the neurons either during training (Figure 24B) when reinforcers were presented or during retrieval of the memory (Figure 24C). The blockade with *DDC-GAL4* during training severely impaired appetitive memory, whereas the same blockade after the training did not significantly affect memory (Figure 24D–E). Similarly, the neurons labelled in *TH-GAL4* were required specifically during acquisition of aversive memory (Figure 24F–G). These results suggest that the neurons differentially labelled with *DDC-GAL4* and *TH-GAL4* mediate the formation of appetitive and aversive visual memories, likely acting as reinforcement signals. As specific subsets of dopamine neurons in *TH-GAL4* and *DDC-GAL4* have been shown to signal sugar reward and shock punishment for olfactory memories (Aso et al., 2012; Burke et al., 2012; Claridge-Chang et al., 2009; Liu et al., 2012), I genetically dissected these populations further to identify the essential neurons for visual memories.

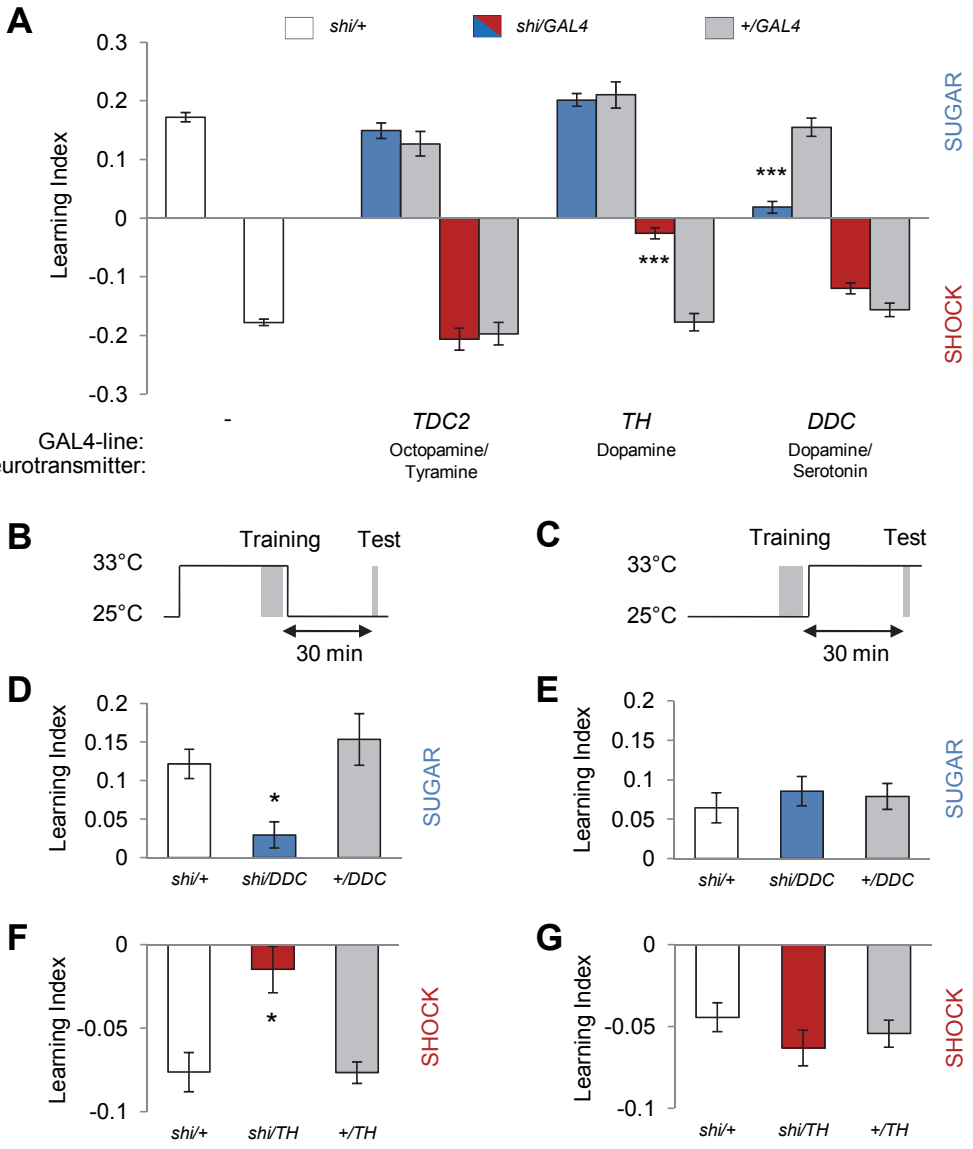

Figure 24 – Different dopamine neurons are required for appetitive and aversive memory acquisition. (**A**) Different aminergic neurons are continuously blocked with corresponding GAL4 drivers. The blockade with *TH-GAL4* and *DDC-GAL4* selectively impairs aversive and appetitive memories, respectively. Blocking octopamine and tyramine neurons does not significantly impair memory (n = 8–61). (**B–C**) Scheme of the temperature shift to block the output of corresponding neurons during training (**B**) or test (**C**). (**D–E**) Output of *DDC-GAL4* labelled neurons is only necessary in appetitive training but dispensable during test (n = 13–38). (**F–G**) Similarly, output of *TH-GAL4* labelled neurons is only necessary during aversive training but dispensable during test (n = 12–16). Memory of the experimental group is compared to the performance of the corresponding control group. Only the most conservative statistical result of multiple pairwise comparisons is stated. Bars and error bars represent mean and SEM, respectively (*p < 0.05; ***p < 0.001).

Genotype	Sugar Response Mean +/- SEM	Shock Response Mean +/- SEM	p<0,05
shi/+	-	-0.429 +/- 0.056	
shi/TH	-	-0.189 +/- 0.019	*
+/TH	-	-0.386 +/- 0.060	
shi/MB504B	-	-0.382 +/- 0.041	
+/MB504B	-	-0.385 +/- 0.051	
shi/+	0.718 +/- 0.020	-	
shi/DDC	0.729 +/- 0.027	-	
+/DDC	0.725 +/- 0.017	-	
shi/+	0.436 +/- 0.053	-	
shi/R58E02	0.544 +/- 0.033	-	
+/R58E02	0.563 +/- 0.036	-	
CS	0.547 +/- 0.041	-0.471 +/- 0.044	
$dumb^2$	0.634 +/- 0.042	-0.289 +/- 0.031	*
$dumb^2$/MB247, $dumb^2$	-	-0.255 +/- 0.028	*
+/MB247	-	-0.452 +/- 0.067	

Table 2 – Sugar and shock responses of the lines with impaired visual memories. No significant defect in naïve sugar preference is detected among the experimental groups and the corresponding control groups (one-way ANOVA, $p > 0.05$) ($n = 8$). No significant difference in naïve shock avoidance is detected among the experimental groups and the corresponding control groups (one-way ANOVA, $p>0.05$), except for *shi/TH*, $dumb^2$ and $dumb^2$/MB247,$dumb^2$ (one-way ANOVA, *post-hoc* pairwise comparisons, $p<0.05$) ($n = 6–10$). Consistent with a study by Lebestky et al. (Lebestky et al., 2009), I observed prolonged arousal after shocking these flies, and this hyperactivity rather than shock sensitivity is a likely cause of the reduced avoidance. Indeed, the $DopR^+$ expression in the MB rescues visual memories, even though shock avoidance is still impaired.

3.2.3 Dopamine neurons of PAM and PPL1 clusters projecting to the MB are necessary and sufficient for appetitive and aversive memories, respectively.

To functionally restrict the neurons in *DDC-GAL4* and *TH-GAL4* into smaller subsets, I selected two specific driver lines for dopamine neurons: *MB504B* and *R58E02*. *R58E02-GAL4* drives GAL4 expression in the PAM cluster neurons that signal reward for olfactory

memory (Figure 25A, C; Liu et al., 2012). This driver co-expresses with *DDC-GAL4*, but rarely with *TH-GAL4,* in the PAM cluster (Liu et al., 2012). *MB504B* is a split-GAL4 line labelling four individual dopamine neurons in the PPL1 cluster: MB-MP1, MB-MV1, MB-V1, and the neuron that projects to the tip of the alpha lobe (Figure 25B). These neurons are a subset of *TH-GAL4* and have been shown, using a less specific line, to induce aversive olfactory memory (Aso et al., 2012). I found that the blockade of these neurons with shi^{ts1} indeed impaired the corresponding aversive or appetitive visual memories (Figure 25C-D). However, the different blocks of synaptic transmission did not significantly affect the reflexive choice of sugar and shock (Table 2), and the flies could discriminate the visual stimuli due to a significant bias in green preference during the test (data not shown). These results demonstrate that visual and olfactory memories share neuronal substrates for appetitive and aversive reinforcements.

To examine whether the activity of these neurons directly drives memories, or carries a regulatory role, I exerted direct control over neuronal activity with *R58E02-GAL4* and *MB504B-GAL4* using a temperature-sensitive cation channel dTRPA1 (Hamada et al., 2008). I paired one of the visual stimuli with thermo-activation of GAL4-expressing neurons by raising ambient temperature to 31 °C and subsequently measured the flies' colour preference (Figure 25E). Thermo-activation of the PAM and PPL1 cluster neurons with *R58E02-GAL4* and *MB504B-GAL4* was sufficient to induce appetitive and aversive memories, respectively (Figure 25F–G). From these results I conclude that these different subsets of dopamine neurons supply appetitive and aversive reinforcement information for visual as well as olfactory memories.

Consistent with results from the block of dopamine neurons, I found severe appetitive and aversive visual memory defects in the mutant for DopR ($dumb^2$; Kim et al., 2007), a D1-like dopamine receptor (Figure 25G, see Table 2 for controls). As both the PAM neurons in *R58E02-GAL4* and the PPL1 neurons in *MB504B-GAL4* terminate in the MBs (Figure 25A-B), I hypothesized that their output is transmitted to MB intrinsic neurons, Kenyon cells (KCs) through DopR. To express $DopR^+$ in the mutant background, I made use of the PiggyBac insertion mutant ($dumb^2$) that contains UAS in at the first intron of the *DopR* gene allowing GAL4-dependent expression of the gene (Kim et al., 2007). Selective expression of $DopR^+$ in the KCs using *MB247-GAL4* significantly rescued the memory defect of the mutant (Figure 25H). Altogether, these results suggest that the same sets of dopamine neurons convey reward and punishment signals to the MBs to induce appetitive and aversive memories of the different sensory modalities.

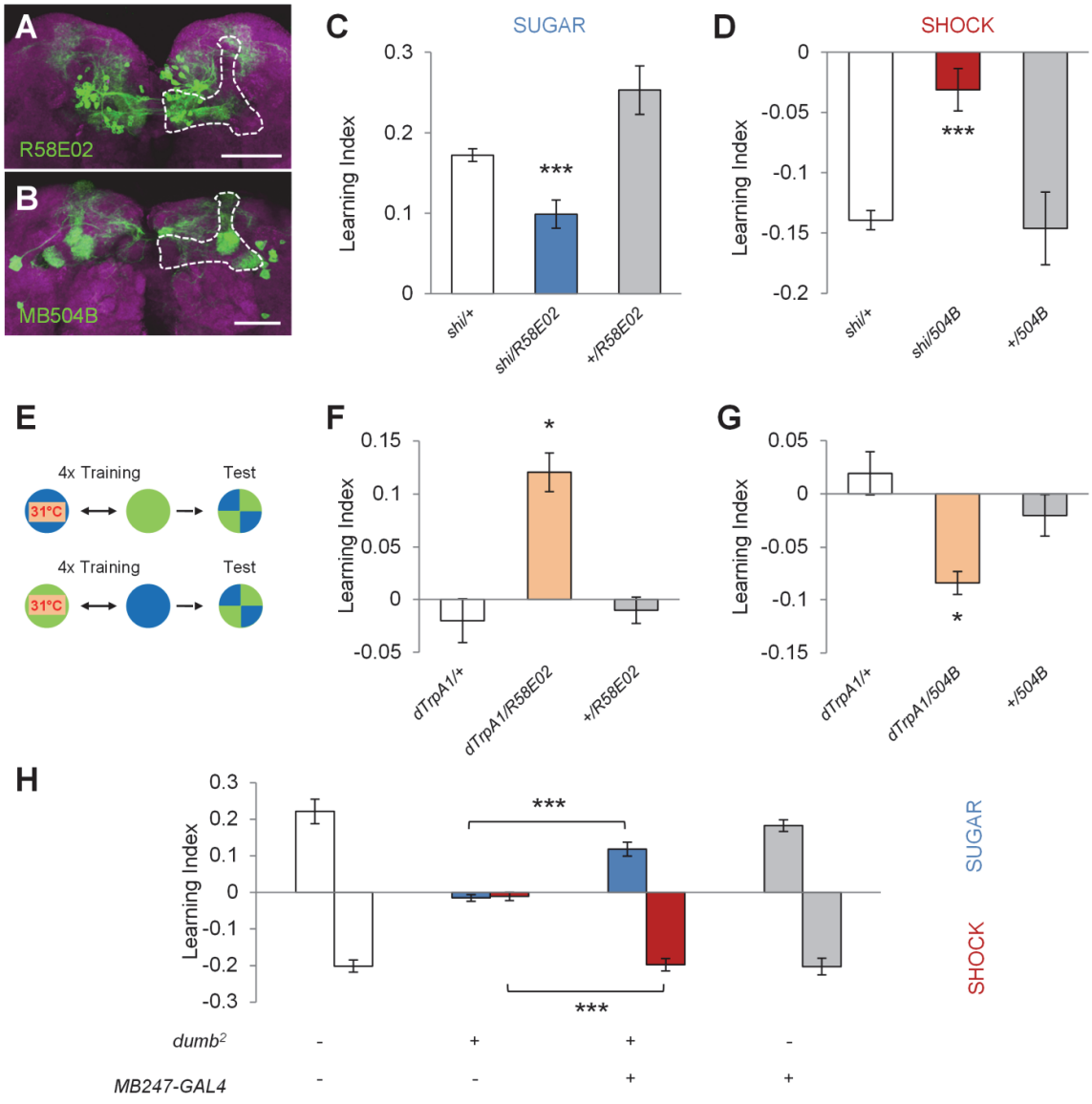

Figure 25 – PAM and PPL1 dopamine neurons projecting to the MB are necessary and sufficient for appetitive and aversive memories, respectively. (**A**–**B**) Expression patterns of *R58E02-GAL4* and *MB504B-GAL4* in the MB region (outlined) are visualized by mCD8::GFP (green) with neuropil counterstaining with synapsin antibody (magenta). Scale bar = 50 µm. (**C**–**D**) Blocking *R58E02* (**C**) and *MB504B* (**D**) subsets of dopamine neurons impairs appetitive and aversive memories, respectively (n = 11–21). (**E**) Scheme of TrpA1 activation used to substitute reinforcement stimuli. One visual stimulus is paired with temperature elevation (31 °C) during training, leading to activation of *dTrpA1*-expressing neurons. (**F**–**G**) Thermo-activation with R58E02 and MB504B induces appetitive and aversive visual memories, respectively (n = 6–18). (**H**) Expression of DopR+ in the MB restores both forms of visual memory of the *dumb*^{2} mutant (n = 8–16). Bars and error bars represent mean and SEM, respectively (*$p < 0.05$; ***$p < 0.001$).

4. Discussion

4.1 Peripheral neural circuits underlying colour discrimination

4.1.1 A new behavioural assay for colour discrimination in flies

While innate phototactic choice has been employed to study spectral preference in *Drosophila* (Fischbach, 1979; Gao et al., 2008; Karuppudurai et al., 2014; Yamaguchi et al., 2010), it is unknown whether this behaviour is related to 'true' colour vision (Menzel and Greggers, 1985). I therefore chose visual discrimination learning – a behavioural paradigm that allows to control intensity invariance (Bicker and Reichert, 1978; Kelber et al., 2003; Menne and Spatz, 1977; Tang and Guo, 2001). I successfully established a new behavioural assay that allows contrasting colour and intensity discrimination in *Drosophila* using a previously developed setup (Schnaitmann et al., 2010), which was further improved to allow narrow-band spectral stimulation with LEDs. When flipping the intensities of the colour stimuli between training and test up to one order of magnitude, flies still showed significant preference for the reinforced colour stimulus, indicating proper colour discrimination independent of intensity (Figure 12B–C). This is further supported by ERG recordings which served to control the response of the diverse photoreceptor cell types in the retina in response to the used stimulation (Figure 19).

Colour discrimination in the here presented assay was restricted to blue/green stimuli. By exchanging the LEDs, the analysis of colour discrimination can be easily extended to the whole spectral range from UV to red light. Especially UV discrimination would be interesting to study, because flies have three photoreceptor types being sensitive in the UV (both R7s and R1–R6). These are excellent prerequisites for high acuity UV discrimination. Indeed, Hernández de Salomon and Spatz (Hernández de Salomon and Spatz, 1983) showed in their aversive visual conditioning assay that flies have second best colour discrimination around 420 nm, though shorter UV discrimination was not tested.

This assay has many similarities with the visual aversive learning paradigm developed by Menne and Spatz (Menne and Spatz, 1977), where coloured illumination of an arena was paired with vigorous shaking as aversive reinforcement. Similar to their setup, the entire arena was illuminated, and freely moving flies were handled as a group. Since Menne and Spatz also applied differential conditioning and a discrimination task, this paradigm was successfully used in studies of colour vision in *Drosophila* (Bicker and Reichert, 1978; Hernández de Salomon and Spatz, 1983; Menne and Spatz, 1977). For unknown reasons,

colour/intensity memories have not been studied using this assay since. Furthermore, the here presented study is since decades the only reported study about the neural mechanisms underlying 'true' colour vision in *Drosophila*. Thus, the newly developed behavioural assay has the potential to finally advance the neurogenetic analysis of colour vision in flies.

4.1.2 Outer and inner photoreceptors contribute to colour discrimination

Combining modelling with genetic manipulations and behavioural experiments, I identified the photoreceptor types for blue/green discrimination in *Drosophila* (Figures 14, 19). Interestingly, I could find significant blue/green discrimination in transgenic flies with only yellow but not in flies with only pale ommatidia (Figure 19A). Therefore, Rh1, Rh4 and/or Rh6, the latter two been found only in yellow ommatidia, must play a crucial role in blue/green discrimination. Indeed, *norpA* rescue flies with either dichromatic combination of Rh1-/Rh4- or Rh4-/Rh6-expressing photoreceptor types only were able to spectrally discriminate blue and green stimuli. In contrast, flies with functional Rh1-/Rh6-expressing photoreceptor types only were not able. The difference in discrimination abilities of flies with dichromatic *norpA* rescues in Rh1-/Rh4- or Rh1-/Rh6-expressing photoreceptor types suggests differential computation underlying the signal integration of the outer photoreceptors and the different inner photoreceptor types (i.e. R7 and R8). These results also point out that R7 (Rh4) is critical for blue/green discrimination and can be used either together with R1–R6 (Rh1) or R8 (Rh6) (Figure 18C). Furthermore, these findings indicate that post-receptoral computations within the same optic cartridge underlie colour vision (Morante and Desplan, 2008). In an optic cartridge all three photoreceptor types could thus feed into opponent mechanisms of downstream cells. Such columnar trichromacy may therefore be identified in future studies.

While flies with only pale ommatidia were not able to discriminate blue and green, this ommatidium type (with Rh3 and Rh5 in R7 and R8, respectively) might however be involved in colour discrimination at presumably shorter wavelengths. Furthermore, Rh3 and Rh5 derived signals might be compared to signals from photoreceptors in yellow ommatidia (inter-cartridge comparison). Alternatively, pale ommatidia might not underlie colour vision but mediate a specific behaviour like e.g. innate phototaxis. Such functional specialization is found for DRA ommatidia in flies (Wernet et al., 2012) and ommatidia types in other insects like butterflies (Koshitaka et al., 2008).

These findings redress the longstanding hypothesis that solely narrow-band inner photoreceptors mediate colour vision (Pichaud et al., 1999; Troje, 1993). Sufficiency of the opsin pair Rh1-Rh4 for blue-green colour discrimination indicates that receptors with a complex and broad spectral sensitivity can provide information on the wavelength composition of a visual stimulus. Considering the sufficiency of inner photoreceptors for blue/green discrimination (Figure 19, 21), the role of the outer photoreceptors may be to create an additional opponency dimension for enhanced colour discrimination. This assumption is supported by the here presented computational model which revealed that the contribution of the outer photoreceptors to colour vision is necessary to explain the published data on wavelength discrimination in *Drosophila* (Figure 13). The outer photoreceptors have predominant functions in achromatic vision, such as motion detection (Heisenberg and Buchner, 1977; Yamaguchi et al., 2008). Yet, exploitation of the outer photoreceptor pathway for multiple visual functions is advantageous, in particular for animals with limited neuronal resources. The recently discovered contribution of *Drosophila* R7/R8 to motion detection further supports our hypothesis of photoreceptors being used for multiple computational tasks instead of single use (Wardill et al., 2012). In addition, several studies claimed the analogy that fly receptors R1–R6 serve a similar function as human rods, while fly receptors R7/R8 are comparable to our cones (Pichaud et al., 1999; Sanes and Zipursky, 2010; Strausfeld and Lee, 1991). This no longer holds, since all these receptors are involved in colour discrimination and since all function similarly at elevated light intensities (Hardie, 1979).

4.1.3 Post-receptoral mechanisms underlying colour vision

The LMCs L1, L2, and L3, which relay R1–R6 information to different layers in the medulla (Fischbach and Dittrich, 1989), were found to be required for blue-green discrimination (Figure 22). However, this study did not test the requirement of individual cell types as the used GAL4 drivers labelled two or three different LMCs at the same time (Figure 22A). Thus, it remained unclear, which of those three cell types contribute to blue-green discrimination. Using recently reported specific driver lines for each LMC type, which have been recently reported, this question can now be addressed (Tuthill et al., 2013). L1, L2, and L3 all have previously been found to provide input to the motion detection system of the fly (Joesch et al., 2010; Katsov and Clandinin, 2008; Rister et al., 2007; Silies et al., 2013). L1 and L2 are critically involved in splitting visual brightness information into ON and OFF components and provide input to motion sensitive T4 and T5 cells via several interneurons (Joesch et al.,

2010; Maisak et al., 2013; Takemura et al., 2013). Additionally they connect to many more cell types in the medulla, some of which also receive input from R7 and R8 (Takemura et al., 2013). Especially L3 has many synaptic connections with cells being also postsynaptic to R7 and R8 (Gao et al., 2008; Takemura et al., 2013). Thus, all three are potentially contributing to colour discrimination and a neural separation of motion and colour processing is suggested to be implemented downstream of the LMCs.

Neuronal comparison of differential receptor outputs may be through colour opponent mechanisms (Hertel, 1980; Kien and Menzel, 1977a; Paulk et al., 2008, 2009b; Yang et al., 2004). Tm5 cells in the medulla neuropil are candidate colour opponent cells comparing Rh4 with Rh1 or Rh6 signals, since they integrate the outputs R7, R8, and R1–R6 (the latter via LMCs; especially L3) (Gao et al., 2008). However, so far no antagonistic input to Tm5 has been identified. In contrast, R7, R8 and L3 are thought to directly or indirectly inhibit Tm5c. While R8 inhibits Tm5c directly, multiple inhibitory R7 signals are conveyed by glutamatergic Dm8 onto Tm5c, which expresses the excitatory glutamate receptor Clumsy (Karuppudurai et al., 2014). Analogous to R7/Dm8/Tm5c circuit, L3 gets inhibited by R1–R6, which presumably has glutamatergic input onto Tm5c (Kolodziejczyk et al., 2008). Therefore, if Tm5c shows colour opponency, the antagonistic input is presumably not mediated by Dm8 or L3. Alternatively, the post-receptoral comparisons may take place further downstream in the optic neuropils (Menzel and Backhaus, 1989), though several studies in honeybees and bumblebees identified colour opponent neurons in the medulla (Hertel, 1980; Kien and Menzel, 1977a; Paulk et al., 2009b). Future behavioural and physiological studies may further elucidate this neuronal computation and may identify neurons with broadband, narrow-band, and colour opponent sensitivity as reported for honey bees and bumblebees (Hertel, 1980; Kien and Menzel, 1977a, 1977b; Paulk et al., 2009b; Yang et al., 2004). Furthermore, such studies might reveal whether colour opponent mechanisms in flies exist that are similar to mechanisms found in vertebrates. It is for example unclear whether insects possess spatial opponency mechanisms found in vertebrates which are amongst others required to compare the contrast of neighbouring colours at the same time (Solomon and Lennie, 2007). To date no receptive field with such spatial opponency is found in any recorded colour opponent cell of honeybees (Hertel, 1980; Kien and Menzel, 1977a).

4.1.4 A comparative view on the function of photoreceptor types in arthropod colour vision

Crustacean and insect compound eyes share many similarities from which to draw information about the evolution of arthropod colour vision. Typically, their ommatidia harbour several photoreceptors with two, three or more different spectral sensitivities (Warrant and Nilsson, 2006). In decapod crustaceans, two anatomical types of photoreceptors are found. Similar to R1–R6 in *Drosophila,* seven long-wavelength sensitive short visual fibres from R1–R7 connect with second-order interneurons in the lamina, the monopolar ganglion cells, which convey visual information to the second optic neuropil, the medulla (Marshall et al., 1999). A single UV-sensitive receptor has a distal rhabdomere and a long visual fibre projecting to the medulla, analogous to R7 in flies (Marshall et al., 1999). Therefore, similar as in *Drosophila,* colour vision must rely on a comparison of both photoreceptor types.

The butterfly *Papilio xuthus* has compound eyes with three ommatidia types. In each type, nine photoreceptors that are divided into six spectral classes (ultraviolet, violet, blue, green, red, and broad-band) contribute to the rhabdomere (Koshitaka et al., 2008). Behavioural analyses have shown that *Papilio xuthus* uses the ultraviolet, blue, green, and red receptors for colour discrimination (Koshitaka et al., 2008). The ultraviolet and blue receptors are terminating in the medulla, whereas the green and red receptors are terminating in the lamina (Hamanaka et al., 2013). This might indicate that also in *Papilio xuthus* processing of wavelength information begins in the lamina.

Honeybees like all insects have six outer photoreceptors projecting to the lamina neuropil (Sommer and Wehner, 1975). They are long-wavelength sensitive and suggested to mediate achromatic vision like the detection of patterns, shape and motion (Osorio and Vorobyev, 2005), thus likely sharing the same function as in *Drosophila* (Heisenberg and Buchner, 1977; Yamaguchi et al., 2008; Zhou et al., 2012). In three types of ommatidia in bees, two UV photoreceptors, two blue photoreceptors or one of each contribute to the distal rhabdomere (Wakakuwa et al., 2005). Together with an additional long-wavelength sensitive receptor which is found at the basal rhabdomere, these receptors project to the medulla, similar as R7 and R8 in *Drosophila* (Sommer and Wehner, 1975). While colour vision in honeybees was found to depend on all three photoreceptor pigments, it is still unknown whether the outer and/or the basal photoreceptors mediate the long-wavelength input to the colour vision circuit (Backhaus, 1991; Menzel and Backhaus, 1989). Given that decapods,

butterflies and flies share the contribution of photoreceptors that terminate in the lamina to colour vision, it is likely that such feature is conserved and also to be found in the honeybee.

4.2 Neural circuits underlying reinforcement signalling of visual memories

4.2.1 High-throughput aversive visual conditioning

Devising a transparent electric shock grid module made it possible to apply the same visual stimulation in aversive and appetitive conditioning assays. Except for the reduced height of the arena in the aversive assay and the reinforcing stimuli, the assays are the same. Having developed these two assays (this thesis; Schnaitmann et al., 2010) that yield comparable and highly significant memory performance, it now became possible contrasting both forms of visual memory and to genetically dissect the underlying neural circuits. As both reinforcing stimuli and behavioural tasks are the same in these visual and the frequently used olfactory conditioning assays, it now became possible to compare the circuits underlying olfactory and visual memory. Fully automated high-throughput data acquisition software was developed to control the presentation of electric shock and visual stimuli while making video recordings of flies' behaviour (Figure 23). In the setup, memory performance is based on altered visual preference in walking flies, a task likely to be less demanding than the constant flight required for flight simulator learning. Flies tend to refuse to fly at elevated temperature that is required for the successful use of the temperature sensitive reversible synaptic inhibitor *shi*^{ts1} (Kitamoto, 2001). This problem hindered the study of neural circuits underlying visual memory so far that can now be advanced. In the presented assay, behaviour at elevated temperature is not compromised. Thus, the setup presented here is a powerful alternative to the so far used flight simulator for studying visual memory. For a collaboration with Yoshinori Aso and Gerry Rubin (Janelia Farm Research Campus, HHMI, USA) I developed a setup incorporating 20 single aversive assays that can be run fully automated. This will facilitate behavioural examination of many genotypes and will allow the screening of MB extrinsic and intrinsic neurons as a follow up of the work presented here.

4.2.2 Associative memories of different modalities share mushroom body circuits

I found that visual and olfactory memories share the same subsets of dopamine neurons that convey reinforcing signals (Figure 24–25). Such shared requirement of the transmitter system between visual and olfactory learning has been described in cockroaches (Mizunami et al., 2009; Unoki et al., 2005, 2006). However the pharmacological manipulation used in the mentioned studies does not allow further circuit dissection. For electric shock reinforcement, identified neurons in the PPL1 cluster, such as MB-MP1, MB-MV1 and MB-V1, drive aversive memories in both visual and olfactory learning (Figure 25 D, G; Aso et al., 2010, 2012; Claridge-Chang et al., 2009), while the MB-M3 neurons in the PAM cluster seem to be involved specifically in aversive olfactory memory (data not shown; Aso et al., 2010, 2012). Thus, overlapping sets of dopamine neurons appear to represent electric shock punishment in both visual and olfactory memory with olfactory aversive memory potentially recruiting a larger set. It was previously shown that the MB-M3 neurons induce aversive olfactory memory that increases stability of other memory components (Aso et al., 2012). Longer lasting olfactory memories may thus require the recruitment of additional dopamine neurons. Whether this holds true for visual memories as well requires future analysis. In appetitive conditioning, PAM cluster neurons play crucial roles in both olfactory and visual memories (Figs. 24–25, Burke et al., 2012; Liu et al., 2012). Which cell types in these clusters are involved and whether there is a cellular distinction between olfactory and visual memory requires further analysis at the single cell level. Most importantly, all these neurons convey dopamine signals to restricted subdomains of the MB. Consistently, dopamine receptor DopR1 is required and its expression in the MB is sufficient to restore visual memory (Figure 25H). This receptor is therefore likely mediating the reinforcement signal input to the KCs.

Though a requirement of octopamine neurons could not be found for visual memories, a recent study showed that sweet taste engages a distributed octopamine signal that reinforces olfactory short-term memory by signalling through dopamine neurons (Burke et al., 2012). Future analyses will reveal whether this pathway is shared as well for visual memories. That this could be the case is supported by studies in crickets which demonstrated an important role of octopamine in visual memory (Mizunami et al., 2009; Unoki et al., 2006).

Recently, the requirement of MB output for visual memory acquisition and retrieval was found by my colleague K. Vogt, which is also consistent with olfactory conditioning, although recruited KC subsets are differentiated (Vogt and Schnaitmann et al., submitted;

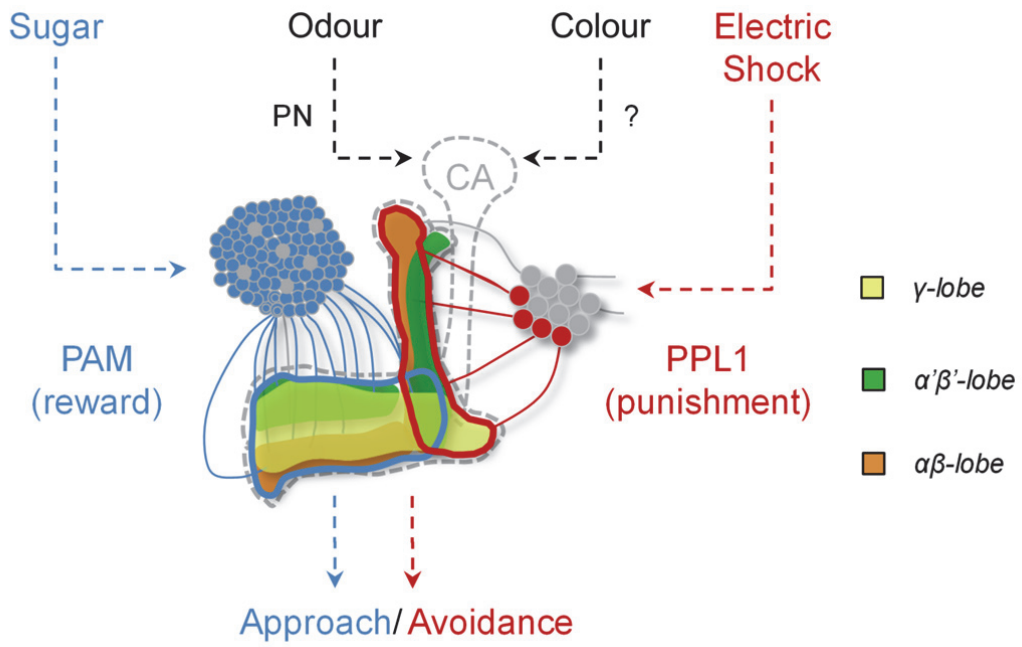

Figure 26 – Suggested circuit model of visual memories. Visual and olfactory information is conveyed to partially overlapping sets of KCs (Vogt and Schnaitmann et al., submitted). Olfactory input to the calyx via projection neurons (PN) is well characterized, whereas the visual input to the MB has not been identified yet. Output of KCs, representing olfactory and visual information, is locally modulated by the different subsets of dopamine neurons (PAM, PPL1) to form appetitive and aversive memories.

Dubnau et al., 2001; Krashes et al., 2007; McGuire et al., 2001; Schwaerzel et al., 2003). The identification of reinforcement signalling neurons that project to the MB (this thesis) and the necessity of the MB Kenyon cells (Vogt and Schnaitmann et al., submitted) together suggest that associative plasticity underlying visual memories is to be found in the MB (Figure 26). Moreover, these findings support the conclusion that coincidence mechanisms are similar for different forms of memories inside the MB (Gerber et al., 2004a; Heisenberg, 2003; Qin et al., 2012). The feature of diverse sensory representations inside the MB may be conserved among insect species. In honeybees for example, different sensory modalities are represented in spatially segregated areas of the calyx (Ehmer and Gronenberg, 2002; Mobbs, 1982; Strausfeld, 2002). The MB might thus have evolved as a centre for multi modal associative modulation. Such centralization of similar brain functions spares the cost of maintaining similar circuit motifs in different brain areas and may be an evolutionary conserved design of

information processing. Such converging inputs of different stimuli into a multisensory area have even been described in humans (Beauchamp et al., 2008).

'Flight simulator' visual learning was shown to require the central complex but not the MB (Liu et al., 2006; Pan et al., 2009; Wolf et al., 1998). Although this appears to contradict this study and the MB requirement for visual memory in the here used assay (Vogt and Schnaitmann et al., submitted), I note that there are important differences between the behavioural paradigms employed. Visual stimulation in 'flight simulator' experiments consisted mostly of patterns in the frontal visual field while in the here presented assay, colour stimuli were presented in the ventral visual field. Furthermore, heat punishment is opposed to sucrose reward and electric shock punishment. Moreover, mixed classical/operant conditioning of single flying flies is a highly different behavioural task compared to classical conditioning of walking flies en masse. Altogether, memory in the used assay sharing many similarities to olfactory conditioning is very different from memory in the previously used visual assay. Therefore, I suspect these differences being reflected in the distinct underlying neural substrates.

While olfactory input to the MB via olfactory projection neurons is well described (Hallem et al., 2004; Masse et al., 2009), visual inputs to the MB in flies have not yet been reported. In other insects, direct connections between optic lobes and MBs have been found (Gronenberg and Hölldobler, 1999; Li and Strausfeld, 1997; Lin and Strausfeld, 2012; Mobbs, 1982; Paulk et al., 2008; Schildberger, 1984). Also afferents originating in the protocerebrum of cockroaches were found to provide multi-modal input to the MB lobes (Li and Strausfeld, 1997). Thus, the MB may also receive indirect visual input in *Drosophila,* possibly via the optic glomeruli (Otsuna and Ito, 2006). Future behavioural and physiological studies may identify these cells and increase our understanding how colour information is conveyed to the MB.

References

Adams, M.D., Celniker, S.E., Holt, R.A., Evans, C.A., Gocayne, J.D., Amanatides, P.G., Scherer, S.E., Li, P.W., Hoskins, R.A., Galle, R.F., et al. (2000). The genome sequence of Drosophila melanogaster. Science *287*, 2185–2195.

Akalal, D.-B.G., Yu, D., and Davis, R.L. (2010). A late-phase, long-term memory trace forms in the γ neurons of Drosophila mushroom bodies after olfactory classical conditioning. J. Neurosci. *30*, 16699–16708.

Anderson, J.C., and Laughlin, S.B. (2000). Photoreceptor performance and the coordination of achromatic and chromatic inputs in the fly visual system. Vision Res. *40*, 13–31.

Arshavsky, V.Y. (2003). Protein translocation in photoreceptor light adaptation: a common theme in vertebrate and invertebrate vision. Sci. Signal. *2003*, 43.

Ashburner, M. (1989). Drosophila. A laboratory handbook. (Cold Spring Harbor Laboratory Press).

Aso, Y., Grübel, K., Busch, S., Friedrich, A.B., Siwanowicz, I., and Tanimoto, H. (2009). The mushroom body of adult Drosophila characterized by GAL4 drivers. J. Neurogenet. *23*, 156–172.

Aso, Y., Siwanowicz, I., Bräcker, L., Ito, K., Kitamoto, T., and Tanimoto, H. (2010). Specific dopaminergic neurons for the formation of labile aversive memory. Curr. Biol. *20*, 1445–1451.

Aso, Y., Herb, A., Ogueta, M., Siwanowicz, I., Templier, T., Friedrich, A.B., Ito, K., Scholz, H., and Tanimoto, H. (2012). Three dopamine pathways induce aversive odor memories with different stability. PLoS Genet *8*, e1002768. doi: 10.1371/journal.pgen.1002768.

Autrum, H., and Zwehl, V. v (1964). Die spektrale Empfindlichkeit einzelner Sehzellen des Bienenauges. Z. Für Vgl. Physiol. *48*, 357–384.

Bachmann, A., and Knust, E. (2008). The use of P-Element transposons to generate transgenic flies. In Drosophila, D.C. Dahmann, ed. (Humana Press), pp. 61–77.

Backhaus, W. (1991). Color opponent coding in the visual system of the honeybee. Vision Res. *31*, 1381–1397.

Bahl, A., Ammer, G., Schilling, T., and Borst, A. (2013). Object tracking in motion-blind flies. Nat. Neurosci. *16*, 730–738.

Baines, R.A., Uhler, J.P., Thompson, A., Sweeney, S.T., and Bate, M. (2001). Altered electrical properties in Drosophila neurons developing without synaptic transmission. J. Neurosci. *21*, 1523–1531.

Barth, M., and Heisenberg, M. (1997). Vision affects mushroom bodies and central complex in Drosophila melanogaster. Learn. Mem. *4*, 219–229.

Bausenwein, B., Dittrich, A.P.M., and Fischbach, K.-F. (1992). The optic lobe of Drosophila melanogaster. Cell Tissue Res. *267*, 17–28.

Beauchamp, M.S., Yasar, N.E., Frye, R.E., and Ro, T. (2008). Touch, sound and vision in human superior temporal sulcus. NeuroImage *41*, 1011–1020.

De Belle, J.S., and Heisenberg, M. (1994). Associative odor learning in Drosophila abolished by chemical ablation of mushroom bodies. Science *263*, 692–694.

Benda, J., Gollisch, T., Machens, C.K., and Herz, A.V. (2007). From response to stimulus: adaptive sampling in sensory physiology. Curr. Opin. Neurobiol. *17*, 430–436.

Benzer, S. (1967). Behavioral mutants of Drosophila isolated by countercurrent distribution. Proc. Natl. Acad. Sci. *58*, 1112.

Bicker, G., and Reichert, H. (1978). Visual learning in a photoreceptor degeneration mutant of Drosophila melanogaster. J. Comp. Physiol. *127*, 29–38.

Bloomquist, B.T., Shortridge, R.D., Schneuwly, S., Perdew, M., Montell, C., Steller, H., Rubin, G., and Pak, W.L. (1988). Isolation of a putative phospholipase C gene of Drosophila, norpA, and its role in phototransduction. Cell *54*, 723–733.

Blum, A.L., Li, W., Cressy, M., and Dubnau, J. (2009). Short- and longterm memory in Drosophila require cAMP signaling in distinct neuron types. Curr. Biol. *19*, 1341–1350.

Borst, A. (2009). Drosophila's view on insect vision. Curr. Biol. *19*, R36–R47.

Borst, A., and Euler, T. (2011). Seeing things in motion: models, circuits, and mechanisms. Neuron *71*, 974–994.

Borst, A., and Haag, J. (2002). Neural networks in the cockpit of the fly. J. Comp. Physiol. A *188*, 419–437.

Braitenberg, V. (1967). Patterns of projection in the visual system of the fly. I. Retina-lamina projections. Exp. Brain Res. *3*, 271–298.

Braitenberg, V. (1970). Ordnung und Orientierung der Elemente im Sehsystem der Fliege. Kybernetik *7*, 235–242.

Braitenberg, V., and Debbage, P. (1974). A regular net of reciprocal synapses in the visual system of the fly, Musca domestica. J. Comp. Physiol. *90*, 25–31.

Brand, A., and Perrimon, N. (1993). Targeted gene-expression as a means of altering cell fates and generating dominant phenotypes. Development *118*, 401–415.

Brembs, B., and Plendl, W. (2008). Double dissociation of PKC and AC manipulations on operant and classical learning in Drosophila. Curr. Biol. *18*, 1168–1171.

Brembs, B., and Wiener, J. (2006). Context and occasion setting in Drosophila visual learning. Learn. Mem. *13*, 618–628.

Buchner, E., Buchner, S., and Bülthoff, I. (1984). Deoxyglucose mapping of nervous activity induced in Drosophila brain by visual movement. J. Comp. Physiol. A *155*, 471–483.

Burke, C.J., Huetteroth, W., Owald, D., Perisse, E., Krashes, M.J., Das, G., Gohl, D., Silies, M., Certel, S., and Waddell, S. (2012). Layered reward signalling through octopamine and dopamine in Drosophila. Nature *492*, 433–477.

Claridge-Chang, A., Roorda, R.D., Vrontou, E., Sjulson, L., Li, H., Hirsh, J., and Miesenböck, G. (2009). Writing memories with light-addressable reinforcement circuitry. Cell *139*, 405–415.

Cole, S.H., Carney, G.E., McClung, C.A., Willard, S.S., Taylor, B.J., and Hirsh, J. (2005). Two functional but noncomplementing Drosophila tyrosine decarboxylase genes: distinct roles for neural tyramine and octopamine in female fertility. J. Biol. Chem. *280*, 14948–14955.

Cronin, T.W., and Marshall, N.J. (1989). A retina with at least ten spectral types of photoreceptors in a mantis shrimp. Nature *339*, 137–140.

Daumer, K. (1956). Reizmetrische Untersuchung des Farbensehens der Bienen. Z. Für Vgl. Physiol. *38*, 413–478.

Delgado, R., Maureira, C., Oliva, C., Kidokoro, Y., and Labarca, P. (2000). Size of vesicle pools, rates of mobilization, and recycling at neuromuscular synapses of a Drosophila mutant, shibire. Neuron *28*, 941–953.

Devary, O., Heichal, O., Blumenfeld, A., Cassel, D., Suss, E., Barash, S., Rubinstein, C.T., Minke, B., and Selinger, Z. (1987). Coupling of photoexcited rhodopsin to inositol phospholipid hydrolysis in fly photoreceptors. Proc. Natl. Acad. Sci. *84*, 6939–6943.

Dubnau, J., Grady, L., Kitamoto, T., and Tully, T. (2001). Disruption of neurotransmission in Drosophila mushroom body blocks retrieval but not acquisition of memory. Nature *411*, 476–480.

Dudai, Y., Jan, Y.-N., Byers, D., Quinn, W.G., and Benzer, S. (1976). dunce, a mutant of Drosophila deficient in learning. Proc. Natl. Acad. Sci. *73*, 1684–1688.

Egelhaaf, M., and Borst, A. (1992). Are there separate ON and OFF channels in fly motion vision? Vis. Neurosci. *8*, 151–164.

Egelhaaf, M., Borst, A., and Reichardt, W. (1989). Computational structure of a biological motion-detection system as revealed by local detector analysis in the fly's nervous system. J. Opt. Soc. Am. A Opt. Image Sci. Vis. *6*, 1070–1087.

Ehmer, B., and Gronenberg, W. (2002). Segregation of visual input to the mushroom bodies in the honeybee (Apis mellifera). J. Comp. Neurol. *451*, 362–373.

Eichner, H., Joesch, M., Schnell, B., Reiff, D.F., and Borst, A. (2011). Internal Structure of the Fly Elementary Motion Detector. Neuron *70*, 1155–1164.

Elliott, D.A., and Brand, A.H. (2008). The GAL4 system : a versatile system for the expression of genes. Methods Mol. Biol. *420*, 79–95.

Ernst, R., and Heisenberg, M. (1999). The memory template in Drosophila pattern vision at the flight simulator. Vision Res. *39*, 3920–3933.

Fischbach, K.F. (1979). Simultaneous and successive colour contrast expressed in “slow” phototactic behaviour of walking Drosophila melanogaster. J. Comp. Physiol. *130*, 161–171.

Fischbach, K., and Dittrich, A. (1989). The optic lobe of Drosophila melanogaster. 1. A Golgi Analysis of wildtype structure. Cell Tissue Res. *258*, 441–475.

Folkers, E. (1982). Visual learning and memory of Drosophila melanogaster wild type CS and the mutants dunce1, amnesiac, turnip and rutabaga. J. Insect Physiol. *28*, 535–539.

Folkers, E., Drain, P., and Quinn, W.G. (1993). Radish, a Drosophila mutant deficient in consolidated memory. Proc. Natl. Acad. Sci. *90*, 8123–8127.

Foucaud, J., Burns, J.G., and Mery, F. (2010). Use of Spatial Information and Search Strategies in a Water Maze Analog in Drosophila melanogaster. Plos One *5*, e15231.

Franceschini, N. (1979). Voltage Clamp by Light - Rapid Measurement of the Spectral and Polarization Sensitivities of Receptor-Cells. Invest. Ophthalmol. Vis. Sci. *18 (Supplement)*, 5.

Friggi-Grelin, F., Coulom, H., Meller, M., Gomez, D., Hirsh, J., and Birman, S. (2003). Targeted gene expression in Drosophila dopaminergic cells using regulatory sequences from tyrosine hydroxylase. J. Neurobiol. *54*, 618–627.

Frisch, K. von (1914). Der Farbensinn und Formensinn der Biene. Zool Jb Physiol *35*, 1–188.

Fukushi, T. (1990). Colour discrimination from various shades of grey in the trained blowfly, Lucilia cuprina. J. Insect Physiol. *36*, 69–75.

Fukushi, T. (1994). Colour perception of single and mixed monochromatic lights in the blowfly Lucilia cuprina. J. Comp. Physiol. A *175*, 15–22.

Gao, S., Takemura, S., Ting, C.-Y., Huang, S., Lu, Z., Luan, H., Rister, J., Thum, A.S., Yang, M., Hong, S.-T., et al. (2008). The neural substrate of spectral preference in Drosophila. Neuron *60*, 328–342.

Garbers, C., Schnaitmann, C., Prech, S., Tanimoto, H., and Wachtler, T. (2012). Novel method for closed-loop electroretinogram measurement of sensitivity in Drosophila. Front. Comput. Neurosci. *Conference Abstract: Bernstein Conference 2012.*

Gegear, R.J., Casselman, A., Waddell, S., and Reppert, S.M. (2008). Cryptochrome mediates light-dependent magnetosensitivity in Drosophila. Nature *454*, 1014–1018.

Gegenfurtner, K.R., and Kiper, D.C. (2003). Color vision. Neuroscience *26*, 181–206.

Gerber, B., Tanimoto, H., and Heisenberg, M. (2004a). An engram found? - Evaluating the evidence from fruit flies. Curr. Opin. Neurobiol. *14*, 737–744.

Gerber, B., Scherer, S., Neuser, K., Michels, B., Hendel, T., Stocker, R.F., and Heisenberg, M. (2004b). Visual learning in individually assayed Drosophila larvae. J. Exp. Biol. *207*, 179–188.

Gong, Z.-F., Xia, S.-Z., Liu, L., Feng, C.-H., and Guo, A.-K. (1998). Operant visual learning and memory in Drosophila mutants dunce, amnesiac and radish. J. Insect Physiol. *44*, 1149–1158.

Griffith, L.C. (2012). Identifying behavioral circuits in Drosophila melanogaster: moving targets in a flying insect. Curr. Opin. Neurobiol. *22*, 609–614.

Gronenberg, W., and Hölldobler, B. (1999). Morphologic representation of visual and antennal information in the ant brain. J. Comp. Neurol. *412*, 229–240.

Guo, J., and Guo, A. (2005). Crossmodal interactions between olfactory and visual learning in Drosophila. Science *309*, 307–310.

Hallem, E.A., Ho, M.G., and Carlson, J.R. (2004). The molecular basis of odor coding in the Drosophila antenna. Cell *117*, 965–979.

Hamada, F.N., Rosenzweig, M., Kang, K., Pulver, S.R., Ghezzi, A., Jegla, T.J., and Garrity, P.A. (2008). An internal thermal sensor controlling temperature preference in Drosophila. Nature *454*, 217–220.

Hamanaka, Y., Shibasaki, H., Kinoshita, M., and Arikawa, K. (2013). Neurons innervating the lamina in the butterfly, Papilio xuthus. J. Comp. Physiol. A *199*, 341–351.

Hardie, R.C. (1979). Electrophysiological analysis of fly retina. I: Comparative properties of R1-6 and R 7 and 8. J. Comp. Physiol. *129*, 19–33.

Hardie, R.C. (1985). Functional organization of the fly retina. Prog Sens Physiol *5*, 1–79.

Hardie, R.C. (1989). A histamine-activated chloride channel involved in neurotransmission at a photoreceptor synapse. Nature *339*, 704–706.

Hardie, R.C. (1991). Whole-cell recordings of the light induced current in dissociated Drosophila photoreceptors: evidence for feedback by calcium permeating the light-sensitive channels. Proc. R. Soc. Lond. B Biol. Sci. *245*, 203–210.

Hardie, R.C., and Franze, K. (2012). Photomechanical responses in Drosophila photoreceptors. Science *338*, 260–263.

Hardie, R.C., and Minke, B. (1992). The trp gene is essential for a light-activated Ca2+ channel in Drosophila photoreceptors. Neuron *8*, 643–651.

Hardie, R.C., Peretz, A., Suss-Toby, E., Rom-Glas, A., Bishop, S.A., Selinger, Z., and Minke, B. (1993). Protein kinase C is required for light adaptation in Drosophila photoreceptors. Nature *363*, 634–637.

Harris, W.A., Stark, J.A., and Walker, W.S. (1976). Genetic dissection of the photoreceptor system in the compound eye of Drosophila melanogaster. J. Physiol. *256*, 415–439.

Hassenstein, B., and Reichardt, W. (1956). Systemtheoretische Analyse der Zeit-, Reihenfolgen-und Vorzeichenauswertung bei der Bewegungsperzeption des Rüsselkäfers Chlorophanus. Z Naturforsch *11*, 513–524.

Hausen, K. (1984). The lobula-complex of the fly: structure, function and significance in visual behaviour. In Photoreception and Vision in Invertebrates, (Springer US), pp. 523–559.

Heisenberg, M. (2003). Mushroom body memoir: from maps to models. Nat. Rev. Neurosci. *4*, 266–275.

Heisenberg, M., and Buchner, E. (1977). The rôle of retinula cell types in visual behavior of Drosophila melanogaster. J. Comp. Physiol. *117*, 127–162.

Heisenberg, M., Borst, A., Wagner, S., and Byers, D. (1985). Drosophila mushroom body mutants are deficient in olfactory learning. J. Neurogenet. *2*, 1–30.

Heisenberg, M., Wolf, R., and Brembs, B. (2001). Flexibility in a single behavioral variable of Drosophila. Learn. Mem. *8*, 1–10.

Von Helmholtz, H. (1866). Handbuch der physiologischen Optik: mit 213 in den Text eingedruckten Holzschnitten und 11 Tafeln (Voss).

Von Helversen, O. (1972). Zur spektralen Unterschiedsempfindlichkeit der Honigbiene. J. Comp. Physiol. A *80*, 439–472.

Hering, E. (1878). Zur Lehre vom Lichtsinne (Druck Und Verlag Von Carl Gerold's Sohn, Wien).

Hernández de Salomon, C.H., and Spatz, H.C. (1983). Colour vision in Drosophila melanogaster: wavelength discrimination. J. Comp. Physiol. A *150*, 31–37.

Hertel, H. (1980). Chromatic properties of identified interneurons in the optic lobes of the bee. J. Comp. Physiol. A *137*, 215–231.

Hildebrand, J.G., and Shepherd, G.M. (1997). Mechanisms of olfactory discrimination: Converging evidence for common principles across phyla. Annu. Rev. Neurosci. *20*, 595–631.

Hori, S., Takeuchi, H., Arikawa, K., Kinoshita, M., Ichikawa, N., Sasaki, M., and Kubo, T. (2006). Associative visual learning, color discrimination, and chromatic adaptation in the harnessed honeybee Apis mellifera L. J. Comp. Physiol. A *192*, 691–700.

Huang, J., Liu, C.-H., Hughes, S.A., Postma, M., Schwiening, C.J., and Hardie, R.C. (2010). Activation of TRP channels by protons and phosphoinositide depletion in Drosophila photoreceptors. Curr. Biol. *20*, 189–197.

Inoue, H., Yoshioka, T., and Hotta, Y. (1985). A genetic study of inositol trisphosphate involvement in phototransduction using Drosophila mutants. Biochem. Biophys. Res. Commun. *132*, 513–519.

Isabel, G., Pascual, A., and Preat, T. (2004). Exclusive consolidated memory phases in Drosophila. Science *304*, 1024–1027.

Ito, K., Okada, R., Tanaka, N.K., and Awasaki, T. (2003). Cautionary observations on preparing and interpreting brain images using molecular biology-based staining techniques. Microsc. Res. Tech. *62*, 170–186.

Jackowska, M., Bao, R., Liu, Z., McDonald, E.C., Cook, T.A., and Friedrich, M. (2007). Genomic and gene regulatory signatures of cryptozoic adaptation: loss of blue sensitive photoreceptors through expansion of long wavelength-opsin expression in the red flour beetle Tribolium castaneum. Front Zool *4*, 24. doi: 10.1186/1742–9994–4–24.

Jacob, K.G., Willmund, R., Folkers, E., Fischbach, K.F., and Spatz, H.C. (1977). T-maze phototaxis ofDrosophila melanogaster and several mutants in the visual systems. J. Comp. Physiol. A *116*, 209–225.

Järvilehto, M., and Zettler, F. (1971). Localized intracellular potentials from pre- and postsynaptic components in the external plexiform layer of an insect retina. Z. Für Vgl. Physiol. *75*, 422–440.

Jenett, A., Rubin, G.M., Ngo, T.-T.B., Shepherd, D., Murphy, C., Dionne, H., Pfeiffer, B.D., Cavallaro, A., Hall, D., Jeter, J., et al. (2012). A GAL4-driver line resource for Drosophila neurobiology. Cell Rep. *2*, 991–1001.

Joesch, M., Schnell, B., Raghu, S.V., Reiff, D.F., and Borst, A. (2010). ON and OFF pathways in Drosophila motion vision. Nature *468*, 300–304.

Johns, D.C., Weerahandi, H., Meyers, J., Cook, S.H., Campbell, J.N., and Ringkamp, M. (2001). Suppression of inflammation induced hyperalgesia by in vivo viral gene transfer of the Kir2.1 potassium channel. Soc. Neurosci. Abstr. *27*, 2170–2170.

Kahsai, L., and Zars, T. (2011). Learning and memory in Drosophila: behavior, genetics, and neural systems. Int. Rev. Neurobiol. *99*, 139–167.

Karuppudurai, T., Lin, T.-Y., Ting, C.-Y., Pursley, R., Melnattur, K.V., Diao, F., White, B.H., Macpherson, L.J., Gallio, M., Pohida, T., et al. (2014). A hard-wired glutamatergic circuit pools and relays UV signals to mediate spectral preference in Drosophila. Neuron *81*, 603–615.

Katsov, A.Y., and Clandinin, T.R. (2008). Motion processing streams in Drosophila are behaviorally specialized. Neuron *59*, 322–335.

Keene, A.C., and Waddell, S. (2007). Drosophila olfactory memory: single genes to complex neural circuits. Nat. Rev. Neurosci. *8*, 341–354.

Kelber, A., and Lind, O. (2010). Limits of colour vision in dim light. Ophthalmic Physiol. Opt. J. Br. Coll. Ophthalmic Opt. Optom. *30*, 454–459.

Kelber, A., and Osorio, D. (2010). From spectral information to animal colour vision: experiments and concepts. Proc. R. Soc. B Biol. Sci. *277*, 1617–1625.

Kelber, A., and Pfaff, M. (1999). True colour vision in the orchard butterfly, Papilio aegeus. Naturwissenschaften *86*, 221–224.

Kelber, A., Vorobyev, M., and Osorio, D. (2003). Animal colour vision — behavioural tests and physiological concepts. Biol. Rev. *78*, 81–118.

Kien, J., and Menzel, R. (1977a). Chromatic properties of interneurons in the optic lobes of the bee. J. Comp. Physiol. A *113*, 35–53.

Kien, J., and Menzel, R. (1977b). Chromatic properties of interneurons in the optic lobes of the bee. J. Comp. Physiol. A *113*, 17–34.

Kim, Y.C., Lee, H.G., and Han, K.A. (2007). D1 dopamine receptor dDA1 is required in the mushroom body neurons for aversive and appetitive learning in Drosophila. J. Neurosci. *27*, 7640–7647.

Kirschfeld, K. (1967). Die Projektion der optischen Umwelt auf das Raster der Rhabdomere im Komplexauge von Musca. Exp. Brain Res. *3*, 248–270.

Kitamoto, T. (2001). Conditional modification of behavior in Drosophila by targeted expression of a temperature-sensitive shibire allele in defined neurons. J. Neurobiol. *47*, 81–92.

Kitamoto, T. (2002). Conditional disruption of synaptic transmission induces male–male courtship behavior in Drosophila. Proc. Natl. Acad. Sci. *99*, 13232–13237.

Klagges, B.R., Heimbeck, G., Godenschwege, T.A., Hofbauer, A., Pflugfelder, G.O., Reifegerste, R., Reisch, D., Schaupp, M., Buchner, S., and Buchner, E. (1996). Invertebrate synapsins: a single gene codes for several isoforms in Drosophila. J. Neurosci. Off. J. Soc. Neurosci. *16*, 3154–3165.

Koenig, J.H., and Ikeda, K. (1983). Evidence for a presynaptic blockage of transmission in a temperature-sensitive mutant of Drosophila. J. Neurobiol. *14*, 411–419.

Kolodziejczyk, A., Sun, X., Meinertzhagen, I.A., and Nässel, D.R. (2008). Glutamate, GABA and acetylcholine signaling components in the lamina of the Drosophila visual system. PLoS One *3*, e2110. doi: 10.1371/journal.pone.0002110.

Konopka, R.J., and Benzer, S. (1971). Clock mutants of Drosophila melanogaster. Proc. Natl. Acad. Sci. *68*, 2112–2116.

Kosaka, T., and Ikeda, K. (1983). Possible temperature-dependent blockage of synaptic vesicle recycling induced by a single gene mutation in drosophila. J. Neurobiol. *14*, 207–225.

Koshitaka, H., Kinoshita, M., Vorobyev, M., and Arikawa, K. (2008). Tetrachromacy in a butterfly that has eight varieties of spectral receptors. Proc. R. Soc. B Biol. Sci. *275*, 947–954.

Krapp, H.G., and Hengstenberg, R. (1996). Estimation of self-motion by optic flow processing in single visual interneurons. Nature *384*, 463–466.

Krapp, H.G., Hengstenberg, B., and Hengstenberg, R. (1998). Dendritic structure and receptive-field organization of optic flow processing interneurons in the fly. J. Neurophysiol. *79*, 1902–1917.

Krashes, M.J., Keene, A.C., Leung, B., Armstrong, J.D., and Waddell, S. (2007). Sequential use of mushroom body neuron subsets during Drosophila odor memory processing. Neuron *53*, 103–115.

Kühn, A. (1927). Über den Farbensinn der Bienen. Z. Für Vgl. Physiol. *5*, 762–800.

Kumar, J.P., and Ready, D.F. (1995). Rhodopsin plays an essential structural role in Drosophila photoreceptor development. Development *121*, 4359–4370.

Labhart, T., and Meyer, E.P. (1999). Detectors for polarized skylight in insects: a survey of ommatidial specializations in the dorsal rim area of the compound eye. Microsc. Res. Tech. *47*, 368–379.

Lai, S.-L., and Lee, T. (2006). Genetic mosaic with dual binary transcriptional systems in Drosophila. Nat. Neurosci. *9*, 703–709.

Land, M.F. (1997). Visual Acuity in Insects. Annu. Rev. Entomol. *42*, 147–177.

Lebestky, T., Chang, J.S.C., Dankert, H., Zelnik, L., Kim, Y.C., Han, K.A., Wolf, F.W., Perona, P., and Anderson, D.J. (2009). Two Different Forms of Arousal in Drosophila Are Oppositely Regulated by the Dopamine D1 Receptor Ortholog DopR via Distinct Neural Circuits. Neuron *64*, 522–536.

Lee, T., and Luo, L. (2001). Mosaic analysis with a repressible cell marker (MARCM) for Drosophila neural development. Trends Neurosci. *24*, 251–254.

Lee, Y.-J., Shah, S., Suzuki, E., Zars, T., O'Day, P.M., and Hyde, D.R. (1994). The Drosophila dgq gene encodes a Gα protein that mediates phototransduction. Neuron *13*, 1143–1157.

Li, Y., and Strausfeld, N.J. (1997). Morphology and sensory modality of mushroom body extrinsic neurons in the brain of the cockroach, Periplaneta americana. J. Comp. Neurol. *387*, 631–650.

Li, H., Chaney, S., Roberts, I.J., Forte, M., and Hirsh, J. (2000). Ectopic G-protein expression in dopamine and serotonin neurons blocks cocaine sensitization in Drosophila melanogaster. Curr. Biol. *10*, 211–214.

Lin, C., and Strausfeld, N.J. (2012). Visual inputs to the mushroom body calyces of the whirligig beetle Dineutus sublineatus: modality switching in an insect. J. Comp. Neurol. *520*, 2562–2574.

Liu, C., Plaçais, P.-Y., Yamagata, N., Pfeiffer, B.D., Aso, Y., Friedrich, A.B., Siwanowicz, I., Rubin, G.M., Preat, T., and Tanimoto, H. (2012). A subset of dopamine neurons signals reward for odour memory in Drosophila. Nature *488*, 512–516.

Liu, G., Seiler, H., Wen, A., Zars, T., Ito, K., Wolf, R., Heisenberg, M., and Liu, L. (2006). Distinct memory traces for two visual features in the Drosophila brain. Nature *439*, 551–556.

Liu, L., Wolf, R., Ernst, R., and Heisenberg, M. (1999). Context generalization in Drosophila visual learning requires the mushroom bodies. Nature *400*, 753–756.

Luan, H., Peabody, N.C., Vinson, C.R., and White, B.H. (2006). Refined spatial manipulation of neuronal function by combinatorial restriction of transgene expression. Neuron *52*, 425–436.

Lubbock, J. (1888). On the senses, instincts, and intelligence of animals: With special reference to insects (Appleton & Co).

Maisak, M.S., Haag, J., Ammer, G., Serbe, E., Meier, M., Leonhardt, A., Schilling, T., Bahl, A., Rubin, G.M., Nern, A., et al. (2013). A directional tuning map of Drosophila elementary motion detectors. Nature *500*, 212–216.

Margulies, C., Tully, T., and Dubnau, J. (2005). Deconstructing memory in Drosophila. Curr. Biol. *15*, 700–713.

Marshall, J., Kent, J., and Cronin, T. (1999). Visual adaptations in crustaceans: spectral sensitivity in diverse habitats. In Adaptive Mechanisms in the Ecology of Vision, (Kluwer, London), pp. 285–327.

Masek, P., and Scott, K. (2010). Limited taste discrimination in Drosophila. Proc. Natl. Acad. Sci. *107*, 14833–14838.

Masse, N.Y., Turner, G.C., and Jefferis, G.S.X.E. (2009). Olfactory information processing in Drosophila. Curr. Biol. *19*, 700–713.

Maxwell, J.C. (1860). On the theory of compound colours, and the relations of the colours of the spectrum. Philos. Trans. R. Soc. Lond. *150*, 57–84.

McGuire, S.E., Le, P.T., and Davis, R.L. (2001). The role of Drosophila mushroom body signaling in olfactory memory. Science *293*, 1330–1333.

McGuire, S.E., Le, P.T., Osborn, A.J., Matsumoto, K., and Davis, R.L. (2003). Spatiotemporal rescue of memory dysfunction in Drosophila. Science *302*, 1765–1768.

Meier, M., Serbe, E., Maisak, M.S., Haag, J., Dickson, B.J., and Borst, A. (2014). Neural circuit components of the Drosophila OFF motion vision pathway. Curr. Biol. *24*, 385–392.

Meinertzhagen, I.A., and O'neil, S.D. (1991). Synaptic organization of columnar elements in the lamina of the wild type in Drosophila melanogaster. J. Comp. Neurol. *305*, 232–263.

Meinertzhagen, I.A., and Sorra, K.E. (2001). Synaptic organization in the fly's optic lamina: few cells, many synapses and divergent microcircuits. Prog. Brain Res. *131*, 53–69.

Menda, G., Bar, H.Y., Arthur, B.J., Rivlin, P.K., Wyttenbach, R.A., Strawderman, R.L., and Hoy, R.R. (2011). Classical conditioning through auditory stimuli in Drosophila: methods and models. J. Exp. Biol. *214*, 2864–2870.

Menne, D., and Spatz, H.-C. (1977). Colour vision inDrosophila melanogaster. J. Comp. Physiol. *114*, 301–312.

Menzel, R., and Backhaus, W. (1989). Color vision honey bees: phenomena and physiological mechanisms (Springer-Verlag, Berlin, Heidelberg etc.).

Menzel, R., and Blakers, M. (1976). Colour receptors in the bee eye—morphology and spectral sensitivity. J. Comp. Physiol. A *108*, 11–13.

Menzel, R., and Greggers, U. (1985). Natural phototaxis and its relationship to colour vision in honeybees. J. Comp. Physiol. A *157*, 311–321.

Menzel, R., Ventura, D.F., Hertel, H., De Souza, J.M., and Greggers, U. (1986). Spectral sensitivity of photoreceptors in insect compound eyes: comparison of species and methods. J. Comp. Physiol. A *158*, 165–177.

Mizunami, M., Unoki, S., Mori, Y., Hirashima, D., Hatano, A., and Matsumoto, Y. (2009). Roles of octopaminergic and dopaminergic neurons in appetitive and aversive memory recall in an insect. BMC Biol. *7*, 46. doi: 10.1186/1741–7007–7–46.

Mobbs, P.G. (1982). The brain of the honeybee Apis mellifera. I. The connections and spatial organization of the mushroom bodies. Philos. Trans. R. Soc. Lond. B Biol. Sci. *298*, 309–354.

Mollereau, B., Wernet, M.F., Beaufils, P., Killian, D., Pichaud, F., Kühnlein, R., and Desplan, C. (2000). A green fluorescent protein enhancer trap screen in Drosophila photoreceptor cells. Mech. Dev. *93*, 151–160.

Montell, C. (1999). Visual transduction in Drosophila. Annu. Rev. Cell Dev. Biol. *15*, 231–268.

Morante, J., and Desplan, C. (2008). The color-vision circuit in the medulla of Drosophila. Curr. Biol. *18*, 553–565.

Morris, R. (1984). Developments of a water-maze procedure for studying spatial learning in the rat. J. Neurosci. Methods *11*, 47–60.

Mota, T., Roussel, E., Sandoz, J.-C., and Giurfa, M. (2011). Visual conditioning of the sting extension reflex in harnessed honeybees. J. Exp. Biol. *214*, 3577–3587.

Mu, L., Ito, K., Bacon, J.P., and Strausfeld, N.J. (2012). Optic glomeruli and their inputs in Drosophila share an organizational ground pattern with the antennal lobes. J. Neurosci. *32*, 6061–6071.

Neumeyer, C. (1980). Simultaneous color contrast in the honeybee. J. Comp. Physiol. *139*, 165–176.

Neuser, K., Triphan, T., Mronz, M., Poeck, B., and Strauss, R. (2008). Analysis of a spatial orientation memory in Drosophila. Nature *453*, 1244–1247.

Ofstad, T.A., Zuker, C.S., and Reiser, M.B. (2011). Visual place learning in Drosophila melanogaster. Nature *474*, 204–207.

Osorio, D., and Vorobyev, M. (2005). Photoreceptor sectral sensitivities in terrestrial animals: adaptations for luminance and colour vision. Proc. R. Soc. B Biol. Sci. *272*, 1745–1752.

Otsuna, H., and Ito, K. (2006). Systematic analysis of the visual projection neurons of Drosophila melanogaster. I. Lobula-specific pathways. J. Comp. Neurol. *497*, 928–958.

Pan, Y., Zhou, Y., Guo, C., Gong, H., Gong, Z., and Liu, L. (2009). Differential roles of the fan-shaped body and the ellipsoid body in Drosophila visual pattern memory. Learn. Mem. *16*, 289–295.

Paulk, A.C., Phillips-Portillo, J., Dacks, A.M., Fellous, J.M., and Gronenberg, W. (2008). The processing of color, motion, and stimulus timing are anatomically segregated in the bumblebee brain. J. Neurosci. *28*, 6319–6332.

Paulk, A.C., Dacks, A.M., Phillips-Portillo, J., Fellous, J.M., and Gronenberg, W. (2009a). Visual processing in the central bee brain. J. Neurosci. *29*, 9987–9999.

Paulk, A.C., Dacks, A.M., and Gronenberg, W. (2009b). Color processing in the medulla of the bumblebee (Apidae: Bombus impatiens). J. Comp. Neurol. *513*, 441–456.

Pavlov, I.P. (1927). Conditioned reflexes (Oxford Univ. Press; New York).

Perisse, E., Yin, Y., Lin, A.C., Lin, S., Huetteroth, W., and Waddell, S. (2013). Different kenyon cell populations drive learned approach and avoidance in Drosophila. Neuron *79*, 945–956.

Pfeiffer, B.D., Ngo, T.-T.B., Hibbard, K.L., Murphy, C., Jenett, A., Truman, J.W., and Rubin, G.M. (2010). Refinement of Tools for Targeted Gene Expression in Drosophila. Genetics *186*, 735–755.

Pichaud, F., Briscoe, A., and Desplan, C. (1999). Evolution of color vision. Curr. Opin. Neurobiol. *9*, 622–627.

Pitman, J.L., DasGupta, S., Krashes, M.J., Leung, B., Perrat, P.N., and Waddell, S. (2009). There are many ways to train a fly. Fly (Austin) *3*, 3–9.

Pollack, I., and Hofbauer, A. (1991). Histamine-like immunoreactivity in the visual system and brain of Drosophila melanogaster. Cell Tissue Res. *266*, 391–398.

Popescu, D.C., Ham, A.-J.L., and Shieh, B.-H. (2006). Scaffolding protein INAD regulates deactivation of vision by promoting phosphorylation of transient receptor potential by eye protein kinase C in Drosophila. J. Neurosci. *26*, 8570–8577.

Potter, C.J., Tasic, B., Russler, E.V., Liang, L., and Luo, L. (2010). The Q system: a repressible binary system for transgene expression, lineage tracing, and mosaic analysis. Cell *141*, 536–548.

Pulver, S.R., Pashkovski, S.L., Hornstein, N.J., Garrity, P.A., and Griffith, L.C. (2009). Temporal dynamics of neuronal activation by Channelrhodopsin-2 and TRPA1 determine behavioral output in Drosophila larvae. J. Neurophysiol. *101*, 3075–3088.

Qin, H., Cressy, M., Li, W., Coravos, J.S., Izzi, S.A., and Dubnau, J. (2012). Gamma neurons mediate Dopaminergic input during aversive olfactory memory formation in Drosophila. Curr. Biol. *22*, 608–614.

Quinn, W.G., Harris, W.A., and Benzer, S. (1974). Conditioned behavior in Drosophila melanogaster. Proc. Natl. Acad. Sci. U. S. A. *71*, 708–712.

Quinn, W.G., Sziber, P.P., and Booker, R. (1979). The Drosophila memory mutant amnesiac. Nature *277*, 212–214.

Ranganathan, R., Harris, G.L., Stevens, C.F., and Zuker, C.S. (1991). A Drosophila mutant defective in extracellular calcium-dependent photoreceptor deactivation and rapid desensitization. Nature *354*, 230–232.

Rister, J., Pauls, D., Schnell, B., Ting, C.Y., Lee, C.H., Sinakevitch, I., Morante, J., Strausfeld, N.J., Ito, K., and Heisenberg, M. (2007). Dissection of the peripheral motion channel in the visual system of Drosophila melanogaster. Neuron *56*, 155–170.

Rister, J., Desplan, C., and Vasiliauskas, D. (2013). Establishing and maintaining gene expression patterns: insights from sensory receptor patterning. Development *140*, 493–503.

Rushton, W.A.H. (1972). Review Lecture. Pigments and signals in colour vision. J. Physiol. *220*, 1–31.

Salcedo, E., Huber, A., Henrich, S., Chadwell, L.V., Chou, W.-H., Paulsen, R., and Britt, S.G. (1999). Blue- and green-absorbing visual pigments of Drosophila: ectopic expression and physiological characterization of the R8 photoreceptor cell-specific Rh5 and Rh6 rhodopsins. J. Neurosci. *19*, 10716–10726.

Sanes, J.R., and Zipursky, S.L. (2010). Design Principles of Insect and Vertebrate Visual Systems. Neuron *66*, 15–36.

Scherer, S., Stocker, R.F., and Gerber, B. (2003). Olfactory learning in individually assayed Drosophila larvae. Learn. Mem. *10*, 217–225.

Schildberger, K. (1984). Multimodal interneurons in the cricket brain: properties of identified extrinsic mushroom body cells. J. Comp. Physiol. A *154*, 71–79.

Schnaitmann, C., Vogt, K., Triphan, T., and Tanimoto, H. (2010). Appetitive and aversive visual learning in freely moving Drosophila. Front. Behav. Neurosci. *4*, 10. doi: 10.3389/fnbeh.2010.00010.

Schnaitmann, C., Garbers, C., Wachtler, T., and Tanimoto, H. (2013). Color Discrimination with Broadband Photoreceptors. Curr. Biol. *23*, 2375–2382.

Schnell, B., Raghu, S.V., Nern, A., and Borst, A. (2012). Columnar cells necessary for motion responses of wide-field visual interneurons in Drosophila. J. Comp. Physiol. A *198*, 389–395.

Scholes, J. (1969). The electrical responses of the retinal receptors and the lamina in the visual system of the fly musca. Kybernetik *6*, 149–162.

Schroll, C., Riemensperger, T., Bucher, D., Ehmer, J., Völler, T., Erbguth, K., Gerber, B., Hendel, T., Nagel, G., Buchner, E., et al. (2006). Light-induced activation of distinct modulatory neurons triggers appetitive or aversive learning in Drosophila larvae. Curr. Biol. *16*, 1741–1747.

Schümperli, R.A. (1973). Evidence for colour vision inDrosophila melanogaster through spontaneous phototactic choice behaviour. J. Comp. Physiol. *86*, 77–94.

Schwaerzel, M., Monastirioti, M., Scholz, H., Friggi-Grelin, F., Birman, S., and Heisenberg, M. (2003). Dopamine and octopamine differentiate between aversive and appetitive olfactory memories in Drosophila. J. Neurosci. *23*, 10495–10502.

Scott, K., Becker, A., Sun, Y., Hardy, R., and Zuker, C. (1995). Gqα protein function in vivo: Genetic dissection of its role in photoreceptor cell physiology. Neuron *15*, 919–927.

Silies, M., Gohl, D.M., Fisher, Y.E., Freifeld, L., Clark, D.A., and Clandinin, T.R. (2013). Modular use of peripheral input channels tunes motion-detecting circuitry. Neuron *79*, 111–127.

Single, S., and Borst, A. (1998). Dendritic Integration and Its Role in Computing Image Velocity. Science *281*, 1848–1850.

Sitaraman, D., LaFerriere, H., Birman, S., and Zars, T. (2012). Serotonin is critical for rewarded olfactory short-term memory in Drosophila. J. Neurogenet. *26*, 238–244.

Skinner, B.F. (1938). The behavior of organisms: an experimental analysis (Appleton-Century, Oxford, England).

Solomon, S.G., and Lennie, P. (2007). The machinery of colour vision. Nat. Rev. Neurosci. *8*, 276–286.

Sommer, E.W., and Wehner, R. (1975). The retina-lamina projection in the visual system of the bee, Apis mellifera. Cell Tissue Res. *163*, 45–61.

Spalthoff, C., Egelhaaf, M., Tinnefeld, P., and Kurtz, R. (2010). Localized direction selective responses in the dendrites of visual interneurons of the fly. BMC Biol. *8*, 36. doi: 10.1186/1741–7007–8–36.

Spradling, A., Stern, D., Kiss, I., Roote, J., Laverty, T., and Rubin, G. (1995). Gene Disruptions Using P-Transposable Elements - an Integral Component. Proc. Natl. Acad. Sci. *92*, 10824–10830.

Stockinger, P., Kvitsiani, D., Rotkopf, S., Tirián, L., and Dickson, B.J. (2005). Neural circuitry that governs Drosophila male courtship behavior. Cell *121*, 795–807.

Straka, H., and Ammermüller, J. (1991). Temporal resolving power of blowfly visual system: effects of decamethonium and hyperpolarization on responses of laminar monopolar neurons. J. Comp. Physiol. A *168*, 129–139.

Strausfeld, N.J. (1976). Atlas of an insect brain (Springer-Verlag Berlin, Heidelberg, New York).

Strausfeld, N.J. (2002). Organization of the honey bee mushroom body: representation of the calyx within the vertical and gamma lobes. J. Comp. Neurol. *450*, 4–33.

Strausfeld, N.J., and Braitenberg, V. (1970). The compound eye of the fly (Musca domestica): connections between the cartridges of the lamina ganglionaris. Z. Für Vgl. Physiol. *70*, 95–104.

Strausfeld, N.J., and Lee, J.-K. (1991). Neuronal basis for parallel visual processing in the fly. Vis. Neurosci. *7*, 13–33.

Stuart, A.E., Borycz, J., and Meinertzhagen, I.A. (2007). The dynamics of signaling at the histaminergic photoreceptor synapse of arthropods. Prog. Neurobiol. *82*, 202–227.

Suster, M.L., Seugnet, L., Bate, M., and Sokolowski, M.B. (2004). Refining GAL4-driven transgene expression in Drosophila with a GAL80 enhancer-trap. Genesis *39*, 240–245.

Van Swinderen, B. (2009). Fly memory: a mushroom body story in parts. Curr. Biol. *19*, 855–857.

Takemura, S., Karuppudurai, T., Ting, C.-Y., Lu, Z., Lee, C.-H., and Meinertzhagen, I.A. (2011). Cholinergic circuits integrate neighboring visual signals in a Drosophila motion detection pathway. Curr. Biol. *21*, 2077–2084.

Takemura, S., Bharioke, A., Lu, Z., Nern, A., Vitaladevuni, S., Rivlin, P.K., Katz, W.T., Olbris, D.J., Plaza, S.M., Winston, P., et al. (2013). A visual motion detection circuit suggested by Drosophila connectomics. Nature *500*, 175–181.

Takemura, S.Y., Lu, Z., and Meinertzhagen, I.A. (2008). Synaptic circuits of the Drosophila optic lobe: the input terminals to the medulla. J. Comp. Neurol. *509*, 493–513.

Tang, S., and Guo, A. (2001). Choice behavior of Drosophila facing contradictory visual cues. Science *294*, 1543–1547.

Tempel, B.L., Bonini, N., Dawson, D.R., and Quinn, W.G. (1983). Reward learning in normal and mutant Drosophila. Proc. Natl. Acad. Sci. *80*, 1482–1486.

Ting, C.Y., Gu, S., Guttikonda, S., Lin, T.Y., White, B.H., and Lee, C.H. (2011). Focusing transgene expression in Drosophila by coupling Gal4 with a novel split-LexA expression system. Genetics *188*, 229–233.

Troje, N. (1993). Spectral categories in the learning behaviour of blowflies. Z. Naturforschung C *48*, 96–96.

Tully, T., and Quinn, W.G. (1985). Classical conditioning and retention in normal and mutant Drosophila melanogaster. J. Comp. Physiol. A *157*, 263–277.

Tully, T., Preat, T., Boynton, S.C., and Del Vecchio, M. (1994). Genetic dissection of consolidated memory in Drosophila. Cell *79*, 35–47.

Tuthill, J.C., Nern, A., Holtz, S.L., Rubin, G.M., and Reiser, M.B. (2013). Contributions of the 12 neuron classes in the fly lamina to motion vision. Neuron *79*, 128–140.

Unoki, S., Matsumoto, Y., and Mizunami, M. (2005). Participation of octopaminergic reward system and dopaminergic punishment system in insect olfactory learning revealed by pharmacological study. Eur. J. Neurosci. *22*, 1409–1416.

Unoki, S., Matsumoto, Y., and Mizunami, M. (2006). Roles of octopaminergic and dopaminergic neurons in mediating reward and punishment signals in insect visual learning. Eur. J. Neurosci. *24*, 2031–2038.

Vogt, K., and Kirschfeld, K. (1984). Chemical identity of the chromophores of fly visual pigment. Naturwissenschaften *71*, 211–213.

Vogt, K., Schnaitmann, C., Dylla, K., Knapek, S., Aso, Y., Rubin, G.M., and Tanimoto, H. Shared mushroom body circuits underlie visual and olfactory memories in Drosophila. (submitted).

Vorobyev, M., and Osorio, D. (1998). Receptor noise as a determinant of colour thresholds. Proc. R. Soc. Lond. B Biol. Sci. *265*, 351–358.

Waddell, S., and Quinn, W.G. (2001). What can we teach Drosophila? What can they teach us? Trends Genet. *17*, 719–726.

Wakakuwa, M., Kurasawa, M., Giurfa, M., and Arikawa, K. (2005). Spectral heterogeneity of honeybee ommatidia. Naturwissenschaften *92*, 464–467.

Wang, Y., Mamiya, A., Chiang, A., and Zhong, Y. (2008). Imaging of an early memory trace in the Drosophila mushroom body. J. Neurosci. *28*, 4368–4376.

Wardill, T.J., List, O., Li, X., Dongre, S., McCulloch, M., Ting, C.-Y., O'Kane, C.J., Tang, S., Lee, C.-H., Hardie, R.C., et al. (2012). Multiple spectral inputs improve motion discrimination in the Drosophila visual system. Science *336*, 925–931.

Warrant, E., and Nilsson, D.-E. (2006). Invertebrate vision (Cambridge University Press).

Werner, A., Menzel, R., and Wehrhahn, C. (1988). Color constancy in the honeybee. J. Neurosci. *8*, 156–159.

Wernet, M.F., Celik, A., Mikeladze-Dvali, T., and Desplan, C. (2007). Generation of uniform fly retinas. Curr. Biol. *17*, 1002–1003.

Wernet, M.F., Velez, M.M., Clark, D.A., Baumann-Klausener, F., Brown, J.R., Klovstad, M., Labhart, T., and Clandinin, T.R. (2012). Genetic dissection reveals two separate retinal substrates for polarization vision in Drosophila. Curr. Biol. *22*, 12–20.

Wertz, A., Gaub, B., Plett, J., Haag, J., and Borst, A. (2009). Robust coding of ego-motion in descending neurons of the fly. J. Neurosci. *29*, 14993–15000.

Wolf, R., Wittig, T., Liu, L., Wustmann, G., Eyding, D., and Heisenberg, M. (1998). Drosophila mushroom bodies are dispensable for visual, tactile, and motor learning. Learn. Mem. *5*, 166–178.

Xia, S.-Z., Feng, C.-H., and Guo, A.-K. (1998). Multiple-phase model of memory consolidation confirmed by behavioral and pharmacological analyses of operant conditioning in Drosophila. Pharmacol. Biochem. Behav. *60*, 809–816.

Xu, X., and Kim, S.K. (2011). The early bird catches the worm: new technologies for the Caenorhabditis elegans toolkit. Nat. Rev. Genet. *12*, 793–801.

Yagi, R., Mayer, F., and Basler, K. (2010). Refined LexA transactivators and their use in combination with the Drosophila Gal4 system. Proc. Natl. Acad. Sci. *107*, 16166–16171.

Yamaguchi, S., Wolf, R., Desplan, C., and Heisenberg, M. (2008). Motion vision is independent of color in Drosophila. Proc. Natl. Acad. Sci. *105*, 4910–4915.

Yamaguchi, S., Desplan, C., and Heisenberg, M. (2010). Contribution of photoreceptor subtypes to spectral wavelength preference in Drosophila. Proc. Natl. Acad. Sci. *107*, 5634–5639.

Yang, E.-C., Lin, H.C., and Hung, Y.S. (2004). Patterns of chromatic information processing in the lobula of the honeybee, Apis mellifera L. Journal of Insect Physiology *50*, 913–925.

Yeh, E., Gustafson, K., and Boulianne, G.L. (1995). Green fluorescent protein as a vital marker and reporter of gene expression in Drosophila. Proc. Natl. Acad. Sci. *92*, 7036–7040.

Yu, D., Akalal, D.-B.G., and Davis, R.L. (2006). Drosophila α/β mushroom body neurons form a branch-specific, long-term cellular memory trace after spaced olfactory conditioning. Neuron *52*, 845–855.

Zars, T. (2009). Spatial orientation in Drosophila. J. Neurogenet. *23*, 104–110.

Zars, T., Fischer, M., Schulz, R., and Heisenberg, M. (2000). Localization of a short-term memory in Drosophila. Science *288*, 672–675.

Zhang, K., Guo, J.Z., Peng, Y., Xi, W., and Guo, A. (2007). Dopamine-mushroom body circuit regulates saliency-based decision-making in Drosophila. Science *316*, 1901–1904.

Zhang, X., Liu, H., Lei, Z., Wu, Z., and Guo, A. (2013). Lobula-specific visual projection neurons are involved in perception of motion-defined second-order motion in Drosophila. J. Exp. Biol. *216*, 524–534.

Zhang, Y., Kim, I.-J., Sanes, J.R., and Meister, M. (2012). The most numerous ganglion cell type of the mouse retina is a selective feature detector. Proc. Natl. Acad. Sci. *109*, 2391–2398.

Zhou, Y., Ji, X., Gong, H., Gong, Z., and Liu, L. (2012). Edge detection depends on achromatic channel in Drosophila melanogaster. J. Exp. Biol. *215*, 3478–3487.

Acknowledgement

First of all, I thank Prof. Dr. Hiromu Tanimoto for his great support throughout my thesis. My intellectual development is mainly attributed to his consistent supervision and our many discussions, as is my strong appreciation for the field of behavioural neuroscience.

My sincere thanks to Prof. Dr. Alexander Borst, who as my PhD supervisor gave me helpful advices regarding the development of my project.

Many thanks as well to PD Dr. Thomas Wachtler and Christian Garbers of the Ludwig-Maximilians-Universität, who supported this work with the computational model of fly colour discrimination, their help with the ERG measurements, and many fruitful discussions about colour vision. I am particularly grateful to the collaboration with Dr. Yoshinori Aso and Prof. Dr. Gerry Rubin of the Janelia Farm Research Campus who provided transgenic lines and who supported my behavioural experiments at their Institute. I also want to thank Katrin Vogt for her fruitful collaboration on the visual memory circuit project.

I deeply appreciate advices from the thesis committee members Prof. Dr. Dr. h.c. Martin Heisenberg, Prof. Dr. Takashi Suzuki, and Prof. Dr. Tim Gollisch.

Special thanks to Dr. Stephan Knapek, Dr. Igor Siwanowicz, Anja Friedrich, Andreas Eckart, Konrad Öchsner, and Stefan Prech for excellent technical assistance.

Prof. Dr. Jan Benda and Dr. Jan Grewe of the Ludwig-Maximilians-Universität I would like to thank for their great intellectual support, the setup and space without which the ERG measurements could not have been done.

I would like to thank my colleagues throughout the Tanimoto Group, Armin Bahl, Dr. Max Jösch, Prof. Dr. Dierk Reiff, Dr. Roni Jortner, Dr. Stephan Ohler, Dr. Irina Hein and Dr. Väinö Haikala for discussions, suggestions and for providing a great work atmosphere.

Many thanks to the Boehringer Ingelheim Fonds, which supported me financially as well as intellectually throughout my stipend. Many thanks also to the Max-Planck-Institute of Neurobiology.

Finally, I would like to thank my wife and family for their love and indispensable support.

Non-self-contributions

The computational model of *Drosophila* colour discrimination (Figure 12) and electrophysiological experiments (Figure 16, 19) were done in collaboration with Christian Garbers and PD Dr. Thomas Wachtler (Ludwig-Maximilians-Universität, München). The transgenic line *MB504B* was kindly provided by Dr. Yoshinori Aso and Prof. Dr. Gerry Rubin (Janelia Farm Research Campus). Anja B. Friedrich and Dr. Stephan Knapek (Max-Planck-Institute of Neurobiology) kindly provided confocal data for *R58E02-GAL4* and *MB504B* (Figure 25).

Curriculum vitae

Personal information

Surname / First name(s) Dominik	Schnaitmann, Christopher
Institution	Max-Planck-Institute of Neurobiology
Address	Am Klopferspitz 18, 82152 Martinsried
Phone	0049.89.857.834.39
E-mail	schnaitmann@neuro.mpg.de
Nationality	German
Marital status	Married
Date of birth	17 February 1983
Languages	German, English, French

Education

2008 – present:	Ph.D. (candidate) Biology, Ludwig-Maximilians-Universität München, Germany. Thesis title: 'Neural circuits underlying colour vision and visual memory in *Drosophila melanogaster*'. Work was conducted at the Max-Planck-Institute of Neurobiology, Martinsried, Germany. Supervisor: Dr. Hiromu Tanimoto
2003 – 2008:	Diploma, Biology, Julius-Maximilians-Universität Würzburg, Germany, Main subjects: Neurobiology, Genetics and Biochemistry, Thesis title: Visual appetitive learning in *Drosophila melanogaster*, Supervisor: Prof. Dr. Dr. h.c. Martin Heisenberg

2002 – 2003: Civil Service, Forschungsinstitut Senckenberg, Research Station of Limnology, Frankfurt/Main, Germany

1993 – 2002: High-School Degree (German Abitur), Hanns-Seidel-Gymnasium, Hösbach, Germany

Honors and Awards

2009 – 2011: PhD Fellowship of the Boeringer-Ingelheim-Fonds

Publications

Schnaitmann, C., Vogt, K., Triphan, T., Tanimoto, H. (2010). Appetitive and aversive visual learning in freely moving Drosophila. Front. Behav. Neurosci. *4*, 10.

Schnaitmann, C., Garbers, C., Wachtler, T., and Tanimoto, H. (2013). Colour Discrimination with Broadband Photoreceptors. Current Biology *23*, 2375–2382.

Vogt, K.*, Schnaitmann, C.*, Dylla, K. V., Knapek, S., Aso, Y., Rubin, G., Tanimoto, H. Shared mushroom body circuits underly visual and olfactory memories in *Drosophila*. (submitted).

*equal contribution

Abstracts / Scientific Presentations

Poster presentation "Peripheral neural circuits underlying colour discrimination in *Drosophila*", 13 – 16 March 2013, 10th Göttingen Meeting of The German Neuroscience Society, Göttingen, Germany

Oral presentation "Colour discrimination and memory in *Drosophila*", 24 April 2012, Albert-Ludwigs-Universität, Freiburg, Germany

Oral presentation “Photoreceptors contributing to colour vision in *Drosophila*”, 21 – 22 March 2012, Fruit Flies and Honeybees – Mini Symposium, Berlin, Germany

Oral presentation “Colour discrimination and memory in *Drosophila*”, 9 February 2012, Janelia Farm, Ashburn, USA

Poster Presentation “Functional analysis of color discrimination in *Drosophila*”, 13 – 16 March 2011, Visual Processing in Insects: From Anatomy to Behavior, Janelia Farm, Ashburn, USA

Poster presentation “Neural circuits underlying visual appetitive and aversive memories in *Drosophila melanogaster*”, 01 – 05 September 2010, Neurofly, Manchester, UK

Oral presentation “Colour discrimination and memory in *Drosophila*”, 28 July 2010, Julius-Maximilians-Universität, Würzburg, Germany

Poster presentation “Toward identification of the neural circuit underlying *Drosophila* visual memories”, 29 September – 03 October 2009, Neurobiology of Drosophila, Cold Spring Harbor Laboratory, New York, USA

Oral Presentation “Visual appetitive learning in *Drosophila melanogaster*”, 13 November 2008, Mark Stopfer Lab, National Institutes of Health (NIH), Bethesda, USA

Poster presentation “Behavioural assay for appetitive visual memory”, 09 – 11 November 2008, Learning and memory: A Synthesis of Flies and Honeybees, Janelia Farm, Ashburn, USA

Poster presentation “Visual appetitive learning in *Drosophila melanogaster*”, 09 – 10 October 2008, Drosophila Regional Meeting, Max-Planck-Institute of Neurobiology, Martinsried, Germany

Poster presentation “Visual appetitive learning in *Drosophila*”, 06 – 11 September 2008, Neurofly, University of Würzburg, Germany

Declaration (Eidesstattliche Versicherung)

Ich versichere hiermit an Eides statt, dass die vorgelegte Dissertation von mir selbständig und ohne unerlaubte Hilfe angefertigt ist.

München, den ....

(Unterschrift)

Erklärung

Hiermit erkläre ich, *

- dass die Dissertation nicht ganz oder in wesentlichen Teilen einer anderen Prüfungskommission vorgelegt worden ist.
- dass ich mich anderweitig einer Doktorprüfung ohne Erfolg **nicht** unterzogen habe.
- dass ich mich mit Erfolg der Doktorprüfung im Hauptfach Biologie bei der Fakultät für Biologie der Ludwig-Maximilians-Universität unterzogen habe.
- ~~dass ich ohne Erfolg versucht habe, eine Dissertation einzureichen oder mich der Doktorprüfung zu unterziehen.~~

München, den ....

(Unterschrift)

*) Nichtzutreffendes streichen